Thermal Conduction in Polymeric Nanofluids and Nanosolids Controlled by Interfacial Scattering: Solutions to Some Selected Problems

Thesis submitted to
Cochin University of Science and Technology
in partial fulfillment of the requirements for the award of the degree of

DOCTOR OF PHILOSOPHY

Nisha M. R.

Department of Instrumentation

Cochin University of Science and Technology

Cochin 682 022

October 2011

Certificate

Certified that the work presented in this thesis is based on the bona fide work done by ***Ms. Nisha M. R.*** *under my guidance in the Department of Instrumentation, Cochin University of Science and Technology, and has not been included in any other thesis submitted previously for the award of any degree.*

Cochin-682022
31 October 2011

Dr. Jacob Philip
Supervising Guide

DECLARATION

Certified that the work presented in this thesis is based on the original work done by me under the guidance of Dr. Jacob Philip, Professor, Department of Instrumentation, Cochin University of Science and Technology, and has not been included in any other thesis submitted previously for the award of any degree.

Cochin-682022 **Nisha M. R.**

31October 2011

Dedication to my Parents and Brother……...

Acknowledgement

It is a pleasure to thank the many people who made this thesis possible.

Before I begin I would like to extend my first and foremost gratitude to the almighty God whose imperial presence was always there throughout my effort to bring out this thesis in the best possible way.

It is difficult to overstate my sincere gratitude to my Ph. D. supervising teacher Dr. Jacob Philip, Director, Sophisticated Test and Instrumentation Centre, Cochin University of Science and Technology. With his enthusiasm, inspiration, and patience he made things easy and helped to make physics fun for me. Throughout my Ph. D. work and thesis-writing period, he provided encouragement, advice, teaching, amity and lots of good ideas. I must appreciate his efforts and guidance without which this would not have materialized.

I am extremely grateful to Dr. A. V. Alex and Dr. N. V. Joshy, physics teachers, St. Paul's college, Kalamassery for their advice and help to join research work at the Department of Instrumentation, Cochin University of Science and Technology.

I would like to express my sincere gratitude to Dr. Stephen Rodriguez, Head of the Department of Instrumentation and Dr. K. N. Madhusudanan, the former Head of the Department who gave the opportunity to utilize all facilities available in the department to make my work a reality.

I would like to thank other faculty members, Dr. Johny Isaac, Dr. K. Rajeev Kumar and non teaching staff of the Department of Instrumentation for their kind help and suggestions with various aspects. I am particularly grateful

to Mrs. Elikutty former section officer, Mr. Murali, Mr. Joshy, Mr. Gopi Menon, Mr. Jose Jacob, Mr. Jose for their kind help and technical support during the time of my Ph. D. work.

I gratefully acknowledge all the support and timely helps of my seniors and my friends Dr. A. V Alex, Dr. O. Raghu, Dr. Alex Mathew, Dr. Preethy, Dr. Rajesh, Dr. Manjusha, Dr. Vimala, Benjamin Sir, Nisha, Viji, Anu, Uma, Maju, Subin, Ginson, Rehna, Savitha, Jayalakshmi, Soumya, Rakhi, Lidiya, Nissam, Abdul Rahman and Amita.

I also like to remember some of my friends at the Department of Chemistry, Cochin University of Science and Technology, for their timely help for doing various sample preparations in my work.

I would like to remember staff of Sophisticated Test and Instrumentation Centre (STIC), for their kind support and help extended throughout my work. No words are enough to express my heartfelt thanks to the staff of Sophisticated Analytical and Instrumentation Facility, STIC especially to Dr. Shibu M. Eapen for his great ideas, kind help and sincere support for realizing various analyses in my work. I also remember the great efforts and timely helps of Mr. Adarsh, Shyam, Saji, Melbin, Ezrah, Aswathy and Smitha who deserve some special mention.

I am indebted to my parents and my lovely brother for being supportive and generous enough to stand by me to achieve whatever I have today.

I am extremely grateful to my loving brothers in my family for the moral support, care that they are giving throughout my life. I recall all other family members, some uncles, aunts, cousins, sisters, brother in laws, niece and nephews for their love, care and the attitude to join in all my difficult times.

I am also grateful to all members of Mytry Residential Association for the enthusiasm, care and support that I have enjoyed with them during the course of this work. Special thanks to all my friends and well wishers for their prayers during each moment in my life.

Last but not the least I extend my warm affection to my friends who have been sportive and suggestive even though I could not really spare time for them and almost failed to reciprocate to their affection due to lack of time. I hope you will excuse me at this time and let me take this as an opportunity to tell you that I really love you all.

Once again remembering the supreme power for guiding me throughout…….

Nisha M. R.

Contents

PREFACE

Nanofluids are a new class of nanotechnology based heat transfer fluids, defined as a uniform suspension of nanometer sized metallic or nonmetallic particles in a base fluid. These nano-suspensions have been found to possess enhanced thermal conductivity at comparatively low concentrations of nanoparticles. Even at very low volume fractions (< 0.1%) of the suspended nanoparticles, enhancements as high as 40% in thermal conductivity have been reported in many nanofluids. Moreover, the percentages of enhancements are found to increase with nanofluid characteristics such as particle concentration, particle size, temperature etc. For the past two decades, scientists and engineers have made significant advances in the precise measurement of thermal conductivity of nanofluids and its variations with various characteristics cited above. Also different theoretical models have been developed to account for the observed enhancements in thermal conductivity and associated properties of nanofluids. Following the conventional effective medium or mean field models and including physical mechanisms specifically applicable to nanofluids, scientists have tried to explain the observed anomalous features of the thermophysical properties of these systems. Researchers have modified the effective medium theory taking into account mechanisms such as adsorption of liquid molecules around nanoparticle surface, formation of nanoparticle clusters in liquid medium, Brownian motion of nanoparticles at finite temperature, scattering of thermal waves at nanoparticle-matrix interfaces etc. However, several questions still remain unanswered and researchers do not seem to agree on the mechanism(s) responsible for the observed results. An associated puzzling issue still remaining unresolved on this subject is the effect of the size and shape of suspended nanoparticles on the effective thermal conductivity of nanofluids.

Most of the work done so far has been on low molecular weight nanofluids such as water based ones with metallic or nonmetallic nanoparticle dispersions, and not much on high molecular weight nanofluids such as polymeric ones has been reported in literature. In low molecular weight based nanofluids the formation and stability of liquid adsorption layer around the nanoparticle couldn't be possible due to the low viscosity of the base medium. Moreover, in high molecular weight polymer based nanofluids, a mechanism such as adsorption of liquid molecule around the nanoparticles will possibly control the thermal conduction process. The higher viscosity of the high molecular weight base medium gives a better stability for adsorbed nanolayer formed around the nanoparticle surface and in a high molecular weight nanofluid system consisting of metallic nanoparticles, the formation of nanoparticle clusters also have a significant role for deciding the effective thermal conductivity of nanofluids. So the validity of these mechanisms has to be checked accurately following a measurement system which possesses high accuracy and precision in experimental values of thermal conductivity.

In this work we have tried to establish the mode of variation of effective thermal conduction properties of polymeric nanofluids with particle concentration and extended our analysis to their condensed form, known as polymeric nanosolids. Generally the thermal properties like thermal conductivity and thermal diffusivity of a material determine the thermal conduction mechanism in a material. Since the heat losses in a sample do not affect its thermal diffusivity value it is better to measure thermal diffusivity than thermal conductivity for monitoring thermal conduction in a sample. The measurement of thermal properties of polymeric nanofluids and their solid counterparts have been done with experimental techniques that are based photothermal effects. The absorption and conversion of optical energy into

thermal energy is common for all light absorbing materials irrespective of whether they are solids, liquids or gases. The subsequent excitation and deexcitation of electronic and atomic energy levels results in the heating in these materials. Such process form the basis of photothermal techniques employed for thermal property analysis. We have also arrived at theoretical conclusions on effective thermal conduction observed with polymeric nanofluids and their solid counterparts following the conventional effective medium theory and its modified forms proposed by previous authors. It has been shown that the experimental results agree with our theoretical predictions within the uncertainty of the experimental results.

We have employed a thermal wave resonant cavity (TWRC) which works based on thermal wave interference to measure the thermal diffusivity of nanofluids. The thermal wave interference technique measures the thermal diffusivity of a fluid filled in a resonant cavity formed between two parallel metallic foils through which thermal waves generated at one metallic foil by modulated optical absorption propagate back and forth resulting in interference maxima and minima. By performing cavity length scan or light modulation frequency scan, the interference peaks can be made to shift from one maximum (or minimum) to the next maximum (or minimum). By measuring the separation between adjacent peaks of the interference maxima or minima in a cavity scan mode or the phase separation in a frequency scan mode, one can determine the thermal diffusivity of the fluid accurately.

We have studied the variation in thermal conduction in condensed polymeric nanosolids with the concentration of nanoparticles. The determination of thermal properties of nanosolids has been made with photopyroelectric (PPE) as well as photoacoustic (PA) thermal wave techniques. In the PPE technique, an intensity modulated beam of light (from a

laser) incident on the sample generates a thermal wave, which propagates through the sample creating a corresponding periodic temperature rise on the opposite side of the sample. This temperature rise is picked up with a pyroelectric detector (such as a PVDF film) attached to the sample. The amplitude and phase of the pyroelectric signal are recorded as a function of modulation frequency with a Lock-in-amplifier. The thermal properties such as thermal conductivity, specific heat capacity as well as thermal diffusivity of the samples have been evaluated from the amplitude and phase values of the thermal wave. The measurements have been carried out on samples with different mass fractions of nanoparticles.

The PA measurement of thermal diffusivity of a solid is based on the sensitive detection of acoustic waves generated by the absorption of modulated electromagnetic radiation, the most popular radiation source nowadays being lasers. It is now well established that the PA effect involves production of acoustic waves as a consequence of the generation of thermal waves in the medium due to non-radiative de-excitation processes in the sample as a result of periodic heating by the absorption of modulated light. The experimental method is based on the analysis of the variations in the amplitude and phase of the PA signal with the light modulation frequency, which is also the frequency of the generated acoustic waves. The sample is kept in an enclosed volume provided with a window to irradiate the sample and a sensitive microphone picks up the PA signal, which is usually amplified and processed with a lock-in amplifier. The experiment needs to be carried out in a vibration free environment so that a sufficiently high signal to noise ratio can be achieved.

In the following paragraphs, we give a chapter wise description of the contents of the thesis.

Chapter 1 is a review on thermal conductivity of nanofluids. The concept, preparation of nanofluids and experimental techniques followed by previous authors are discussed in this chapter. The experimental investigations on the dependence of various parameters such as nanoparticle volume fraction, nanoparticle size, temperature, type of nanoparticle, type of base fluid on effective thermal conductivity of nanofluids are also included. Various theoretical models proposed by previous researchers to describe the anomalous enhancements observed with nanofluids are put in proper perspective. A somewhat comprehensive study on the anomalous enhancement observed with thermal conductivity of nanofluids is described in one of the sections. Investigations on the validity of mechanisms such as formation of adsorption layer around the nanoparticle for describing the effective thermal conductivity of polymeric nanofluids is one of the main themes of the work presented in this thesis. This is discussed along with the thermal conduction studies performed in polymeric nanosolids.

Chapter 2 describes the experimental techniques followed for the measurements reported in this thesis. It describes the design and fabrication of a thermal wave resonant cavity (TWRC) cell that we have employed for measuring the thermal diffusivity of polymeric nanofluids. The main parts of a thermal wave resonant cavity are i) a resonant cavity formed between two parallel metallic foils ii) stepper motor controller attached to one of the metallic foils for varying the cavity length to produce thermal wave interference. The stepper motor is driven by signals from a programmed PC. A computer program has been developed in visual basic to control the step size in the cavity length scan experiment. Sensitive detection of the interference maxima and minima have been performed with a PVDF detector and its output has been analyzed with a Lock-in-amplifier which has been interfaced to the PC.

Experimental investigations on effective thermal conductivity and the thermal diffusivity of polymeric nanosolids have been performed with the conventional photoacoustic and photopyroelectric techniques. A description of the basic principles and measurement of these techniques are also discussed in this chapter.

Chapter 3 outlines the various theoretical models that we have followed to describe the experimentally observed thermal conductivity of polymeric nanofluids and polymeric nanosolids. The concept and derivation of conventional effective medium theory for effective thermal conductivity of two component mixtures, originally proposed by Maxwell, are discussed in this chapter. The modified form of effective medium model proposed by previous authors based on the mechanisms such as adsorption layer formation around the nanoparticle, nanoparticle clustering etc. for describing the anomalous enhancement observed with these nanofluids have also been discussed in this chapter. As a second part of this chapter various theoretical models for effective thermal conductivity of nanosolid materials, such as the model developed by Nan considering the interfacial scattering in nanosolids, the model developed by Cheng and Vachon following the diffusion of thermal waves through nanoparticles and others have been discussed. Our predictions on effective thermal conductivity of condensed polymeric nanosolids are also presented by combining the concepts of Nan's model and Cheng-Vachon model.

Chapter 4 describes the results on the effect of nanoparticle volume fraction on the effective thermal diffusivity of polymeric nanofluids and others investigated by thermal wave resonant cavity technique. The variation in thermal conduction in nanofluids is done by varying the concentration of nanofluids. The preparation of different concentrations of polymeric

nanofluids has been done following two step method which includes the nanoparticle synthesis, dispersion of nanoparticles in the base fluid etc. These are described in this chapter. Measurement of thermal diffusivity of polymeric nanofluids and results obtained with these high molecular weight nanofluid systems are given in this chapter. A comparison of experimental results and theoretical analysis that we have carried out in the same system following the theoretical models proposed by previous authors are also presented and discussed in this chapter. In order to isolate the effect of adsorption layer on effective thermal conductivity of nanofluids, we have also investigated the variations of effective thermal diffusivity/thermal conductivity of water based nanofluids with the concentration of nanoparticles. The experimental results obtained with these are also presented and analyzed in this chapter.

Chapter 5 discusses the effect of nanoparticle size on effective thermal diffusivity and thermal conductivity of polymeric and water based nanofluid systems investigated by a thermal wave resonant cavity. The preparation of polymeric and water based nanofluids with variations in the size of nanoparticles are also described in this chapter. Finally, the validity of mechanisms such as adsorption of liquid layer around nanoparticle surfaces and clustering of nanoparticles in determining the particle size dependence of effective thermal conductivity of nanofluids are discussed.

Chapter 6 describes the results on the investigations that we have carried out on effective thermal conductivity and thermal diffusivity of polymeric nanosolids by varying the concentration of nanoparticles. The measurements have been carried out using photopyroelectric and photoacoustic techniques. Comparison of observed experimental results with various theoretical models are presented and discussed in this chapter.

Chapter 7 gives a summary and conclusion of work done in this thesis. Scope for future work in polymeric nanofluids and polymeric nanosolids are presented in the last section of the thesis.

A good part of the work presented in this thesis has been either published or submitted for publication. The following papers have been published or submitted for publication.

Papers published: 1

1. J. Philip and M. R. Nisha, "*Thermal diffusion in dilute nanofluids investigated by photothermal interferometry*", Journal of Physics: Conference Series, Vol. **214** (2009) 012035

Papers submitted for publication: 3

1. M. R. Nisha and J. Philip, "*Thermal conduction in polymeric nanofluids under mean field approximation: Role of interfacial adsorption layers*", Int. J.ThermoPhysics .
2. M. R. Nisha and J. Philip, "*Dependence of particle size on the effective thermal diffusivity and conductivity of nanofluids: Role of base fluid properties*", Journal of Heat and Mass Transfer.
3. M. R. Nisha, M. S. Jayalakshmi and J. Philip, "*Role of interfacial resistance on effective thermal conductivity of condensed polymeric nanofluids (nanosolids)*", Material Science and Applications.

Papers published in Conference proceedings: 3

1. "*Thermo physical Properties of Nanofluids: New Findings on the influences of Particle size*". 21st Kerala Science Congress 2009, January 28-31, Kollam, Kerala, India.
2. "*Thermal diffusion in dilute nanofluids investigated by photo thermal interferometry.*" 15th International Conference on Photoacoustic and Photo- thermal Phenomena, 2009, July 19-23, Leuven, Belgium.
3. "*Thermal diffusion in dilute polymeric nanofluids: Role of interfacial scattering*. Proc. Int. Conf. on Nanostructured Materials, 2010, Thiruchengode, India.

Chapter 1

Introduction to Nanofluids

1.1 Introduction

Thermal properties of liquids play a decisive role in heating as well as cooling applications in industrial processes. Thermal conductivity of a liquid is an important physical property that decides its heat transfer performance. Conventional heat transfer fluids have inherently poor thermal conductivity which makes them inadequate for ultra high cooling applications. Scientists have tried to enhance the inherently poor thermal conductivity of these conventional heat transfer fluids using solid additives following the classical effective medium theory (Maxwell, 1873) for effective properties of mixtures. Fine tuning of the dimensions of these solid suspensions to millimeter and micrometer ranges for getting better heat transfer performance have failed because of the drawbacks such as still low thermal conductivity, particle sedimentation, corrosion of components of machines, particle clogging, excessive pressure drop etc. Downscaling of particle sizes continued in the search for new types of fluid suspensions having enhanced thermal properties as well as heat transfer performance.

All physical mechanisms have a critical scale below which the properties of a material changes totally. Modern nanotechnology offers physical and chemical routes to prepare nanometer sized particles or nanostructured materials engineered on the atomic or molecular scales with enhanced thermo-physical properties compared to their respective bulk forms. Choi (1995) and other

researchers (Masuda *et al.,* 1993; Lee *et al.,* 1999) have shown that it is possible to break down the limits of conventional solid particle suspensions by conceiving the concept of nanoparticle-fluid suspensions. These nanoparticle-fluid suspensions are termed nanofluids, obtained by dispersing nanometer sized particles in a conventional base fluid like water, oil, ethylene glycol etc. Nanoparticles of materials such as metallic oxides (Al_2O_3, CuO), nitride ceramics (AlN, SiN), carbide ceramics (SiC, TiC), metals (Cu, Ag, Au), semiconductors (TiO_2, SiC), single, double or multi walled carbon nanotubes (SWCNT, DWCNT, MWCNT), alloyed nanoparticles ($Al_{70}Cu_{30}$) etc. have been used for the preparation of nanofluids. These nanofluids have been found to possess an enhanced thermal conductivity (Shyam *et al.,* 2008; Choi *et al.,* 2001; Eastman *et al.,* 2001) as well as improved heat transfer performance (Xuan *et al.,* 2003; Yu *et al.,* 2003; Vassalo *et al.,* 2004; Artus, 1996) at low concentrations of nanoparticles. Even at very low volume fractions (< 0.1%) of the suspended particles, an attractive enhancement up to 40% in thermal conductivity has been reported on these nanotechnology based fluids (Wang *et al.,* 1999) and the percentage of enhancement is found to increase with temperature (Das *et al.,* 2003) as well as concentration of nanoparticles (Shyam *et al.,* 2008). The effective thermal conductivity of these nanofluids are usually expressed as a normalized thermal conductivity value obtained by dividing the overall thermal conductivity of the nanofluid by the base fluid thermal conductivity or sometimes as a percentage of the effective value with respect to the base fluid value.

1.1.1 Properties of nanofluids

It may be noted that particle size is an important physical parameter in nanofluids because it can be used to tailor the nanofluid thermal properties as well as the suspension stability of nanoparticles. Researchers in nanofluids have

been trying to exploit the unique properties of nano particles to develop stable as well as highly conducting heat transfer fluids.

The key building blocks of nanofluids are nanoparticles; so research on nanofluids got accelerated because of the development of nanotechnology in general and availability of nanoparticles in particular. Compared to micrometer sized particles, nanoparticles possess high surface area to volume ratio due to the occupancy of large number of atoms on the boundaries, which make them highly stable in suspensions. Thus the nano suspensions show high thermal conductivity possibly due to enhanced convection between the solid particle and liquid surfaces. Since the properties like the thermal conductivity of the nano sized materials are typically an order of magnitude higher than those of the base fluids, nanofluids show enhancement in their effective thermal properties. Due to the lower dimensions, the dispersed nanoparticles can behave like a base fluid molecule in a suspension, which helps us to reduce problems like particle clogging, sedimentation etc. found with micro particle suspensions. The combination of these two features; extra high stability and high conductivity of the dispersed *'nanospecies'* make them highly preferable for designing heat transfer fluids. The stable suspensions of small quantities of nanoparticles will possibly help us to design lighter, high performance thermal management systems.

Cooling is indispensable for maintaining the desired performance and reliability of a wide variety of industrial products such as computers, power electronic circuits, car engines, high power lasers, X-ray generators etc. With the unprecedented increase in heat loads and heat fluxes caused by more power in miniaturized products, high tech industries such as microelectronics, transportation, manufacturing, metrology and defense face cooling as one of the top technical challenges. For example, the electronics industry has provided

computers with faster speeds, smaller sizes and expanded features, leading to ever increasing heat loads, heat fluxes and localized hot spots at the chip and package levels. Such thermal problems are also found in power electronics, optoelectronic devices etc. So the enhanced heat transfer characteristics of nanofluids may offer the development of high performance, compact, cost effective liquid cooling systems.

1.2 Nanofluid thermal conductivity research: A review

Practical applications of nanofluids discussed above are decided by the thermophysical characteristics of nanofluids. In the last decade, significant amounts of experimental as well as theoretical research were done to investigate the thermophysical behavior of nanofluids. All these studies reveal the fact that micro structural characteristics of nanofluids have a significant role in deciding the effective thermal conductivity of nanofluids. There are many reviews on nanofluid thermal conductivity research (Wang *et al.,* 2007; Murshed *et al.,* 2008a; Choi *et al.,* 2009; Wen *et al.,* 2009). In all reviews on nanofluid thermal conductivity, both theoretical models as well as experimental results have been discussed. By closely analyzing the experimental results and theoretical models followed by previous authors we get a good picture of the conflicting reports on the effective thermal conductivity of nanofluids and the mechanisms supporting these reports. Experimental work done by a good number of research groups worldwide has revealed that nano fluids exhibit thermal properties superior to base fluid or conventional micrometer sized particle-fluid suspensions. Choi *et al.* (2001) and Eastman *et al.* (2001) have shown that copper and carbon nanotube (CNT) nano fluid suspensions possess much higher thermal conductivities compared to those of base fluids and that CNT nanofluids have showed a non linear relationship between thermal conductivity and concentration at low volume fractions of CNTs (Choi *et al.,* 2001).

Initial work on nanofluids was focused on thermal conductivity measurements as a function of concentration, temperature, and particle size. Measurements of the thermal conductivity of nanofluids started with oxide nanoparticles (Masuda *et al.,* 1993; Lee *et al.,* 1999) using transient hot wire (THW) method. Nanofluids did not attract much attention until Eastman *et al.* (2001) showed for the first time that copper nanofluids, have more dramatic increases than those of oxide nanofluids produced by a two step method. Similarly Choi *et al.* (2001) performed thermal conductivity measurement of MWCNTs (Multi walled Carbon nano tubes) dispersed into a host fluid, synthetic poly (α-olefin) oil, by a two step method and measured the effective thermal conductivity of carbon nanotube-oil suspensions. They discovered that nanofluids have an anomalously large increase in thermal conductivity, up to 150% for approximately 1 vol % of nanotubes, which is by far the highest thermal conductivity ever achieved in a liquid. This measured increase in thermal conductivity of nanotube based nanofluids is an order of magnitude higher than that predicted using existing theories (Maxwell, 1873; Hamilton and Crosser, 1962). The results of Choi *et al.* (2001) show another anomaly that the measured thermal conductivity is non linear with nanotube loadings, while all theoretical models predict a linear relationship. This non linear relationship is not expected in conventional fluid suspensions of microsized particles at such low concentrations. Soon, some other distinctive features such as strong temperature dependent thermal conductivity (Das *et al.,* 2003) and strong particle size dependent thermal conductivity (Chon *et al.,* 2005) were discovered during the thermal conductivity measurement of nanofluids.

Although experimental work on convection and boiling heat transfer in nanofluids are very limited compared to experimental studies on conduction in nanofluids, discoveries such as a two fold increase in the laminar convection

heat transfer coefficient (Faulkner *et al.,* 2004) and a three-fold increase in the critical heat flux in pool boiling (You *et al.,* 2003) were reported. The potential impact of these discoveries on heat transfer application is significant. Therefore, nanofluids promise to bring about a significant improvement in cooling technologies. As a consequence of these discoveries, research and development on nanofluids have drawn considerable attention from industry and academia over the past several years.

Most of the experimental studies on effective thermal conductivities of nanofluids have been done by using a transient hot wire (THW) method, as this is one of the most accurate methods to measure the thermal conductivities of fluids. Another method generally employed is the steady state method. All the experimental results obtained by these methods have shown that the thermal conductivity of nanofluids depend on many factors such as particle volume fraction, particle material, particle size, particle shape, base fluid properties and temperature. More detailed descriptions about the effect of these parameters on effective thermal conductivity of nanofluids are discussed below.

1.2.1 Effect of particle volume fraction

Particle volume fraction is a parameter that has been investigated in almost all of the experimental studies and most of the results are generally in agreement qualitatively. Most of the research reports show an increase in thermal conductivity with an increase in particle volume fraction and the relation found is, in general, linear. There are many studies in literature on the effect of particle volume fraction on the thermal conductivity of nanofluids. Masuda *et al.* (1993) measured the thermal conductivity of water based nanofluids consisting of Al_2O_3 (13nm), SiO_2 (12nm) and TiO_2 (27nm) nanoparticles, the numbers in the parenthesis indicating the average diameter of

the suspended nanoparticles. An enhancement up to 32.4% was observed in the effective thermal conductivity of nanofluids for a volume fraction about 4.3% of Al_2O_3 nanoparticles. Lee *et al.* (1999) studied the room temperature thermal conductivity of water as well as ethylene glycol (EG) based nanofluids consisting of Al_2O_3 (38.5nm) and CuO (23.6nm) nanoparticles. In this study a high enhancement of about 20 % in the thermal conductivity was observed for 4% volume fraction of CuO in CuO/EG nanofluid. Later Wang *et al.* (1999) repeated the measurement on the same type of nanofluids based on EG and water with Al_2O_3 (28nm) as well as CuO (23nm) as inclusions. The measurements carried out by these groups showed that for water and ethylene glycol-based nanofluids, thermal conductivity ratio showed a linear relationship with particle volume fraction and the lines representing this relation were found to be coincident.

Measurements on other nanofluid systems such as TiO_2 in deionized water (Chopkar *et al.,* 2008) and multi walled carbon nanotube (MWCNT) in oil (Choi *et al.,* 2001) show a non linear relation between the effective thermal conductivity and particle volume fraction which indicate the interactions between the particles in the system.

1.2.2 Effect of particle material

Most of the studies show that particle material is an important parameter that affects the thermal conductivity of nanofluids. For example, Lee *et al.* (1999) considered the thermal conductivity of nanofluids with Al_2O_3 and CuO nanoparticles mentioned in the previous section. They found that nanofluids with CuO nanoparticles showed better enhancement compared to the nanofluids prepared by suspending Al_2O_3 nanoparticles in the same base fluid. It may be noted that as a material Al_2O_3 has higher thermal conductivity than CuO.

Authors explain this behavior as due to the formation clusters of Al_2O_3 nanoparticles in the fluid.

Chopkar *et al.* (2008) made room temperature measurements in water and EG based nanofluids consisting of Ag_2Al as well as Ag_2Cu nanoparticles and it was found that the suspensions of Ag_2Al nanoparticles showed enhancement in thermal conductivity slightly more than Ag_2Cu nanoparticle suspensions. This was explained as due to the higher thermal conductivity of Ag_2Al nanoparticles. Also, the suspensions of carbon nanotubes in different fluids were found to possess a surprising enhancement upto about 160% (Choi *et al.,* 2001) in the effective thermal conductivity value.

1.2.3 Effect of base fluid

According to the conventional effective medium theory (Maxwell, 1873), as the base fluid thermal conductivity decreases, the effective thermal conductivity of a nanofluid increases. Most of the experimental reports agree with the theoretical values given by this conventional mean field model. As per Wang *et al.*'s (1999) results on the thermal conductivity of suspensions of Al_2O_3 and CuO nanoparticles in several base fluids such as water, ethylene glycol, vacuum pump oil and engine oil, the highest thermal conductivity ratio was observed when ethylene glycol was used as the base fluid. EG has comparatively low thermal conductivity compared to other base fluids. Engine oil showed somewhat lower thermal conductivity ratios than Ethylene Glycol. Water and pump oil showed even smaller ratios respectively. However, CuO/EG as well as CuO/water nanofluids showed exactly same thermal conductivity enhancements at the same volume fraction of the nanoparticles. The experimental studies reported by Xie *et al.* (2002b) also supported the values given by the mean field theory.

Chopkar *et al.* (2008) contradicted the above results based on mean field theory statement by reporting higher thermal conductivity enhancement for nanofluids with a base fluid of higher thermal conductivity. The theoretical analysis made by Hasselmann and Johnson (1987) have shown that the effective thermal conductivity of fluid-particle mixtures were nearly independent of base fluid thermal conductivity.

1.2.4 Effect of particle size

The advent of nanofluids offers the processing of nanoparticles of various sizes in the range of 5-500 nm. It has been found that the particle sizes of nanoparticles have a significant role in deciding the effective thermal conductivity of nanofluids. There are many studies reported in literature regarding the dependence of nanoparticle size on effective thermal conductivity of nanofluids. Chopkar *et al.* (2006) studied the effect of the size of dispersed nanoparticles for $Al_{70}Cu_{30}$ /EG nanofluids by varying the size of $Al_{70}Cu_{30}$ nanoparticles in the range from 9 nm to 83 nm. In another study on water and EG based nanofluids consisting of Al_2Cu and Ag_2Al nanoparticles, Chopkar *et al.* (2008) also investigated the effect of particle size on effective thermal conductivity of nanofluids. In all these cases it has been found that the effective thermal conductivity of a nanofluid increases with decreasing nanoparticle size. Also, the results of Eastman *et al.* (2001) and Lee *et al.* (1999) support this conclusion drawn by Chopkar *et al.* (2008) on the particle size effect on the effective thermal conductivity of nanofluids.

In another study of the effect of particle size on the thermal conductivity of nanofluids, reported by Beck *et al.* (2009) in water as well as EG based nanofluids consisting of Al_2O_3 nanoparticles, the normalized thermal conductivity of nanofluids vary in such a way that it decreases with decreasing

the nanoparticle size. Thus conflicting reports have appeared in literature on the dependence of particle size on the thermal conductivity of nanofluids.

1.2.5 Effect of particle shape

For experimentation, spherical as well as cylindrical shaped nanoparticles are commonly used for nanofluid synthesis. The cylindrical particles have larger aspect ratio (length to diameter ratio) than spherical particles. The wide differences in the dimensions of these particles do influence the enhancement in effective thermal properties of nanofluids. Xie *et al.* (2002a) measured the thermal conductivity of water as well as EG based nanofluids consisting of both cylindrical as well as spherical SiC nanoparticles. It was observed that in water based nanofluids, the cylindrical suspensions had higher thermal conductivity enhancement of about 22.9% than the spherical particles for the same volume fraction (4.2%). Also the theoretical values based on Hamilton-Crosser model (1962) are found to be in good agreement with this comparatively higher enhancement for cylindrical particle suspensions.

Another experimental study reported by Murshed *et al.* (2005) in water based nanofluids consisting of spherical as well as rod shaped TiO_2 nanoparticles showed a comparatively higher enhancement for rod shaped particles (32.8%) than spherical particles (29.7%) at a volume fraction of 5%.

In addition to these experimental results a general observation is that nanotube suspensions show a higher enhancement than the spherical particle suspension due to rapid heat transfer along a larger distance through a cylindrical particle since it has a length of the order of a micrometer. However, the cylindrical particle suspension need higher pumping power due to its enhanced viscosity (Timofeeva *et al.,* 2009) which limits its usage, possible application as a heat transfer fluid.

1.2.6 Effect of temperature

The temperature of a two component mixture, such as a nanofluid, depends on the temperature of the solid component as well as that of the host media. In a nanofluid the increase in temperature enhances the collision between the nano particles (Brownian motion) and the formation of nanoparticle aggregates (Li *et al.,* 2008a), which result in a drastic change in the thermal conductivity of nanofluids. Masuda *et al.* (1993) measured the thermal conductivity of water-based nanofluids consisting of Al_2O_3, SiO_2, and TiO_2 nanoparticles at different temperatures. It was found that thermal conductivity ratio decreased with increasing temperature. But the experimental results of others have been contradictory to this result. The temperature dependence of the thermal conductivity of Al_2O_3 /water and CuO/water nanofluids, measured by Das *et al.* (2003), have shown that for 1 vol.% Al_2O_3/water nanofluid, thermal conductivity enhanced from 2% at 21^0C to 10.8% at 51^0C. Temperature dependence of 4 vol. % Al_2O_3 nanofluid was much more significant, an increase from 9.4% to 24.3% at 51^0C. The investigations of Li *et al.* (2006) in CuO/water as well as Al_2O_3/water reveal that the dependence of thermal conductivity ratio on particle volume fraction get more pronounced with increasing temperature. In spite of these experimental results, the theoretical results based on Hamilton-Crosser model (1962) do not support the argument of any significant variation in thermal conductivity with temperature. Researchers have explained the enhancement in thermal conductivity with temperature in terms of the Brownian motion of particles since it increases the micro convection in nanoparticle suspensions.

1.2.7 Effect of sonication time

The ultrasonic vibration technique is the most commonly used technique for producing highly stable, uniformly dispersed nano suspensions by two step process. It has been found that the duration of the application of the ultrasonic vibration has a significant effect on the thermal conductivity of nanofluids (Hong *et al.,* 2006) since it helps to reduce the clustering of nanoparticles.

1.2.8 Effect of the preparation method followed

The enhanced heat transfer characteristics of nanofluids depend on the details of their microstructural properties like the component properties, nanoparticle volume fraction, particle geometry, particle dimension, particle distribution, particle motion, particle interfacial effects as well as the uniformity of dispersion of nanoparticles in host phase. So, the nanofluids employed in experimental research need to be well characterized with respect to particle size, size distribution, shape and clustering of the particles so as to render the results most widely applicable.

As per the application, either a low or high molecular weight fluid can be used as the host fluid for nanofluid synthesis. The dispersion of nanoparticles in a base fluid has been done either by a two step method or by a single step method. In either case, a well-mixed and uniformly dispersed nanofluid is needed for successful reproduction of properties and interpretation of experimental data. As the name implies the two step method involves two stages, first stage is the processing of nanoparticles following a standard physical or chemical method and in the second step proceeds to disperse a desired volume fraction of nanoparticles uniformly in the base fluid. Techniques such as high shear and ultrasound vibration are used to create uniform, stable fluid-particle suspensions. The main drawback of this technique

is that the particles will remain in an aggregated state even after the dispersion in host fluids. The single-step method provides a procedure for the simultaneous preparation and dispersion of nanoparticles in the base fluid.

Most of the metallic oxide nanoparticle suspensions are prepared by the two step method (Kwak *et al.,* 2005). The two step method works well for oxide nanoparticles as well, but it is not as effective for metallic nanoparticles such as copper. Zhu *et al.* (2004) developed a one step chemical method for producing stable Cu-in ethylene glycol nanofluids and have shown that the single step technique is preferable over the two step method for preparing nanofluids containing highly thermal conducting metals.

1.3 Experimental methods

As mentioned above, thermal conductivity is the most important parameter that decides the heat transfer performance of a nanofluid. Thus, researchers have tried to achieve higher enhancements in effective thermal conductivity of nanofluids by varying the nano particle volume fraction, nano particle size, nano particle shape, temperature, the host fluid type as well as the ultra sonication time required for preparing nanofluids. For all these measurements researchers have followed either a two step or a single step method for the preparation of nanofluids. They have employed experimental techniques such as the transient hot wire method (Hong *et al.,* 2005; Beck *et al.,* 2009) and the steady state method (Amrollahi *et al.,* 2008) for the measurement of the thermal conductivity of nanofluids. Other methods such as temperature oscillation method (Das *et al.,* 2003) and hot strip method (Vadasz *et al.,* 1987) are seldom used for thermal conductivity measurements. In all these methods the basic principles of measurement are the same, but differ in instrumentation

and measurement techniques followed. The salient features of each of these measurement techniques outlined below.

1.3.1 The Transient hotwire technique

The transient hot wire (THW) method to measure the thermal conductivity of nanofluids has got established itself as an accurate, reliable and robust technique. The method consists of determining the thermal conductivity of a selected material/fluid by observing the rate at which the temperature of a very thin platinum wire of diameter (5-80 μm) increases with time after a step voltage has been applied to it. The platinum wire is embedded vertically in the fluid, which serves as a heat source as well as a thermometer. The temperature of the platinum wire is established by measuring its electrical resistance using a Wheatstone's bridge, which is related to the temperature through a well-known relationship (Bentley *et al.,* 1984).

If *'i'* is the current following through the platinum wire and *'V'* is the corresponding voltage drop across it, then the heat generated per unit length of the platinum wire is given by,

$$q_l^* = iV/l \tag{1.1}$$

If T_1 and T_2 are the temperatures recorded at two times t_1 and t_2 respectively, the temperature difference (T_1-T_2) can be used to estimate the thermal conductivity using the relationship,

$$k = \frac{iV}{4\pi(T_2 - T_1)l}\left[\ln\left(\frac{t_2}{t_1}\right)\right] \tag{1.2}$$

where '*l*' is the length of the platinum wire.

The advantages of this method are its almost complete elimination of the effects of natural convection and the high speed of measurement compared to other techniques.

1.3.2 The steady state technique

In the steady state method (SSM), a thin layer of the fluid with unknown thermal conductivity is subjected to a constant heat flux. The layer has one dimension thickness very small compared to the other dimensions, so that the one-dimensional Fourier equation can be used to define the heat flow in the system. By measuring the temperature on both sides of this layer the thermal conductivity of the liquid can be determined. Many steady state thin layer experimental systems have been developed for the determination of thermal conductivity of fluids including nanofluids (Xuan *et al.,* 2000; Belleet and Sengelin 1975; Schrock and Starkman 1958). Among them the coaxial cylinders method is probably the best steady state technique for the determination of the thermal conductivity of nanofluids. The major advantages of this method are the simplicity of its design and the short response time of the measuring procedure. By this method the thermal conductivity measurement is possible with an accuracy of ±0.1%. This method is applicable to electrically conducting liquids as well as toxic and chemically aggressive substances. The apparatus built for measurements based on this technique include two coaxial aluminum cylinders with different diameters and lengths. The region between the two cylinders is filled with the liquid of unknown thermal conductivity. Both ends of the system are well insulated, ensuring no heat loss from the ends. An electrical heater is inserted at the middle of the inner cylinder, fitting well in the hole drilled for this purpose. Then the simultaneous recording of the

temperature of the layers is possible with the help of temperature sensors having high accuracy positioned on either side of the layer.

For a steady state situation the thermal conductivity of the fluid can then be evaluated using the equation (Xuan *et al.,* 2000),

$$k_f = q\frac{Ln(R_2/R_1)}{2\pi\ell(T_1 - T_2)} \tag{1.3}$$

Knowing the thermal conductivity k_{al} of aluminium cylinders which is estimated accurately to be 75 W m^{-1} K^{-1}, the thermal conductivity of the nanofluid can be determined following the equation (Xuan *et al.,* 2000),

$$q = k_{nf}\beta_1(T_1 - T_2) = k_{al}\beta_2(T' - T_1) \tag{1.4}$$

where β_1 and β_2 are the equipment shape factors, T' and T_1 are the temperatures on either side of the layer and the cylinder.

1.4 Theoretical models for thermal conductivity of nanofluids.

For the past one and half decades there has been a great deal of interest in understanding the anomalous enhancement in thermal conductivity observed in several types of nanofluids. This is mainly due to the fact that in several experimental results reported in literature, the observed enhancements in thermal conductivity are far more than those predicted by the well-established mean field models. Even in the case of the same nanofluid system, enhancements reported by different groups have shown wide differences. The conventional mean filed models such as the Maxwell-Garnett model, Hamilton-Crosser model as well as Bruggemann model were originally derived for solid mixtures and then to relatively large solid particle suspensions. But, these models have been derived from standard reference models for effective thermal conductivity of mixtures. Therefore, it is questionable whether these models are

able to predict the effective thermal conductivity of nanofluids. Nevertheless, these models are utilized frequently due to their simplicity in the study of nanofluids to compare theoretical and experimental values of thermal conductivity. In the following sections we briefly outline the salient features of the theoretical models widely used to explain the observed thermal conductivity of nanofluids. More detailed description of these models are presented and discussed in chapter 3.

1.4.1 Maxwell-Garnett model

Maxwell (1873) developed the first theoretical model for effective thermal conductivity of two component mixtures considering negligible interfacial resistance at the interface between the host phase and inclusions. This model defines the effective thermal conductivity of isotropic, linear, non-parametric mixtures with randomly distributed spherical inclusions. The inclusions are considered to be small compared to volume of the effective medium and are separated by distances greater than their characteristic sizes. Extension of this model to nanofluids expresses the thermal conductivity of nanofluids as an effective value of the thermal conductivities of the inclusions, and the base fluid, which takes the form (Maxwell, 1873)

$$k_{eff} = \frac{k_p + 2k_f + 2(k_p - k_f)\phi_v}{k_p + 2k_f - (k_p - k_f)\phi_v} \tag{1.5}$$

Here k_p is given by (Chen *et al.,* 1996)

$$k_p = \left(\frac{3a^*/4}{3a^*/4 + 1} \right) k_b \tag{1.6}$$

where k_{eff}, k_p and k_f are the thermal conductivities of the nanofluid, nanoparticles (in bulk) and the base fluid, respectively and ϕ_v is the volume fraction of

dispersed particles. It may be noted that the interaction between the particles is neglected in the derivation. As can be seen from the above expression, the effect of the size and shape of the particles are not included in the analysis.

More detailed descriptions of these models are available in literature (Maxwell, 1873; Das *et al.,* 2007)

1.4.2. Hamilton-Crosser model

Later, Maxwell model was modified for non-spherical inclusions by Hamilton and Crosser (Hamilton and Crosser, 1962). They expressed the effective thermal conductivity of a binary mixture by the expression,

$$k_{eff} = \frac{k_p + (n-1)k_f - (n-1)\phi_v(k_f - k_p)}{k_p + (n-1)k_p + \phi_v(k_f - k_p)} \tag{1.7}$$

where $n = \frac{3}{\psi}$ is the empirical shape factor, ψ being the sphericity of the dispersed particle. When n=3, Equation (1.7) reduces to the expression for effective thermal conductivity given by the Maxwell-Garnett model (Equation 1.5).

1.4.3 Bruggemann model

The two models outlined above have not considered the interaction between the inclusion phases. The model developed by Bruggeman, known as the Bruggeman model (Bruggeman, 1935), includes the interactions among the randomly distributed spherical inclusions in the host phase.

For a binary mixture of homogeneous spherical inclusions, the Bruggeman model gives an expression for effective thermal conductivity as,

$$k_{eff} = (3\phi_v - 1)k_p + [3(1-\phi_v) - 1)]k_f + \sqrt{\Delta} \tag{1.8}$$

where,

$$\Delta = (3\phi_v - 1)^2 k_p{}^2 + [3(1-\phi_v) - 1)]^2 k_f{}^2 + 2[2 + 9\phi_v(1-\phi_v)]k_p k_f \qquad (1.9)$$

Most of the experimental findings show that thermal conductivities of several nanofluids are far more than the values predicted by these mean field models. The mean field models failed to explain the following experimental findings,

(i) Nonlinear behavior that have appeared in effective thermal conductivity enhancements of nanofluids (Chopkar *et al.,* 2006; Li *et al.,* 2000; Kang *et al.,* 2006; Hong *et al.,* 2005; Jana *et al.,* 2007; Shaikh *et al.,* 2007; Xie *et al.,* 2002).

(ii) Effect of particle size and shape on thermal conductivity enhancements (Xie *et al.,* 2002; Chon *et al.,* 2005; Kim *et al.,* 2007; Li *et al.,* 2007 ;Chen *et al.,* 2008 ;Shima *et al.,* 2009).

(iii) Dependence of thermal conductivity enhancement on fluid temperature (Chopkar *et al.,* 2006; Li *et al.,* 2006; Chon *et al.,* 2005; Wen *et al.,* 2004).

So researchers tried to rennovate these conventional mean filed models by including other mechanisms like Brownian motion of nanoparticles (Jang and Choi, 2004), clustering of nanoparticles (Prasher *et al.,* 2006; Wang *et al.,* 2003), formation of liquid layer around the nanoparticles (Yu and Choi, 2003; Keblinski *et al.,* 2002), ballistic phonon transport in nanoparticles (Keblinski *et al.,* 2002), interfacial thermal resistance (Nan *et al.,* 1997; Vladkov and Barrat, 2006) etc. The following sections describe features of the various models based on these mechanisms.

1.4.4 Brownian motion of nanoparticles

Jang and Choi (2004) modeled the thermal conductivity of nanofluids by considering the effect of Brownian motion of nanoparticles. This model is based on the aspect that energy transport in a nanofluid consist of four modes; heat conduction in the base fluid, heat conduction in nanoparticles, collisions between nanoparticles and micro-convection caused by the random motion of the nanoparticles. Among these modes, the random motion of suspended nanoparticles, the so called Brownian motion, transports energy directly by nanoparticles. This model gives a general expression for effective thermal conductivity of nanofluids by combining the four modes of energy transport in nanofluids. Among the four modes of energy transport the first mode is the collision between base fluid molecules, which physically represents the thermal conductivity of the base fluid. Assuming that the energy carriers travel freely only over the mean free path l_{BF}, after which the base fluid molecules collide; the net energy flux J_U across a plane at z is given by (Kittel, 1969)

$$J_U = -\frac{1}{3} l_{BF} \hat{C}_{V,BF} \bar{C}_{BF} (1-\phi_v) \frac{dT}{dz} (1-\phi_v) = -k_{BF} \frac{dT}{dz} (1-\phi_v) \qquad (1.10)$$

where $\hat{C}_{V,BF}$, $\bar{C}_{BF}$, T are the heat capacity per unit volume, mean speed, and temperature of the base fluid molecules, respectively, and ϕ_v and k_{BF} are the volume fraction of nanoparticles and thermal conductivity of the base fluid.

The second mode is the thermal diffusion in nanoparticles embedded in fluids, the net energy flux J_U at z plane is given by,

$$J_U = -\frac{1}{3} l_{nano} \hat{C}_{V,nano} \bar{v} \phi_v \frac{dT}{dz} = -k_{nano} \frac{dT}{dz} \phi_v \qquad (1.11)$$

where k_{nano} and $\bar{v}$ are the thermal conductivity of the suspended nanoparticles and the mean speed of electron or phonon, respectively. The thermal conductivity of suspended nanoparticles involving the Kapitza resistance is given by (Keblinski *et al.,* 2002),

$$k_{nano} = \beta k_p \tag{1.12}$$

The third part of motion is the collision between nanoparticles due to Brownian motion. The nanoparticle collision in a fluid medium is a very slow process (Keblinski *et al.,* 2002); the contribution of this mode to thermal conductivity is much smaller than the other modes and can be neglected.

The last mode is the thermal interactions of dynamic or dancing nanoparticles with base fluid molecules. The random motion of nanoparticles averaged over time is zero. The vigorous and relentless interactions between liquid molecules and nanoparticles at the molecular and nano scales translate into conduction at the macroscopic level, because there is no bulk flow of matter. Therefore the Brownian motion of nanoparticles in nanofluids produces convection like effects at the nano scales. So the fourth mode can be expressed as,

$$J_U = h(T_{nano} - T_{BF})\phi_v = h\delta_T\phi_v \frac{(T_{nano} - T_{BF})}{\delta_T} \propto -h\delta_T\phi_v \frac{dT}{dz} \tag{1.13}$$

where h and δ_T are heat transfer coefficient for flow past nanoparticles and thickness of the thermal boundary layer, respectively.

Here $h \propto \frac{k_{BF}}{d_{nano}} \mathrm{Re}^2_{d_{nano}} \mathrm{Pr}_f^2$

Neglecting the effect of the third mode, we can write the expression for effective thermal conductivity of the nanofluid as,

$$k_{eff} = k_{BF}(1-\phi_v) + k_{nano}\phi_v + \phi_v h \delta_T \tag{1.14}$$

$$\delta_T = \frac{3d_{BF}}{\mathrm{P}_{rf}} \tag{1.15}$$

The proposed model is a function of not only thermal conductivities of the base fluid and nanoparticles, but also depends on the temperature and size of the nanoparticles. So Equation (1.14) can be modified for effective thermal conductivity of nanofluid as,

$$k_{eff} = k_f(1-\phi_v) + k_p{}^*\phi_v + 3C_1 \frac{d_f}{d_p} k_f \,\mathrm{Re}_d{}^2 \,\mathrm{Pr}_f \,\phi_v \tag{1.16}$$

C_1 is a proportionality constant, d_f is the diameter of fluid molecules, d_p is the diameter of the nanoparticle, P_{rf} is the Prandtl number of the base fluid, which represent the ratio of the viscous diffusion rate to thermal diffusion rate of the base media and $k_p{}^*$ is the thermal conductivity of the particle considering the interfacial thermal resistance known as the Kapitza resistance, 'β' is a constant and Re_d is the Reynold's number given by,

$$\mathrm{Re}_d = \frac{C_{R,M} d_p}{v_f} \tag{1.17}$$

where $C_{R,M}$ is the random motion velocity of nanoparticles and v_f is the kinematic viscosity of the base fluid. $C_{R,M}$ can be determined using the relation,

$$C_{R,M} = \frac{D_0}{l_{BF}} \tag{1.18}$$

where $D_0 = \dfrac{k_B T}{3\pi\mu_f d_p}$ is the nanofluid diffusion coefficient, where k_B is the Boltzmann constant, T is the temperature in K and μ_f is the dynamic viscosity of the base fluid. When the dependence of the model on nanoparticle size is

considered, it is seen that the thermal conductivity of nanofluid increases with decreasing particle size, since the decreasing particle size increases the effect of Brownian motion. In the derivation of this model, the thickness of the thermal boundary layer around the nanoparticles was taken to be equal to $3d_f / \mathrm{P_{r\,}}_f$ where d_f is the diameter of the base fluid molecule. As the volume fraction of nanoparticle increases, the effective thermal conductivity of nanofluids tend to increase with Brownian motion of nanoparticles since it depends on the volume fraction and temperature. There are many other studies that appeared in literature on the effect of Brownian motion on the thermal conductivity of nanofluids. But, the validity of this mechanism has been questioned by its room temperature dependence on thermal conductivity since this model describe the effective thermal conduction in nanofluids as an overall effect of micro convective heat transport through nanoparticles.

1.4.5 Effect of clustering of nanoparticles

This model is based on the phenomenon of clustering of nanoparticles (Prasher *et al.,* 2006; Wang *et al.,* 2003) in the host media; the formation of these particle clusters or aggregates of nanoparticles tend to enhance the thermal conductivity of nanofluids. The interconnected particle clusters, which grow as fractal structures, as reported by some authors (Wang *et al.,* 2003), form easy channels for thermal waves to propagate resulting in an overall enhancement in thermal conductivity and this mechanism of particle clustering increases with concentration of particles in the fluid. The theoretical expression for thermal conductivity of nanofluids by particle clustering has been worked out by previous workers (Prasher *et al.,* 2006; Wang *et al.,* 2003). The expression for the effective thermal conductivity of nanofluids with particle clusters takes the form (Prasher *et al.,* 2006),

$$k_{clust} = \left(\frac{([k_a + 2k_f] + 2\phi_a[k_a - k_f])}{([k_a + 2k_f] - \phi_a[k_a - k_f]} \right) k_f \tag{1.19}$$

where k_p is the single nanoparticle thermal conductivity and k_a is the thermal conductivity of the clustered nanoparticle, given by

$$k_a = (1 - \phi_{\text{int}}).k_f + \phi_{\text{int}}.k_p \tag{1.20}$$

where ϕ_a is the cluster volume fraction and ϕ_{int} is the volume fraction of the particles in a cluster $\phi_a = \frac{\phi_v}{\phi_{\text{int}}}$

Equation (1.19) implies that the effective thermal conductivity of nanofluids increases with increase in cluster size. Evans *et al.* (2008) proposed that clustering can result in fast transport of heat over relatively large distances since the heat can be conducted much faster by solid particles when compared to the liquid matrix. They investigated the dependence of thermal conductivity of nanofluids on clustering and interfacial thermal resistance and have shown that the effective thermal conductivity increases with increasing cluster size. However, as the particle volume fraction increases, the nanofluid with clusters show relatively smaller thermal conductivity enhancement. When it comes to interfacial resistance, it is found that the interfacial resistance decreases with the enhancement in thermal conductivity, but this decrease diminishes for nanofluids with large clusters.

According to previous reports the nanoparticle clusters increase the effective thermal conductivity of nanofluids, but the enhancement due to clustering at higher particle concentrations is questioned by phenomena like sedimentation of clustered nanoparticles.

1.4.6 Formation of semisolid layer around nanoparticles

It has been speculated that (Yu and Choi 2003; Keblinski *et al.,* 2002) molecules of the base fluid form a semi-solid layer around the nanoparticles by the adsorption of the base fluid molecules. This ordered semi-solid layer, which has a higher thermal conductivity than the base fluid, increases the effective particle volume fraction and hence the effective thermal conductivity of the nanofluid. Thickness of this adsorption layer is given by Langmuir formula (Li *et al.,* 2008; Yan *et al.,* 1986).

$$t = \frac{1}{\sqrt{3}}\left(\frac{4M}{\rho_f N_A}\right)^{1/3} \tag{1.21}$$

where 'M' is the molecular weight and ρ_f is the mass density of the fluid. N_A is the Avagadro's number.

As per Langmuir formula the thickness of the adsorption layer is found to be of the order of 10^{-9}m for a liquid like water. Yu and Choi (2003) modified the Maxwell (1873) model including the effect of liquid layering around nanoparticles and assumed some possible values for the thermal conductivity of the nanolayer. This model considered the nanoparticle with liquid layer as a single particle and the thermal conductivity of this particle was determined following effective medium theory. This renovated Maxwell model gives the effective thermal conductivity of a nanofluid as

$$k_{eff} = \frac{k_{pe} + 2k_f + 2(k_{pe} - k_f)(1+\beta)^3\phi_v}{k_{pe} + 2k_f - (k_{pe} - k_f)(1+\beta)^3\phi_v} k_f \tag{1.22}$$

Here k_{pe} is the thermal conductivity of the layered nanoparticle, given by

$$k_{pe} = \frac{[2(1-\gamma) + (1+\beta^3)(1+2\gamma)]\gamma}{-(1-\gamma) + (1+\beta)^3(1+2\gamma)} k_p \tag{1.23}$$

where $\gamma = \frac{k_l}{k_p}$ where k_l is the thermal conductivity of the nanolayer, and β is a constant defined as $\beta = \frac{t}{r_p}$, where r_p is the radius of the particle and t is the thickness of adsorption layer given by Equation (1.21).

In addition to this, Yu *et al.* (2004) modified the Hamilton-Crosser model (1962) for non spherical particle suspensions by considering the adsorption effect on nanoparticle surfaces.

Wang *et al.* (2003) have presented another expression for effective thermal conductivity of nanofluids based on particle clustering and the surface adsorption effects of nanoparticles. According to this model the effective thermal conductivity of clustered particle-fluid suspension is given by,

$$\frac{k_{eff}}{k_f} = \frac{(1-\phi_v) + 3\phi_v \int_0^\infty \frac{k_{cl}(r)n(r)}{k_{cl}(r)+2k_f} dr}{(1-\phi_v) + 3\phi_v \int_0^\infty \frac{k_f(r)n(r)}{k_{cl}(r)+2k_f} dr} \tag{1.24}$$

where *n(r)* is the radius distribution function given by,

$$n(r) = \frac{1}{r_{cl}\sqrt{2\pi}\ln\sigma} \exp\left\{ -\left[\frac{\ln(r_{cl} / \bar{r}_{cl})}{\sqrt{2\pi}\ln\sigma} \right]^2 \right\} \tag{1.25}$$

and k_{cl} is the equivalent thermal conductivity of the cluster, which can be determined by replacing ϕ_v by ϕ_v^* in the thermal conductivity expression given by Bruggeman model and k_{cl} can be written as,

$$k_{cl} = (3\phi_v^* - 1)k_p + [3(1-\phi_v^*) - 1]k_f + \sqrt{\Delta} \tag{1.26}$$

where

$$\Delta = (3\phi_v^* - 1)^2 k_p{}^2 + [3(1-\phi_v^*) - 1]^2 k_f{}^2 + 2[2 + 9\phi_v^*(1-\phi_v^*)]k_p k_f \quad (1.27)$$

and ϕ_v^* is given by,

$$\phi_v^* = (r_{cl} / r_p)^{d_f - 3} \quad (1.28)$$

Here r_{cl} is the radius of the clustered nanoparticle and r_p is the thermal conductivity of the bare nanoparticle and d_f is the fractal dimension having values in the range 1.8 - 2.2.

While considering the effect of liquid layering the k_p in the above expression have to be replaced with k_{cp}, the thermal conductivity of the layered nanoparticle, and is given by

$$k_{cp} = k_l \frac{(k_p + 2k_l) + 2A^3(k_p - k_l)}{(k_p + k_l) - A^3(k_p - k_l)} \quad (1.29)$$

where k_l is the thermal conductivity of the adsorption layer and $A = 1 - t/(t+a)$, and r_p is replaced by (r_p+t) and ϕ_v by $\left(\frac{r_p + t}{r_p}\right)^3 \phi_v$. The main drawback of the above mechanism is that there is no experimental data available on the thickness and thermal conductivity of the adsorbed nanolayers, which raise serious questions about the validity of the model.

1.4.7 Models based on interfacial thermal resistance

According to researchers, various mechanisms described above are responsible for enhancement in the effective thermal conductivity of nanofluids, and all the models based on these have been derived without considering the interfacial effects at fluid-particle boundaries. If these effects are taken into

account it has been found that there is a possibility for de-enhancement in effective thermal conductivity of nanofluids. Xuan *et al.* (2003) and Koo *et al.* (2004) have modified the Maxwell-Garnett model in order to arrive at an expression for effective thermal conductivity of nanofluids in this regime. By performing molecular dynamics simulation Vladkov and Barratt (2004) have developed an expression for effective thermal conductivity of nanofluids considering the effects such as interfacial thermal resistance (Kapitza resistance) at the nanoparticle-fluid interface and Brownian motion heat transfer between the particles and fluid molecules.

The expression for effective thermal conductivity in this regime can be written as,

$$\frac{k_{eff}}{k_f} = \frac{(\frac{k_p}{k_f}(1+2\alpha)+2)+2\phi_v(\frac{k_p}{k_f}(1-\alpha)-1)}{(\frac{k_p}{k_f}(1+2\alpha)+2)-\phi_v(\frac{k_p}{k_f}(1-\alpha)-1)} \tag{1.30}$$

where $\alpha = {R_k k_f}/{r_p}$, R_k being the Kapitza resistance. This model predicts an enhancement in effective thermal conductivity of nanofluids for α >1, and a decrease for α <1 .This is because of the effective increase in Kapitza resistance due to scattering of thermal waves at the solid-liquid interfaces, which is determined by the value of α.

Nan *et al.* (1997) generalized the Maxwell –Garnett model, considering the interfacial thermal resistance at the fluid-particle boundary which arises due to the scattering of thermal waves at the interfaces. According to this model the normalized thermal conductivity of nanofluids having particles shaped as prolate spheroids with principal axes $a_{11}=a_{22} < a_{33}$, take the form,

$$\frac{k_{eff}}{k_f} = \frac{3+\phi_v[2\beta_{11}(1-L_{11})+\beta_{33}(1-L_{33})]}{3-\phi_v(2\beta_{11}L_{11}+\beta_{33}L_{33})} \tag{1.31}$$

where,

$$\left.\begin{aligned} L_{11} &= \frac{p^2}{2(p^2-1)} - \frac{p}{2(p^2-1)^{3/2}}\cosh^{-1} p, \\ L_{33} &= 1-2L_{11}, p = a_{33}/a_{11} \\ \beta_{ii} &= \frac{k_{ii}-k_f}{k_f + L_{ii}(k_{ii}^{\,c}-k_f)}, \\ k_{ii} &= \frac{k_p}{1+\gamma L_{ii}k_p/k_f} \\ \gamma &= (2+1/p)R_{bd}k_f/(a_{11}/2) \end{aligned}\right\} \tag{1.32}$$

Here R_{bd} is the Kapitza interfacial thermal resistance.

1.4.8 Model based on Ballistic phonon transport in nanoparticles

In nanoparticles the diffusive heat transport is valid if the mean-free path of phonons is smaller than the characteristic size of the particle under consideration. In a nanoparticle if the diameter is less than the phonon mean free path, the heat transport is not diffusive, but is rather ballistic. This fact prevents the application of conventional theories for modeling the thermal conductivity of nanofluids. Keblinski *et al.* (2002) noted that ballistic heat transport still cannot explain the anomalous thermal conductivity enhancements, because temperature inside the nanoparticles is nearly constant and this fact does not depend on the mode of heat transfer.

1.4.9 Summary of theoretical models

The above are the commonly used theoretical models developed by previous authors to interpret the observed thermal conductivity enhancements

in nanofluids. In order to get the best fitting with experimental results some authors have also tried different combinations of the above mechanisms (Xuan *et al.,* 2003; Koo *et al.,* 2004) and defined the effective thermal conduction in nanofluids as a combined effect of two or more mechanisms. But these mechanisms have faced inadequacies to interpret the wide variations in the experimental data reported in literature since there often exist physically unrealistic situations with these proposed mechanisms. Table I summarizes some of the experimental data of nanofluid thermal conductivity reported by previous authors and their deviations from the proposed theoretical models based on the Brownian motion of nanoparticles, clustering effects of nanoparticles and other effects. In association to the Brownian motion of nanoparticles, the main question is about the possibility of micro convection of nanoparticles at room temperature. So the temperature dependence of Brownian motion as well as its influence on clustering of nanoparticles need to be verified with experimental data.

Other models based on mechanisms such as formation of nanolayer around the nanoparticles also are found to be limited to resolve the inconsistencies of the experimental results. The main problems that arise with these models are

(i) The variation of the thickness of the adsorption layer with nanoparticle size couldn't be predicted.

(ii) There is no experimental data available in literature on the thermal conductivity of the adsorbed nanolayer.

(iii) The very existence of a semisolid monolayer is questionable.

Table 1 presents a summary of the experimental findings reported by previous authors for various nanofluids and the corresponding mechanisms proposed for each. The wide differences in the experimental results that have appeared in the case of the same nanofluid system increases the depth of the issues involved. The main reason for the observed controversies may be due to the differences in the experimental techniques employed, differences in sample preparation methods, variations in particle sizes etc.

Recently, an elaborate inter-laboratory comparison initiated by International Nanofluid Property Benchmark Exercise (INPBE) done by 34 organizations across the world has been published (Buongiorno *et al.,* 2009). This has helped to resolve some of the outstanding issues in this field. In this exercise different research groups have measured thermal conductivity of identical samples of colloidal stable dispersions of nanoparticles using different experimental techniques such as transient hot wire technique, steady state technique and optical methods.

The samples tested in the INPBE exercise comprised of aqueous and nonaqueos base fluids, metal and metallic oxide particles, spherical and cylindrical particles at low and high particle concentrations. The main conclusions drawn from the exercise are the following.

(i) The thermal conductivity of nanofluids increases with increasing particle loading as well as the aspect ratio of the dispersed particles, which is in tune with the classical effective medium theory, originally proposed by Maxwell (1873)

Table 1.1 Summary of experimental findings and corresponding models for thermal conductivity of nanofluids

Citation to Experimental methods	Nanofluid type	Particle Volume fraction ϕ_v (%)	Particle size (nm)	Max. Enhancement (%)	Consistency/in-consistency with the proposed mechanisms	Details of analysis
Masuda *et al.,* (1993)	Al_2O_3 -Water SiO_2- Water TiO_2- Water	1.30–4.30 1.10–2.40 3.10–4.30	13 12 27	32.4 1.1 10.8	Inconsistent with Brownian motion of nanoparticles	2-step 31.85–86.85^{0}C
Lee *et al.,* (1999)	Al_2O_3-Water/EG CuO- Water/EG	1.00-4.30/1.00-5.00 1.00-3.41/1.004.00	38.4 23.6	10/18 12/23	Inconsistent with mean field models	2-step (THW) Room temperature
Wang *et al.,* (1999)	Al_2O_3/Water/EG Al_2O_3/EO/PO CuO/Water/EG	3.00–5.50/5.00–8.00 2.25–7.40/5.00–7.10 4.50–9.70/6.20–14.80	28 28 23	16/41 30/20 34/54	Inconsistent with mean field models	Room temperature (SSM)
Eastman *et al.,* (2001)	Cu -EG	0.01–0.56	<10	41	Inconsistent with mean field models	2-step (THW) Room temperature1.5 % error
Xie *et al.,* (2002a)	SiC/Water/EG SiC/Water/EG	0.78–4.18/0.89–3.501.00–4.00	26 sphere 600 cylinder	17/13 24/23	Consistent with H-C models	Effect of particle shape and size is Examined (THW)
Xie *et al.,* (2002b)	Al_2O_3 Water/EG Al_2O_3 /PO/glycerol	5.00 5.00	60.4 60.4	23/29 38/27	Consistent with H-C model	Room temperature & effect of base fluid verified (THW)
Das *et al.,* (2003)	Al_2O_3/ Water CuO/ Water	1.00–4.00 1.00–4.00	38.4 28.6	24 36	Consistent with H-C model	21–51 ^{0}C The dependence of temperature Verified 2-step
Murshed *et al.,* (2005)	TiO_2 /Water TiO_2/ Water	0.50–5.00 0.50–5.00	15 sphere 10 x 40 rod	30 33	Consistent with H-C model	Room temperature 2-step (THW)
Hong *et al.,* (2006)	Fe/ EG	0.10–0.55	10	18	Consistent with Brownian motion of nanoparticle	Effect of clustering was investigated (THW)
Li and Peterson (2006)	Al_2O_3/ Water CuO /Water	2.00–10.00 2.00–6.00	36 29	29 51	Inconsistent with mean field models	27.5–34.7 ^{0}C 28.9–33.4 ^{0}C (temperature oscillation technique)
Chopkar *et al.,* (2008)	Al_2Cu /Water/EG Ag_2Al/ Water/EG	1.00–2.00 1.00–2.00	31/68/101 33/80	96/76/6 106/93	Inconsistent with mean field models	Effect of particle size was

						examined
Citation to Experimental methods	Nanofluid type	Particle Volume fraction $\phi_v(\%)$	Particle size (nm)	Max. Enhancement (%)	Consistency/in-consistency with the proposed mechanisms	Details of analysis
Beck *et al.,* (2009)	Al_2O_3/ Water	1.86–4.00	8–282	20	Inconsistent with mean field models	Effect of particle size was examined (THW)
Mintsa *et al.,* (2009)	Al_2O_3/ Water CuO /Water	0–18 0–16	36/47 29	31/31 24	Inconsistent with Brownian motion of nanoparticles	20–48 ^{0}C
Turgut *et al.,* (2009)	TiO_2 /Water	0.2–3.0	21	7.4	Inconsistent with Brownian motion of nanoparticles	13–55 ^{0}C
Choi *et al.,* (2001)	MWCNT/ PAO	0.04–1.02	25 x50000	57	Inconsistent with mean field models	Room temperature (THW)
Assael *et al.,* (2005)	DWCNT /Water MWCNT /Water	0.75–1.00 0.60	5 (diameter) 130 x 10000	8 34	Consistent with clustering effect	Effect of sonication time was examined
Liu *et al.,* (2005)	MWCNT -EG/EO	0.20–1.00/1.00–2.00	20 ~ 50 (diameter)	12/30	Consistent with mean field models	Room temperature & base fluid effect was examined

(ii) At least for the samples tested in the exercise, there is no anomalous enhancement of thermal conductivity as reported by previous workers. The observed variations are within the limits set by the respective measurement techniques.

(iii) The measurement technique such as THW found to possess an error up to 3% and the preparation techniques followed for nanofluid synthesis also affects the overall thermal conductivity.

The overall of conclusion of the INPBE is that the reports on anomalous thermal conductivity reported by previous authors are experimental artifacts.

Even though the INPBE resolved the general controversies on the effective thermal conductivity enhancement as mentioned above, the effect of

particle size on the thermal conductivity of nanofluids has not been completely understood yet. It is expected that the Brownian motion of nanoparticles result in higher thermal conductivity enhancement with decreasing particle size. However, some of the experiments show that thermal conductivity decreases with decreasing particle size. The controversial reports on this aspect could be due to the formation of nanoparticle clusters. There are many more issues about which the INPBE exercise is silent about.

Particle size distribution is another important parameter that controls the thermal conductivity of nanofluids. Most of the standard characterization techniques give the average particle size in a sample and it is suggested that average particle size is not sufficient to characterize a nanofluid due to the nonlinear relation between particle size and thermal transport. It is also noted that particle shape is effective on the thermal conductivity of nanofluids since the rod shaped particles offer higher thermal conductivity than spherical ones. More systematic investigations need to be made on this aspect to resolve the outstanding issues. Temperature dependence is another important parameter while discussing the thermal conductivity of nanofluids. Since only limited studies have done on this aspect, more investigations on thermal performance of nanofluids at higher temperatures have to be done, which may broaden the applications of nanofluids.

Even though a large number of theoretical models have been developed to resolve the controversies on the various experimental results available on the thermal conductivity of nanofluids, none of them does satisfactorily explain the dependence of micro structural characteristics of nanoparticles as well as the temperature on effective thermal conductivity of nanofluids. More systematic experimentation as well as theoretical modeling are needed to understand the thermal transport mechanisms in a nanofluid completely.

1.5 Work presented in this thesis

Most of the work done so far on nanofluids has been on nanofluids prepared with low molecular weight base fluids such as water, oil, ethylene glycol etc., which are the common heat transfer fluids used in industries. Since a great deal of physics has emerged on the mechanisms of thermal conductivity in such nanofluids, it is interesting to investigate thermal properties of nanofluids prepared with high molecular weight base fluids, such as polymeric fluids. Another interesting aspect is that polymeric nanofluids can be condensed to form the corresponding solid nanosolids. This opens up the possibility of investigating thermal properties of such condensed nanofluids or nanosolids. It is interesting to investigate the physics involved in the mechanism and suggest possible applications for such materials.

In the present work we had tried to investigate the validity of some mechanisms proposed to be responsible for observed thermal conductivity enhancements in polymeric nanofluids and extended the studies to their solid counterpart. We have carried out the measurement of the relevant thermal properties of such nanofluids to understand the role of mechanisms like interfacial thermal wave scattering at nanoparticle-matrix boundaries.

In order to study the thermal conduction in polymeric nanofluids we prepared two sets of polymer based nanofluids, TiO_2/ PVA (*) and Copper/ PVA (**) and measured the thermal diffusivity following a thermal wave interference technique. The nanofluid preparation was done following a two step method.

The thermal diffusivity of the prepared nanofluids has been measured in a Thermal Wave Resonant Cavity (TWRC) cell, which works based on thermal wave interference. We varied the concentration of nanoparticles as well as the dispersed particle size to study the overall variation in effective thermal

conduction in nanofluids. As a result we obtained enhancements in the normalized thermal conductivity/diffusivity for TiO_2/PVA and Cu/ PVA nanofluids. It has been found that the effective thermal conductivity of polymeric nanofluids decreases with increasing nanoparticle size. In order to define the effective thermal conduction in polymeric nanofluids we have followed appropriate theoretical models for effective thermal conductivity proposed by previous workers.

In addition to the above, measurements have been carried out and theoretical calculations done for TiO_2 /water and Cu/water nanofluids as well for completeness. The variations of thermal conductivity/diffusivity obtained with variations in particle volume fractions are in tune with the mean field theory. For these samples also no deenhancement of any kind in thermal conductivity or diffusivity at low particle volume fractions has been obtained.

As a second part of the work we have extended the studies to the condensed state of nanofluids and investigated the respective variations in effective thermal conductivity of condensed nanofluids, or the corresponding nanosolids, with concentration of nanoparticles. The main goal of this study has been to achieve tunability in thermal properties of nanosolids from negative to positive with respect to base fluid value. Then we carried out the thermal conductivity measurements on these condensed samples following the photopyroelectric (PPE) technique. We have measured the variations of the normalized thermal conductivity as a function of concentration for the two sets of samples, TiO_2/PVA and Cu/PVA.

For the TiO_2/ PVA nanosolid system the normalized thermal conductivity is found to decrease with particle volume fraction in the beginning and then it increases. In the case of Cu/ PVA nanocomposite system the variation of thermal conductivity with particle volume fraction is opposite to

*TiO_2 nanoparticles dispersed in PolyVinyl Alcohol
**Copper nanoparticles dispersed in PolyVinyl Alcohol

that for TiO_2/PVA system. Up to about 4% increases in nanoparticle concentration, the thermal conductivity of the nanosolid increased by a small value (about 7%). This increase in thermal conductivity has been attributed to the high thermal conductivity of copper nanoparticles. In order to explain our experimental results, we developed at a theoretical expression for effective thermal conductivity and diffusivity of nanosolids by combining ideas from models proposed by previous authors.

From the present work we have concluded that for low molecular weight nanofluids thermal conduction is controlled by the diffusion of thermal waves while in polymeric nanofluids mechanisms of interfacial conduction and diffusion of thermal waves decide the overall thermal conductivity nanofluids. From the experimental studies it is found that it is possible to tune the thermal conductivity of polymeric nanofluids and their solid counterparts by dispersing them with appropriate nanoparticles in desired concentrations. The tunability range can be varied from negative to positive with a proper choice of nonmetallic or metallic nanoparticles and their concentrations. Further work with other base fluids and nanoparticles is necessary to evaluate the commercial viability of this class of materials.

Chapter 2

Experimental Methods

2.1 Introduction

The characterization of a material involves the determination of its characteristic physical properties following established experimental techniques under known conditions. Generally the word characterization stands for analysis of the structural (material identification) as well as characteristic physical properties of a material. Generally material identification or structural analysis are done in crystalline materials for the identification of the type of constituent phases, identification of unit cell dimensions, surface morphology, grain sizes etc. In addition, the determination of characteristics physical properties and the relevant physical constants or variables of the sample are carried out. By performing characterization of a material, various physical and chemical properties of a material can be identified and determined, which are important for its applications in technology.

The main goal of the work presented in this thesis is the thermal characterization of selected polymeric nanofluids and the corresponding nanosolids prepared in the laboratory. In this chapter we discuss the principles and methods of the different experimental techniques we have followed for the characterization of the prepared nanofluids and nanosolids. The characterization methods described in the present work starts with the techniques adopted for the preparation of nanoparticles, which are the prime components for the preparation of nanofluids and nanosolids. These nanoparticles determine the

effective thermal properties of these materials. Normally the structural identification and material analysis of these special material composites are done by standard characterization techniques such as Powder X-ray Diffraction (XRD), Scanning Electron Microscopy (SEM), Transmission Electron Microscopy (TEM) etc.

The characteristic thermal properties such as thermal diffusivity, thermal conductivity and specific heat capacity of the prepared polymeric nanofluids and nanosolid samples have been determined by a set of photothermal techniques; the thermal wave interference technique using a thermal wave resonant cavity (TWRC) (Shen and Mandelis, 1996), Photopyroelectric technique (PPE) (Menon and Philip, 2000), Photoacoustic (PA) technique (Madhusoodanan *et al.,* 1987) etc. A homemade thermal wave resonant cavity (Shen and Mandelis, 1996) is used to measure the thermal diffusivity of the prepared nanofluid samples. A TWRC cell works on the principle of thermal wave interference occurring in a thermal wave resonant cavity. The other photothermal techniques are based on photopyroelectric (Mandelis, 1985) and photoacoustic (Rosenswaig, 1980) effects and these have been used for the measurement of thermal properties such as thermal conductivity, thermal diffusivity, and specific heat capacity of the condensed nanosolid materials. The common principle of these two techniques is the detection of the temperature fluctuations in a sample due to the absorption of intensity modulated electromagnetic radiation by the sample. Detailed descriptions of the various measurement techniques that we have followed to determine the characteristic as well as thermal properties of the nano material based samples (liquids and solids) are described in the following sections.

2.2 Standard characterization techniques

The thermophysical properties of materials are determined by their micro structural characteristics such as structure and chemical composition of the constituent phases. While downscaling a material into nanoparticles with dimensions in nano meter ranges, these characteristic properties show a wide difference from its respective bulk form due to the differences in the number of constituent atoms and their spatial distribution in crystal lattices. So the synthesis and characterization of nanomaterials are the first and foremost steps in experimental research on nano materials. The synthesis of nano materials is usually done following physical or chemical routes. Proper selection of synthesis parameters and procedures for a nano material and the appropriate characterization techniques help to carry out evaluation of its desired properties and potential applications. The standard characterization techniques include techniques adopted to determine properties like particle size, particle shape, microstructure etc. by experimental techniques under standard conditions. There exist several advanced and sophisticated techniques for structural and morphological characterization of nanocrystalline materials. In this work we have followed some of the well known techniques for the structural characterization of the nano crystalline materials and nanosolids.

We have employed characterization techniques like powder X-ray diffraction technique and Scanning Electron Microscopy for material identification and structure analysis of the prepared nanoparticles. In addition to these, standard thermal analysis technique like differential scanning calorimetry has been used for the evaluation of specific heat capacity of the prepared nanomaterials. The principle and methodology of these measurement techniques are described in the following sections.

2.2.1 Powder X-Ray diffraction technique

Most of the nanostructures are essentially crystalline particles characterized by a large value for the ratio of the number of surface atoms to interior atoms. Most of the interesting properties of nanomaterials are brought about by the large number of surface atoms in the particle material.

The powder X-ray diffraction technique (XRD) is a general technique used for the determination of crystal structures and atomic spacing. This technique is based on Bragg's law of diffraction of X-rays from different symmetry planes of a crystal. The regular arrangement of atoms along the cleavage planes of a crystal act as grating elements which diffract X-rays. The Bragg's law of diffraction relate the wavelength (λ) of the incident X-ray radiation with inter planar spacing (*d'*) in a crystal. According to this law the constructive interference in the diffraction pattern is obtained only when the interfering reflected rays satisfy the condition,

$$2d' \sin\theta = n\lambda \qquad (2.1)$$

where θ is the angle of diffraction.

In the present studies we have used a Bruker AXS D8 Advance X-ray Powder diffractometer to identify the structure and estimate the average size of the nanocrystalline particles. Identification of the phases of the nanocrystalline samples are done by scanning the sample through a range of angles of incidence 2θ for X-rays. Then, at each of the incident angles, the diffracted rays are detected, processed and analyzed. Here all the possible directions of diffraction are obtained by the random orientation of the powdered material; conversion of the diffraction peaks into *d*-spacing identifies a crystalline material since each

material has a set of unique *d*-spacing. Typically, this is achieved by comparison of *d*-spacing with standard reference patterns.

The thickness *(t)* of a thin crystalline sample or the approximate sizes of nanoparticles can be evaluated from an X-ray diffraction peak (Cullity, 1978), as outlined below.

Consider a nano crystal having size *(t)* composing of *(m+1)* crystalline planes. Let X-rays be incident on adjacent crystalline planes at angles θ_1, θ_2… θ_m. The constructive and destructive interference occurring in this entire crystal lattice produces an intensity variation shown in Figure 2.1.

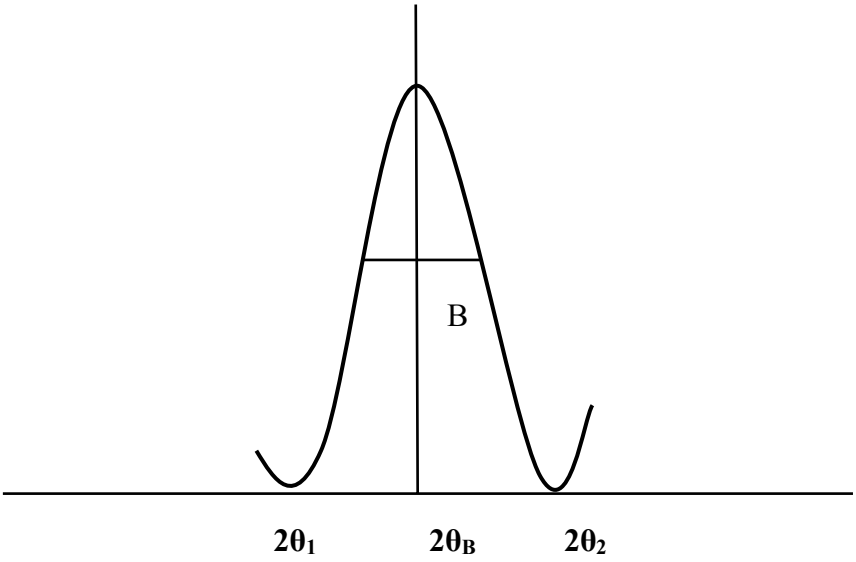

Figure 2.1 A typical X-ray diffraction pattern from a crystal

Here $2\theta_1$ and $2\theta_2$ are the diffraction angles at which the intensity of the diffracted beams drop down to zero. The width of the diffraction peak increases as the thickness of the crystal decreases because the angular range $(2\theta_1\text{-}2\theta_2)$ increases as *m* decreases. Here the width of the curve *B* is usually measured in radians, at intensity equal to half the maximum intensity. As a rough measure of

B, we can take half the difference between the two extreme angles at which the intensity is zero, which amounts to assuming that the diffraction peak is triangular in shape. Therefore,

$$B = \frac{1}{2}(2\theta_1 - 2\theta_2) = \theta_1 - \theta_2 \qquad (2.2)$$

As with Equation (2.1), now we write the path difference for these two angles as related to the entire thickness of the crystal rather than to the distance between adjacent planes:

Therefore

$$2t \sin \theta_1 = (m + 1)\lambda$$

$$2t \sin \theta_2 = (m - 1)\lambda$$

By subtraction we find

$$t(\sin \theta_1 - \sin \theta_2) = \lambda$$

Here $\theta_1 \approx \theta_2 \approx \theta_B$, so that $2t\cos\left(\frac{\theta_1 + \theta_2}{2}\right)\sin\left(\frac{\theta_1 - \theta_2}{2}\right) = \lambda$

$$\theta_1 + \theta_2 \approx 2\theta_B$$

and

$$\sin\left(\frac{\theta_1 - \theta_2}{2}\right) = \left(\frac{\theta_1 - \theta_2}{2}\right)$$

$$\therefore \quad 2t\left(\frac{\theta_1 - \theta_2}{2}\right)\cos\theta_B = \lambda$$

Simplification of this equation gives,

$$t \approx \frac{0.9\lambda}{B\cos\theta_B} \tag{2.3}$$

This equation is known as Debye-Scherrer formula, is generally used to estimate nanoparticle sizes.

2.2.2 Scanning Electron Microscopy (SEM)

The scanning electron microscopy is a widely used technique to visualize and analyze the surface morphology and micro structural characteristics of materials (Muralidharan and Subrahmania, 2009).

The scanning electron microscope (SEM) uses a focused beam of high energy electron beam to generate a variety of signals at the surface of solid specimens. The signals that are derived from electron-sample interactions reveal information about the sample including surface morphology (texture), chemical composition, crystalline structure and orientation of the constituent material particles of a sample. This instrument images a sample by scanning it with high energy electrons following a raster scan method. In most of the applications the data are collected over a selected area of the surface of the sample, and a 2D image is generated that displays spatial variations in the surface properties of a material. In SEM, a specimen is irradiated by an electron beam and data on the specimen are delivered by secondary electrons emitted from the surface layer of thickness ~ 5nm and by backscattered electrons emitted from the volume of linear size ~ 0.5μm. Due to its high depth of focus SEM is frequently used for studying fracture on material surfaces.

In a scanning electron microscope, a high energetic accelerated electrons interact with a sample and produce signals corresponding to ejected secondary

electrons (that produces SEM images), back scattered electrons (BSE), diffracted back scattered electrons (EBSD-that are used to determine the crystal structures and orientation of minerals), characteristic X-rays, electromagnetic radiation and heat. SEM analysis is considered to be non-destructive, because the X-rays generated due to electron beam - sample interaction do not lead to any volume loss in the sample. The electrons emitted from the sample are detected to form a magnified image which allows the examination of the structure and morphology of the materials surface. In this work we have employed a scanning electron microscope (JEOL Model JSM - 6390LV) having an image resolution of ~ 3nm at an accelerating electron voltage of 30kV.

2.2.3 Differential Scanning Calorimetry (DSC)

Differential scanning calorimetry is an instrumental method for the measurement of changes in enthalpy of a sample as the sample temperature is varied. In differential scanning calorimetry (DSC), the sample material is generally subjected to a linear temperature program, and the heat flow rate into the sample is continuously measured; this heat flow rate is proportional to the instantaneous specific heat of the sample (O'Neill *et al.*, 1964; Waston *et al.,* 1964). Two sample holders are mounted symmetrically inside an enclosure which is normally held at room temperature. A primary temperature control system controls the average temperature of the two sample holders, using platinum resistance thermometers and heating elements embedded in the sample holders. A secondary temperature control system measures the temperature difference between the two sample holders, and adjusts this difference to zero by controlling a differential part of the total heating power. This differential power is measured and recorded. The plot of the variation of the differential power with the programmed temperatures is known as the DSC curve. In this

work we have used a Differential Scanning Calorimeter, Make Metler-Toledo, Model 822^e, for some of the measurements.

In order to measure the specific heat capacity (c_p) of an unknown sample having a known mass (m), the DSC curve is plotted with and without sample (baseline). Comparison of these heat flow rates with that of a standard reference material with known specific heat capacity (c_p') with known mass (m') (ratio method), gives the specific heat capacity of the unknown sample. Figure 2.2 shows a set of typical DSC curves, which can be used to measure the specific heat capacity of an unknown sample. Here the baseline is the DSC curve obtained without any sample in the sample pans.

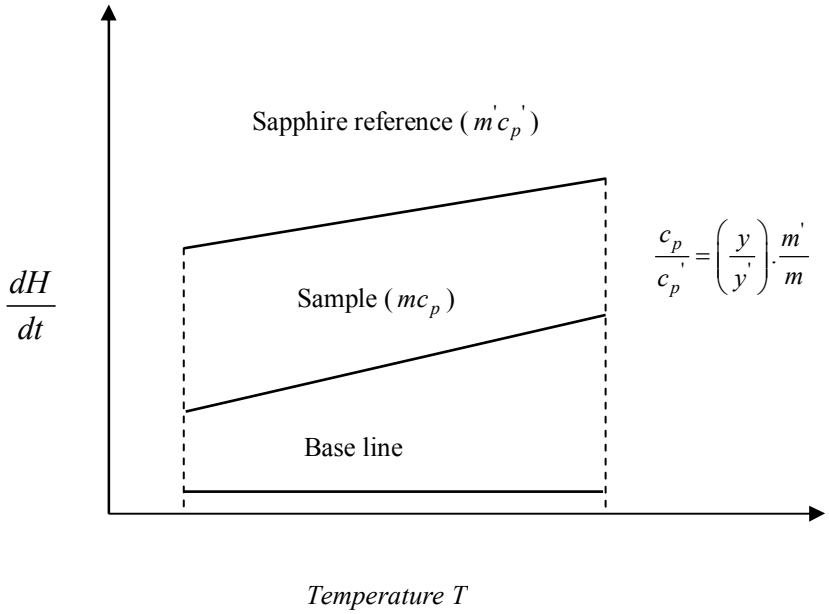

Figure 2.2 A typical DSC curves used for the specific heat capacity measurement of an unknown sample following ratio metric method

Here the rates of heat flow into the sample and reference materials can be written as,

$$\frac{dH}{dt} = y \quad = c_p m \frac{dT}{dt} \tag{2.4}$$

$$\frac{dH'}{dt} = y' = c_p' m' \frac{dT}{dt} \tag{2.5}$$

For the simplicity of the calculation here we have assumed that $m = m'$, so the specific heat capacity of the sample is given by,

$$\frac{c_p'}{c_p} = \frac{my'}{m'y} \tag{2.6}$$

Generally sapphire is used as the reference material in these measurements. The thermal properties of the nanofluid and nanosolid samples investigated in this work have been analyzed following the DSC technique. In certain cases the heat capacities of the samples has been determined by the ratio method, as outlined above.

2.3 Thermal diffusivity measurement by thermal wave interference technique

Thermal wave propagation through a sample is determined by the thermal diffusivity of the material; so the measurement of thermal diffusivity of materials helps to design various heat transfer systems. Since thermal diffusivity is directly related to thermal conductivity through the relation,

$$\alpha = \frac{k}{\rho C} \tag{2.7}$$

where k is the thermal conductivity, ρ is the density and C is the specific heat capacity of the medium, a measurement of thermal diffusivity directly leads to determination of thermal conductivity. Conventionally, the photo thermal

techniques, such as the photopyroelectric (PPE) and photoacoustic (PA) techniques have been used to measure the thermal diffusivity of samples by recording the frequency or time dependence of the amplitude or phase of thermal waves in a fixed volume material (Mandelis *et al.,* 1993a; John *et al.*, 1986; Munidasa *et al.,* 1994). The development of a new Photothermal technique with a variable sample to source distance (Mandelis *et al.,* 1993b; Vanniasinkam, 1994) has opened up the possibility of measuring spatial dependence of amplitude and phase of thermal waves, in a sample leading to the development of the thermal wave interference technique. Thermal wave interferometer is a device that employs interference of counter propagating thermal waves to measure the thermal diffusivity of samples in their gaseous as well as liquid phases. The working principle of this technique is analogous to that of a resonance column used to determine the velocity of sound waves. In a thermal wave interferometer the spatial dependence of thermal wave amplitude is recorded to measure the thermal diffusivity of a fixed length of a fluid filled inside a cavity.

2.3.1 Principle of the technique

The heart of a thermal wave interferometer is a Thermal Wave Resonant Cavity (TWRC) cell; which works based on the phenomenon of interference of thermal waves inside a resonant column (Shen *et al.,* 1996; Shen *et al.,*1995). The resonant column or cavity is made up of two parallel plates; one made up of a thin metallic foil of copper and the other of a metal coated Poly Vinylidine Di Fluoride (PVDF) film. Here the copper foil launches thermal waves into the cavity by the absorbing an intensity modulated laser radiation. The PVDF film acts as a thermal wave reflector as well as a thermal wave detector to monitor the temperature fluctuations due to the thermal wave propagation through the fluid sample filled inside the cavity. Thermal waves propagating through the

sample inside the cavity get reflected from the PVDF film attached opposite side of the thermal wave resonant column.

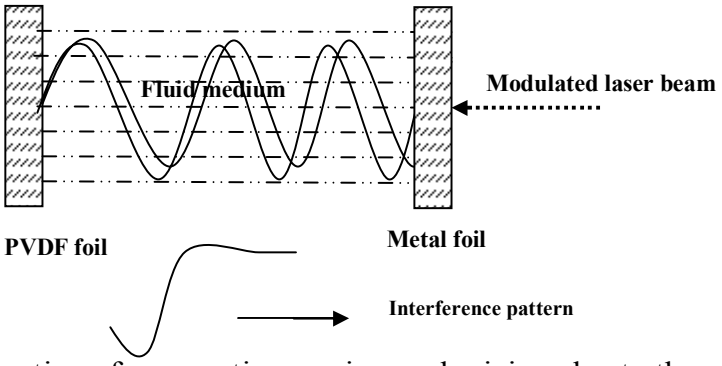

Figure 2.3 Formation of consecutive maxima and minima due to thermal wave interference in a resonant cavity cell (TWRC).

A cavity length scan at a fixed modulation frequency for light or modulation frequency scan for a fixed cavity length produces interference maxima and minima inside the cavity. Figure 2.3 shows a schematic illustration of the formation of interference maximum and minimum during the cavity length scan in a thermal wave resonant cavity. The spatial variations of the amplitudes and phases of the thermal waves inside the cavity are recorded as an in-phase and quadrature outputs of a Lock-in-amplifier with the help of the PVDF the thermal wave transducer. The resonance like extrema obtained in the in-phase (IP) and quadrature (Q) outputs are used to determine the thermal diffusivity of the fluid sample with high precision.

Since the copper foil is opaque, assuming a one dimensionality for the thermal response of the cavity, the general expression for PPE signal detected by the PVDF detector can be derived from the value of average pyroelectric voltage as follows (Vanniasinkam *et al.,* 1994; Mandelis *et al.,* 1993a),

$$V(L,\alpha_g,f)=\frac{2I_o b_{gs}}{K_p\sigma_p(1+b_{gp})(1+b_{gs})^2}\left(\frac{e^{-\sigma_s l}}{1-\gamma_{gs}{}^2\gamma_{gp}e^{-2\sigma_s l}}\right)\left(\frac{e^{-\sigma_g l}}{1-\gamma_{gs}\gamma_{gp}e^{-2\sigma g L}}\right) \tag{2.8}$$

where $\sigma_j=(1+i)\sqrt{\pi f/\alpha_j}$ (2.9)

is the complex thermal diffusion coefficient and α_j denotes the thermal diffusivity ; j=*g, s, p (g*-fluid, *s*-copper wall, *p*-PVDF wall); f is the modulation frequency; and l is the thickness of copper foil, γ_{jk} are the thermal coefficients at *j-k* interface, defined as

$$\gamma_{jk}=\frac{(1-b_{jk})}{(1+b_{jk})}$$

$$b_{jk}=\frac{K_j\sqrt{\alpha_k}}{K_k\sqrt{\alpha_j}} \tag{2.10}$$

The mathematical steps to arrive at Equation (2.8) are not reproduced here as these are well documented in literature (Mandelis *et al.,* 1993b). The real part of Equation (2.8) Re [$V(L,\alpha_g,f)$], stands for in-phase signal, the IP-PPE while Im [$V(L,\alpha_g,f)$] stands for the quadrature signal, Q-PPE.

2.3.2 Cavity length scanning

In a cavity length scanning experiment, modulation frequency f of the incident light is fixed. For a given fluid Equation (2.8) can be written as,

$$V(L)=C\times\frac{e^{-\sigma_g L}}{1-\gamma_{gs}\gamma_{gp}e^{-2\sigma_g L}} \tag{2.11}$$

where C is complex constant independent of cavity length. The IP-PPE and Q-PPE signals thus vary with cavity length and their extrema occur at (Shen *et al.,* 1995),

$$L_n^{(IP)} = (n - \frac{1}{2})\frac{\lambda}{2} \quad ; \quad \text{n=1, 2, 3…..} \tag{2.12}$$

for the case of In-Phase signal, and

$$L_n^{(Q)} = n\frac{\lambda}{n} \; ; \text{n=1, 2, 3, 4….} \tag{2.13}$$

for the quadrature channel,

$$\text{where } \lambda = 2\sqrt{\pi\alpha_g / f} \tag{2.14}$$

is the thermal wave length corresponding to the modulation frequency f and α_g is the thermal diffusivity of the fluid sample. The conditions for IP-channel and Q-channel extrema are the same as the antinodal conditions for a standing wave in a pipe resonator with a capped end and with an open end respectively (Kinsler and Fray, 1962). By locating the cavity lengths corresponding to these thermal wave extrema, the thermal diffusivity can be calculated. Owing to exponential decay of thermal waves in space, the extrema corresponding to n=1 and n=2 alone are significant as shown in Figure 2.4(a) and 2.4(b). Note that thermal waves are highly dissipative in nature. From Equations (2.12), (2.13) and (2.14) we can write the following expressions for thermal diffusivity.

$$\left.\begin{aligned} \alpha &= \frac{f}{\pi}\left(L_2^{(IP)} - L_1^{(IP)}\right)^2 \\ \alpha &= \frac{4f}{\pi}\left(L_1^{(Q)} - L_1^{(IP)}\right)^2 \\ \alpha &= \frac{4f}{\pi}\left(L_2^{(IP)} - L_1^{(Q)}\right)^2 \end{aligned}\right\} \tag{2.15}$$

where $L_1^{(IP)}$ and $L_2^{(IP)}$ are the extrema corresponding to the in-phase PPE signal and $L_1^{(Q)}$ maximum extrema corresponding to the quadrature output. Any of the above expressions can be used to calculate the thermal diffusivity of the fluid medium.

The precise determination of the extremal positions is critical in cavity length scanning experiments. The PPE signal (amplitude and phase) is recorded as a function of the cavity length. An eighth order polynomial fit on the experimental data helps to determine the positions of these extrema precisely. It is found experimentally that using two extrema in the IP channel, $L_1^{(IP)}$ and $L_2^{(IP)}$ yield very reproducible results, but when the $L_1^{(Q)}$ in the Q-channel is used the reproducibility is not so good. The superior reproducibility while using the extrema in the IP channel is probably due to the fact that positions of extrema in the same channels shift by the same amount if noise or instrumental phase shift is introduced during the experiment.

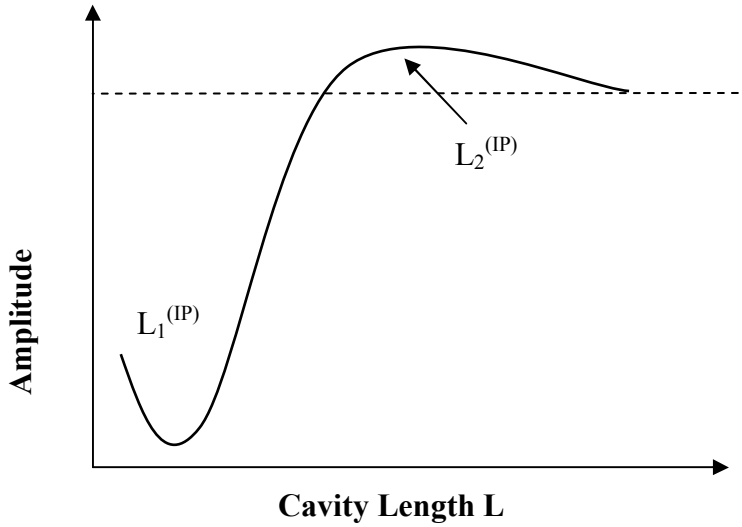

Figure 2.4(a): Variation of the amplitude of the resonance signal with cavity length in a cavity length scan experiment (in-phase output).

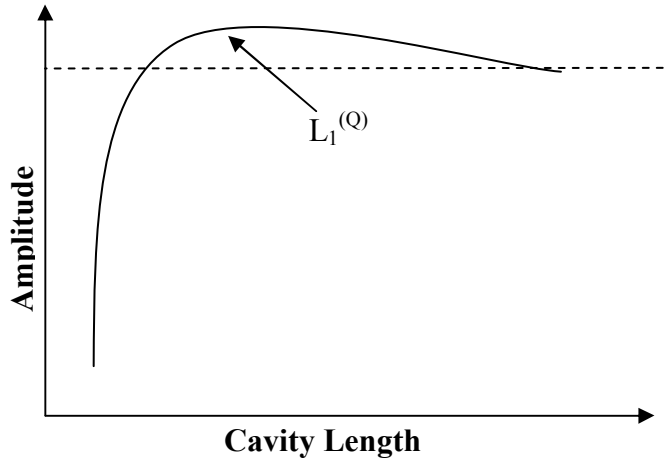

Figure 2.4 (b) Variation of the amplitude of the resonance signal with cavity length in a cavity length scan experiment (quadrature output).

The formation of typical interference maxima and minima as a function of cavity length in a cavity length scan experiment is shown in Figures 2.4(a) and 2.4(b) for IP and Q channels respectively.

2.3.3 Frequency scanning

In a modulation-frequency scan experiment, the modulation frequency of the incident radiation is varied keeping the cavity length fixed, to get the interference maxima and minima inside the cavity. Here the relation between cavity length L and the frequency corresponding to the n^{th} extremum in the IP channel, $f_n^{(IP)}$, is found to be (Shen *et al.,* 1995)

$$L = (n - \frac{1}{2})\frac{\lambda_n^{(IP)}}{2}\text{; n=1, 2, 3…} \tag{2.16}$$

$$\text{where } \lambda_n^{(IP)} = 2\sqrt{\pi\alpha_g / f_n^{(IP)}} \tag{2.17}$$

For the Q-channel the extreme condition can also be expressed as (Shen *et al.*1995)

$$\text{or } L_n \approx \frac{n\lambda_n^{(Q)}}{2} \tag{2.18}$$

$$\lambda_n^{(Q)} = 2\sqrt{\pi\alpha_g / f_n^{(Q)}} \tag{2.19}$$

where n=1, 2, 3, 4…

In the frequency scan experiment, the PPE signal amplitude and phase are measured as a function of modulation frequency. The interference maxima are obtained by normalizing the measured PPE signal with a reference PPE signal, obtained by performing the corresponding frequency scanning experiment with air inside the cavity. In this experiment the first trough in the IP signal is used to calculate the thermal diffusivity of the sample inside the cavity. In this case also, the first extremum corresponding to n=1 is significant. So from Equations (2.16)-(2.19), we can write the expression for thermal diffusivity as,

$$\alpha_g = \left(\frac{L}{0.3315}\right)^2 \frac{f_1^{(IP)}}{\pi} \tag{2.20}$$

In a frequency scanning experiment, the types of variations of the in-phase and quadrature outputs are similar to those of the cavity scan experiment.

In all our experiments we have used the cavity length scan technique to measure thermal diffusivity of the fluid filled in the cavity.

2.3.4. Technical description of the TWRC cell

A diagram of the Thermal Wave Resonant Cavity cell that we have designed and fabricated in the laboratory is shown in Figure 2.5. The main part of this TWRC cell is a Thermal wave Resonant Cavity formed between two reflecting walls for thermal waves. One cavity wall is made of a 35 μm thick copper foil attached to a fixed cylindrical tube so as to form a stretched flat surface about 1cm in diameter. The other wall was formed by a metal coated PVDF film, which also acts as a pyroelectric detector, of thickness 28 μm and 1cm diameter fixed on a copper disc at the bottom of the thermal wave resonator cavity. One side of the copper foil acts as a thermal wave generator formed by the absorption of optical radiation from a modulated He-Ne laser (20 mW, 632.8 nm). The outer surface of the copper foil has been blackened to enhance optical absorption. The copper foil remains thermally thin at all modulation frequencies less than 30Hz (thermal diffusion lengths in copper at all these frequencies are much greater than the physical thickness of copper foil). The holder bearing the PVDF film is attached to a micrometer stage, which allows variations in cavity length L with a resolution of 2.5 μm in one step. The forward and backward movements of the sample holder (or PVDF foil) are made possible by this micrometer stage which is controlled by a stepper- motor driven by a computer. The upper and lower surfaces of the PVDF detector is electrically connected to a dual- phase Lock –in –amplifier (Stanford Research Systems model SRS 830) which detects the resonant maxima and minima. A more detailed view of the experimental set up for the TWRC cell is shown in the Figure 2.6

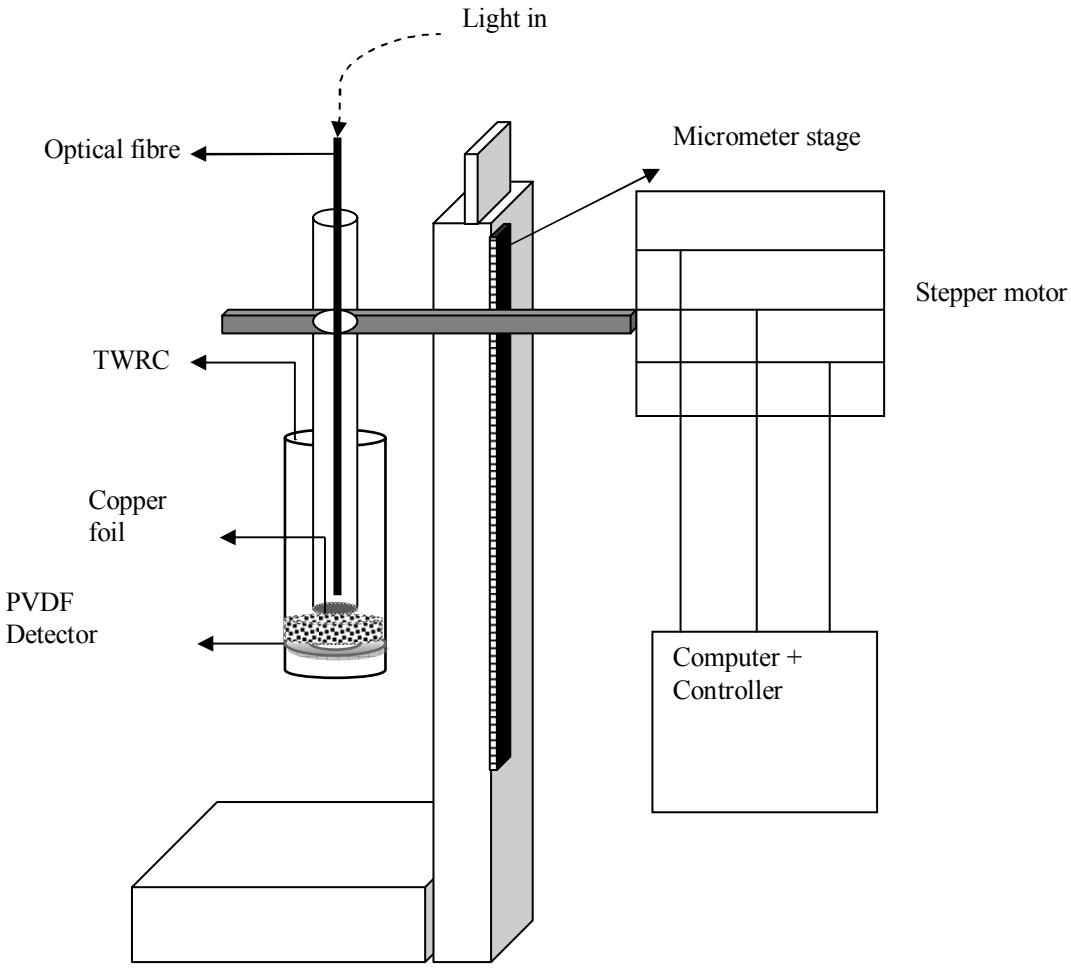

Figure 2.5 Technical Parts of a Thermal Wave Resonant Cavity (TWRC) cell

2.3.5 Measurement Method

The thermal diffusivity values of the different nanofluids in this work have been measured following the cavity scan experiment described above. This experiment offers a new degree of spatial freedom, which allows measurement of thermal diffusivity of fluids in the intra cavity region of the Thermal wave Resonant Cavity. As has been described earlier, the cavity length

scan experiment records the thermal wave resonances at a single modulation frequency. Furthermore, no normalization is needed, which leads to a fast, precise measurement of the thermal diffusivity of fluids with uncertainties less than $\pm 2\%$. The method has been tested with known liquids prior to adapting it to nanofluids. We think that this technique is more convenient and accurate than other techniques such as transient hot wire or parallel hot plate methods for measurement of thermal conductivity of nanofluids.

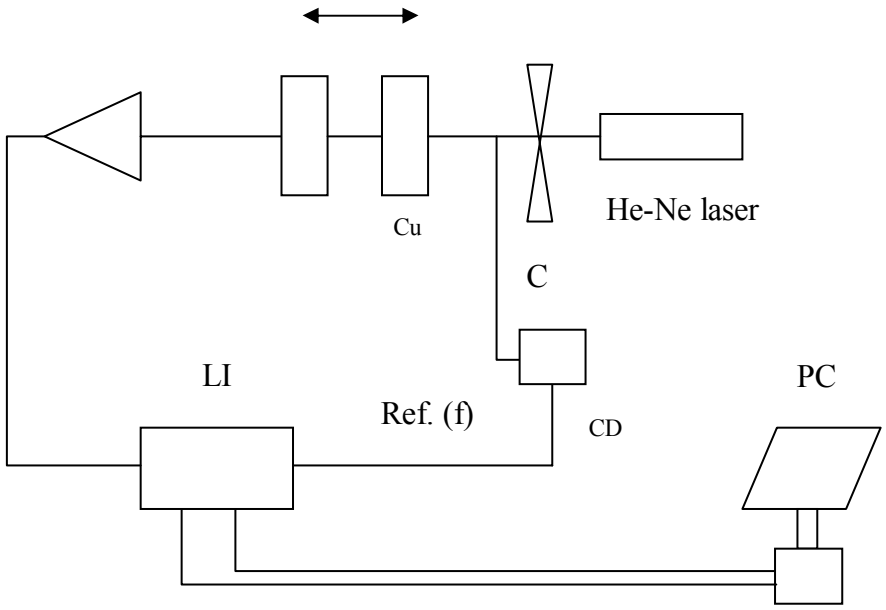

D-PVDF detector, Cu-Copper foil, LI-Lock-in-amplifier, C- Mechanical chopper CD-Chopper driver, PC-Personal computer

Figure 2.6 Experimental set up for the measurement of thermal diffusivity of fluid samples using the TWRC cell by thermal wave interference method.

Figure 2.6 shows the experimental set up of TWRC cell that we have configured to measure the thermal diffusivity of nanofluid samples. A modulated optical radiation from a 20mW He-Ne laser (632.8 nm) impinges normally on the copper foil. A multimode plastic optical fiber (core diameter 2 mm) is used to guide the laser beam on to the copper foil. The PVDF transducer detects the thermal waves launched by the optically heated copper foil and produces an electrical signal. After pre-amplification by a low noise amplifier, the signal is fed into a Lock-in amplifier (SRS 830).

A computer program in Visual Basic developed by us controls the operation of the experimental set up. The program is designed in such a way that the micrometer moves step by step and data acquisition is done by the Lock-in-amplifier at each step. The Lock-in-amplifier is interfaced to the computer to make the whole experiment fully automated.

The interference extrema obtained inside the cavity when the cavity length is varied are detected by the In-Phase and Quadrature channels of the Lock-in amplifier. The Lock-in amplifier readouts have been obtained by interfacing it to a Dell Vostro 1015 PC. We have plotted the thermal wave interference obtained as a function of the cavity spacing and an eighth order polynomial fit on experimental data helped to find the extrema $L_1^{(IP)}$, $L_2^{(IP)}$, $L_1^{(Q)}$ etc. Substituting these values in Equations (2.15) we have evaluated the thermal diffusivity of the nanofluid samples.

2.4 Photo acoustic (PA) technique

Photo acoustic (PA) technique for the measurement of thermal properties of solids is based on the sensitive detection of acoustic waves generated by the absorption of modulated electromagnetic radiation, the most popular radiation source nowadays being lasers. It is now well established that

the PA effect (Rosenwaig *et al.,* 1980) involves production of acoustic waves as a consequence of the generation of thermal waves in the medium due to periodic heating by the absorption of modulated light as a result of non-radiative de-excitation processes in the sample. The PA technique constitutes a comparatively simple and reliable experimental tool (Adams *et al.,*1977), which has been extensively used for the measurement of thermal properties such as thermal diffusivity and conductivity of solid samples (Charpentier *et al.,* 1982; Madhusoodanan *et al.,* 1987).

The method is based on the analysis of the variations of the amplitude and phase of the PA signal with the light modulation frequency, which is also the frequency of the generated acoustic waves. Figure 2.7 shows parts of a basic photoacoustic set up that we have used to measure thermal diffusivity of solid samples. The sample having thickness l_s is mounted on a high thermal conduction backing material such as copper. A modulated laser radiation from a He-Ne laser (632.8 nm), absorbed by the sample generates temperature fluctuation on the surface of the sample, immediately generates acoustic waves, which are detected by a sensitive microphone and a lock-in amplifier processes the detected acoustic signals. The experiment needs to be carried out in a vibration free environment so that a sufficiently high signal to noise ratio can be accomplished. In the present work we have measured the variations of the PA amplitude with modulation frequency to arrive at the thermal diffusivity of the samples.

The sample thicknesses chosen in a PA experiments are such that at low modulation frequencies (say < 50 Hz) the thermal diffusion length of the sample is more than the physical thickness of the sample, in which case the sample is said to be thermally thin. By increasing the modulation frequency to

higher values (say > 100 Hz) the thermal diffusion length decreases and at a high enough modulation frequency, it becomes

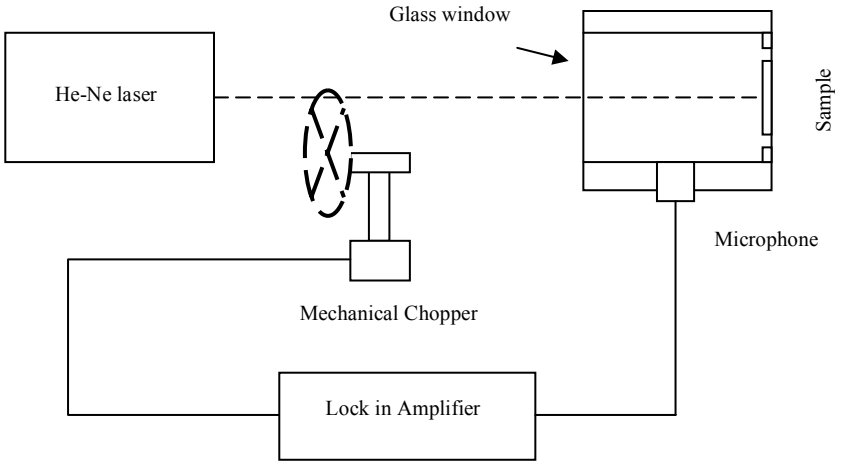

Figure 2.7 Parts of a basic photoacoustic set up used to measure thermal diffusivity of solid samples.

less than the physical thickness of the sample. This takes the sample to a thermally thick regime. The modulation frequency at which the sample switches from a thermally thin state to thermally thick regime is called the critical frequency. Critical frequency can be determined by measuring the variations of the PA amplitude or phase with modulation frequency, which appears as a distinct change in slope in the PA amplitude plot or as a maximum in the phase plot. Once the critical frequency f_c is determined, thermal diffusivity α can be determined from the relation (Madhusoodanan *et al.,*1987)

$$\alpha = \pi f_c l_s^2 \tag{2.21}$$

where l_s is the sample thickness.

This technique has been employed by a good number of previous workers to determine thermal diffusivities of a variety of solid samples (Philip and Madhusoodanan, 1988; Parthasarathy *et al.,* 1988).

2.5 Photopyroelectric (PPE) technique

Pyroelectric effect involves the induction of spontaneous, rapid, polarization in a non-centrosymmetric, and generally piezoelectric, material due to changes in temperature of the material. The Photopyroelectric effect consists of generation of spontaneous polarization in a pyroelectric material due to the absorption of intensity modulated electromagnetic radiation followed by the corresponding rise in temperature. The theory of photopyroelectric effect in solid samples giving the relevant expressions to determine thermal properties such as thermal conductivity and thermal effusivity of a material were originally developed by Mandelis and Zver (1985).

A modified PPE technique for the thermal characterization of condensed solids was developed earlier (Menon and Philip, 2000). This technique enables simultaneous measurement of the thermal conductivity, thermal diffusivity and specific heat capacity of a solid sample.

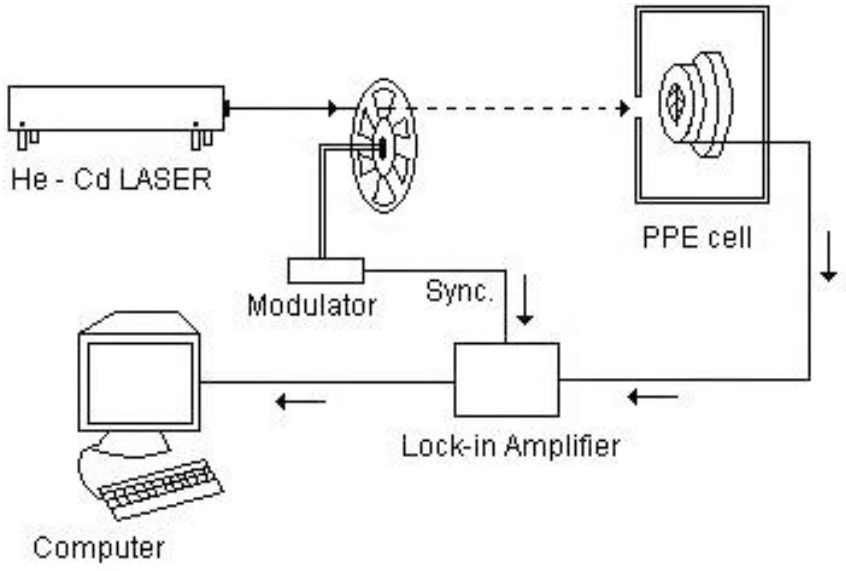

Figure 2.8 A schematic diagram of the Photopyroelectric experimental set up.

In this work we have followed the same method for the simultaneous determination of thermal diffusivity, thermal conductivity and specific heat capacity of polymeric nanosolid samples described in chapter 6 of the thesis. A schematic diagram of the PPE experimental set up that we have used for the thermal characterization of the prepared nanosolid samples is shown in Figure 2.8.

In this technique, an intensity modulated beam of light (from a laser) incident on the sample generates a thermal wave, which propagates through the sample resulting in a corresponding temperature rise on the opposite side of the sample. This temperature rise is picked up with a pyroelectric detector (PVDF film of coated on both sides with a conducting film) attached on the back side of the sample. The temperature variations sensed by the detector give rise to an electrical current, which is proportional to the rate of change of the average heat content, given by

$$i_d = PA\left(\frac{\partial\theta(t)}{\partial t}\right) \tag{2.22}$$

where P is the pyroelectric coefficient of the detector and A is its area. $\theta(t)$ is the spatially averaged temperature variation over the thickness of the detector L_d, and is given by,

$$\theta(t) = \left(\frac{1}{L_d}\right)\int_0^{L_d}\theta(x,t)dx \tag{2.23}$$

Assuming that the sample and pyroelectric detector are thermally thick (thermal diffusion length $\mu = \sqrt{\alpha/\pi f}$ less than the physical thickness of the sample; α being the thermal diffusivity and f the modulation frequency), one can obtain the following expressions for the amplitude and phase of the PPE signal at the output of the detector (Menon and Philip, 2000)

$$V(f,T)=\frac{I_0\eta_s AR_d}{L_d\left[1+\left(f/f_c\right)^2\right]^{1/2}}\frac{P(T)}{P_d(T)C_{pd}(T)}x\frac{\exp\left[-\left(\pi f/\alpha_s\right)^{1/2}L_s\right]}{\frac{e_s(T)}{e_d(T)}+1} \tag{2.24}$$

$$\phi(f,T)=-\tan^{-1}\left(f/f_c\right)-\left(\frac{\pi f}{\alpha_s(T)}\right)^{1/2}L_s \tag{2.25}$$

Here f is the modulation frequency of light, T is the temperature, I_0 is intensity of radiation falling on the sample, η_s is a constant for a sample, R_d is the detector leakage resistance, f_c is the critical frequency at which sample goes from a thermally thin to a thermally thick regime. L, ρ and C_p are the thickness, density and specific heat capacity of the medium respectively, with subscripts d and s standing for detector and sample respectively. The pyroelectric coefficient of the detector film is P=30×10^{-10}C. cm^{-2} K^{-1} at room temperature. The parameter $P(T)/\left[\rho_d(T)C_{\rho d}(T)\right]$ for the detector has been determined by measuring the PPE amplitude and phase at fixed modulation frequency as a function of temperature from 25^{0}C to 50^{0}C in a calibration run. From the Equations (2.24) and (2.25) it is clear that the thermal diffusivity α_s of the sample can be determined from the variation of phase with frequency of the PPE signal. Fitting the experimental PPE phase curve with Equation (2.25) yields α_s. Substitution of α_s into the amplitude expression gives thermal effusivity e_s of the sample. From these the thermal conductivity $k_s(T)$ and heat capacity $C_{ps}(T)$ can be obtained from the following relations

$$k_s(T)=e_s(T)\left[\alpha_s(T)\right]^{1/2} \tag{2.26}$$

$$C_{ps}(T)=\frac{e_s(T)}{\rho_s(T)[\alpha_s(T)]^{1/2}} \tag{2.27}$$

A temperature calibration of the PPE detector with reference materials such as Copper (α_s=1.12×10^{-4}m^{2}s^{-1}) and Polymer nylon (α_s=1.26×10^{-7} m^{2}s^{-1}) yield all necessary parameters in Equations (2.24) and (2.25).

The amplitude and phase of the pyroelectric signal are recorded as a function of modulation frequency with a Lock-in-amplifier. From the amplitude and phase values of the PPE signal, thermal properties like thermal conductivity, specific heat capacity and thermal diffusivity can be evaluated. All the experimental and technical details of this method are described in detail elsewhere, (Preethy C. Menon, Ph.D. thesis, 2001, CUSAT; Menon and Philip, 2000).

2.6 Measurements in different systems

In this present work we have followed experimental techniques described earlier to perform the thermal characterization of the different types of polymeric nanofluids and solid nanosolids. Here the preparation of nanofluids and nanosolids has been done by a two step method, in which a uniform dispersion of the synthesized nanoparticle in a base fluid produced the nanofluid and their solid counterpart provided the nanosolid.

The most essential part of these polymeric nanofluids and nanosolids are the nanometer sized metallic and metallic oxide nanoparticles prepared following chemical routes. As mentioned in chapter 1, the structure and size of these nanoparticles strongly influence the thermal properties of nanofluids and nanosolids. So before performing the thermal transport measurements we have identified the structure, shape and size of the prepared nanoparticles such as TiO_2, copper etc. using the XRD and SEM analysis. These techniques identified the structure, shape, size, morphology and composition of the nanoparticles used for the preparation of the desired nanofluids and nanosolids.

Using the thermal wave interference technique, thermal diffusivity of the prepared nanofluids of different concentrations and particle sizes have been measured. Experimental variations of thermal diffusivity as a function of the concentration and size of the dispersed nanoparticles have been plotted, which yield information about the thermal conduction properties of the nanofluids of interest.

In the second part of the experimental work we have carried out the thermal characterization of condensed nanofluids (nanosolids) by measuring their thermal properties such as thermal conductivity, thermal diffusivity, specific heat capacity etc. For this we have employed the photothermal techniques such as photo acoustic and photopyro electric techniques. The photo acoustic technique has been used for measuring the thermal diffusivity of condensed polymeric nanofluids (nanosolids) first. Then a more complete thermal characterization has been done by measuring of thermal conductivity, thermal diffusivity and specific heat capacity following the photopyro electric technique. This enabled us to compare the thermal diffusivity values of these samples measured following these two techniques. We have also measured the specific heat capacity of the nanosolid samples using differential scanning calorimetry following the ratio method. This helped us to compare the specific heat capacity values of nanosolids measured by two different techniques. More detailed description of the experimental techniques and their descriptions are given in the respective chapters.

Chapter 3

Theoretical Models for Thermal Conduction in Polymeric nanofluids and nanosolids

3. 1 Introduction

The theoretical models describing effective thermal conductivity of two component mixtures have been derived based on the assumption that all mixtures constitute a continuous base medium called the matrix with a discontinuous solid component called particles embedded in it. As mentioned in chapter 1, thermal properties of a two component mixture depend on the details of their microstructures, such as component properties, component volume concentrations, particle dimensions, particle geometry, particle distribution, particle motion and matrix-particle interfacial effects. The transport properties of heterogeneous mixtures have attracted the interest of researchers ever since the time of Maxwell in the nineteenth century. The reason for this interest is, of course, due to the enormous variety of physical systems in which inhomogeneities occur and their practical applications. Among various transport properties, the conductivity properties, comprising the dielectric constant, magnetic permeability, electrical conductivity and thermal conductivity, may be treated together in an analogous manner because of the comparable form of conduction laws. Maxwell was one of the first to investigate conduction properties analytically for a mixture consisting of particles embedded in a base medium following the effective medium theory

(Effective Medium Theory or Effective Medium Approximation denoted as EMT or EMA). The effective medium theory describes the macroscopic properties of a medium based on the properties of the components and their relative volume fractions. Later, using a mean field approach, Maxwell and Garnett modified the effective medium theory originally developed by Maxwell (Maxwell, 1873) to derive the expressions for effective dielectric properties of a two component mixture. Then, it has been extended to thermal conductivity so as to express the effective thermal conductivity or simply thermal conductivity of a binary mixture in terms of its corresponding component properties.

3.2 The Maxwell- Garnett model

The Maxwell - Garnett model or M-G model (Maxwell, 1873) is the first theoretical model used to describe the effective thermal conductivity of two component mixtures. Maxwell had followed an effective medium theory to express effective properties of a binary mixture. The properties considered have generally been the electrical conductivity σ as well as the dielectric constant ε of the medium. The conductivity σ and dielectric constant ε are interchangeable due to the wide applicability of the Laplace transforms. An analogous approach has been adopted to arrive at the effective thermal conductivity of a homogeneous mixture in terms of the thermal conductivity of its constituent phases.

3.2.1 M-G model for effective dielectric constant of a binary mixture

Maxwell and Garnett followed a self consistent approximation or Mean Field Theory (MFT) to derive effective properties of homogeneous mixtures. The main idea of MFT has been to replace all multiple body interactions in a system to any single body one with an average or effective interaction between

them. This reduces any multi-body problem into an effective one-body problem. A many-body system with interactions is generally very difficult to solve exactly, except for extremely simple cases. In the effective medium approach, an n-body system is replaced by a one-body system with a chosen good external field. The external field replaces the interactions of all the other particles to an arbitrary single particle. The ease of solving problems following MFT provides some insight into the overall behavior of the system on an average, which suffices for most applications. In order to derive the effective dielectric properties of a medium, Maxwell- Garnett model considered systems under the following conditions.

(i) a mixture which is electro dynamically isotropic, non parametric and linear (none of its constitutive parameters depends on the intensity of electromagnetic field).

(ii) inclusions are separated by distances greater than their characteristic sizes.

(iii) the characteristic size of inclusions is small compared to the wavelength of the electromagnetic field in the effective medium.

(iv) inclusions are arbitrary randomly distributed.

Consider an effective medium consisting of a matrix medium with dielectric constant ε_m and inclusions of dielectric constant ε_p having volume fraction ϕ_v . Suppose the effective medium is subjected to an electric field **E**. In order to derive the Maxwell-Garnett equation, let us start with an array of polarizable particles. By using the Lorentz local field concept, it is rather straightforward to get the Clausius Mosotti Equation (Griffith, 1999) as

$$\frac{\varepsilon-1}{\varepsilon+2}=\frac{4\pi}{3}\sum_{j}N_j\alpha_j \qquad (3.1)$$

where α_j is the polarizability of the j^{th} component and N_j is the number of components. By using elementary electrostatics, we get the following expression for the polarizability for a spherical inclusion with radius r as

$$\alpha=\frac{(\varepsilon_i-1)}{(\varepsilon_i+2)}r^3 \qquad (3.2)$$

If we combine this with the Clausius - Mosotti equation we get,

$$\left(\frac{\varepsilon_{eff}-1}{\varepsilon_{eff}+2}\right)=\phi_v\left(\frac{\varepsilon_p-1}{\varepsilon_p+2}\right) \qquad (3.3)$$

where ε_{eff} is the effective dielectric constant of the mixture. As the model of Maxwell and Garnett is a composition of a matrix medium with inclusions we rewrite the above equation for such a system as

$$\left(\frac{\varepsilon_{eff}-\varepsilon_m}{\varepsilon_{eff}+2\varepsilon_m}\right)=\phi_v\left(\frac{\varepsilon_{eff}-\varepsilon_m}{\varepsilon_{eff}+2\varepsilon_m}\right) \qquad (3.4)$$

This is the Maxwell-Garnett equation. When ε belongs to the real number set, we can simplify the Maxwell-Garnett equation to obtain the following expressions for ε_{eff}

$$\varepsilon_{eff}=\varepsilon_m\frac{\varepsilon_p(1+2\phi_v)-\varepsilon_m(2\phi_v-2)}{\varepsilon_m(2+\phi_v)+\varepsilon_m(1-\phi_v)} \qquad (3.5)$$

This is the Maxwell- Garnett equation which expresses the effective dielectric properties of a mixture in terms of its component values. Due to the interchangeability of conduction laws, it is possible to convert the above

expression into respective thermal conductivity terms by replacing the dielectric constant of the effective medium, matrix and inclusion by the corresponding thermal conductivities. Obviously, one has to rewrite the relevant steps of the derivation of Maxwell –Garnett formula (Maxwell, 1873) for effective thermal conductivity of mixtures following Laplace equation with the temperature T as the forcing field instead of the electric field **E**.

3.2.2 M-G model for effective thermal conductivity of a binary mixture

In order to derive an expression for the effective thermal conductivity of a binary mixture following Maxwell's idea, (Maxwell, 1873), M-G model considers a very dilute suspension of spherical particles by ignoring interactions between particles. For a mixture containing identical spherical particles of radius r_p in a field of temperature T and temperature gradient G, the steady state-condition can be defined by the Laplace equation,

$$\nabla^2 T(r) = 0 \tag{3. 6}$$

By introducing a large sphere of radius r_0 containing all the spherical particles dispersed in the matrix and being surrounded by the matrix, one can calculate the temperature T outside the sphere r_0 at a distance $r > r_0$ in the following two ways (Stratton, 1941; Van Beek, 1967).

First, the sphere r_0 is considered to consist of a heterogeneous system with an effective thermal conductivity k_{eff} embedded in a matrix with a thermal conductivity k_m. The temperature T outside the sphere r_0 can therefore be expressed as,

$$T(r) = \left(-1 + \frac{k_{eff} - k_m}{2k_m + k_{eff}} \frac{{r_0}^3}{r^3} \right) G.r \tag{3. 7}$$

This is obtained by solving Laplace Equation together with the following boundary conditions:

$$T(r)\big|_{r\to\infty} = -G.r \qquad T(r)\big|_{r\to r_0^-} = T(r)\big|_{r\to r_0^+} \tag{3. 8a}$$

$$k_e \left.\frac{\partial T(r)}{\partial r}\right|_{r\to r_0^-} = k_m \left.\frac{\partial T(r)}{\partial r}\right|_{r\to r_0^+} \tag{3. 8b}$$

Second, the temperature T is considered to be produced by all the spherical particles with thermal conductivity k_p, embedded in a matrix with a thermal conductivity k_m, and by following a similar procedure it can be calculated from the superposition principle as

$$T(r) = \left(-1 + \frac{k_p - k_m}{2k_m + k_p} \frac{\phi_v r_0^3}{r^3} \right) G.r \tag{3. 9}$$

From the above equations, the effective thermal conductivity k_{eff} of a two component medium can be readily obtained after simple algebraic manipulations as

$$k_{eff} = k_m + 3\phi_v \frac{k_p - k_m}{2k_m + k_p - \phi_v(k_p - k_m)} \tag{3. 10}$$

Rearranging terms in the above equation, we can write

$$\frac{k_{eff}}{k_m} = \frac{(1-\phi_v)(k_p + 2k_m) + 3\phi_v k_p}{(1-\phi_v)(k_p + 2k_m) + 3\phi_v k_m} \tag{3. 11}$$

This is the conventional Maxwell –Garnett effective medium self consistent approximation that has been used to describe the effective thermal conductivity of two component mixtures. The Maxwell equation takes into account only the particle volume concentration and the thermal conductivities

of the particle and base medium. Later researchers introduced other classical models which include the effects of particle shape (Hamilton and Crosser, 1962), particle distribution (Cheng and Vachon, 1969), and particle-particle interactions (Jeffrey, 1973). However, all of these models predict more or less identical enhancements in thermal conductivity at low particle concentrations (<1 vol. %) for nanofluids under investigation. Therefore, the Maxwell model is used in this study as representative of all classical models. In this thesis we have used the Maxwell-Garnett model (Maxwell, 1873) and some of its extended forms (Yu and Choi, 2004; Liang and Tsai, 2011; Nan *et al.,* 1997; Cheng and Vachon, 1969) to establish the mechanisms responsible for the observed enhancements in thermal conductivity and thermal diffusivity of Polymeric nanofluids and their solid counterparts, known as Polymeric nanosolids. In the following sections we discuss the details of the theoretical models that have been used for the theoretical calculations for comparison with experimental results.

3.3 Thermal Conduction in Polymeric nanofluids

3.3.1 Effect of adsorption layer on thermal conductivity

Adsorption is the adhesion of atoms or molecules of a fluid on to a rigid solid surface. This process creates a thin film of the adsorbate (the molecules or atoms being accumulated) on the surface of the adsorbant. In 1919, Langmuir introduced a model to quantify the amount of adsorbate adsorbed on an adsorbant as a function of the partial pressure or concentration of absorbate molecule at a given temperature. Langmuir's model considers adsorption of fluid molecules onto an idealized surface.

The main physical process that determine adsorption as per this model are

i) the adsorbed fluid transforms into an immobile state or phase.

ii) all sites are equivalent.

iii) each site can hold at most one molecule (mono-layer coverage only).

iv) there are no interactions between adsorbate molecules on adjacent sites.

In a typical nanofluid system, it is assumed that the adsorption of liquid molecules on a nanoparticle surface is thought to be monolayer one. The way the molecules get organized on particle surface is generally considered to be hexagonal in nature. From the Langmuir formula of monolayer adsorption of molecules, the thickness of adsorption layer can be expressed as (Hua *et al*., 2008; Wang *et al.,* 2009),

$$t = \frac{1}{\sqrt{3}}\left(\frac{4M}{\rho_f N_A}\right)^{1/3} \qquad (3.12)$$

where M is molecular weight of the base fluid, ρ_f is the density of the liquid, and N_A is Avogadro's constant (6.023×10^{23} / mol).

For a typical water based nanofluid system, the thickness of adsorption layer calculated using Langmuir formula, is 1. 8- 2.3 nm. The involved for the derivation of Equation (3.12) is well documented in literature and available elsewhere (Yan, 1986). Researchers have tried to establish the anomalous enhancement observed in effective thermal conductivity of low molecular weight based nanofluids (Yu and Choi, 2003; Yu and Choi, 2004; Xie *et al*., 2005; Wang *et al*., 2003) in terms of the phenomenon of adsorption of base fluid molecules around nanoparticle surfaces. But experimental studies (Buongiorno *et al*., 2009) have shown that this adsorption layers have no significant influence on the effective thermal conductivity of nanofluids made from low molecular weight base nanofluids like water, Ethylene Glycol etc.

However, for a polymer based nanofluid consisting of solid particle suspensions embedded in a polymer fluid, the adsorption of liquid molecules on the surface of solid material is a well defined phenomenon (Becker *et al*., 1989; Klein and Luckham, 1986). There are a number of studies reported in literature (Klein and Luckham , 1986; Glass, 1968; Witt and Ven, 1992; Nash *et al*., 1996) on the adsorption characteristics of a polymer liquid like PVA. Schematic illustration of the formation of a polymer layer around solid nanoparticle is shown in Figure 3. 1.

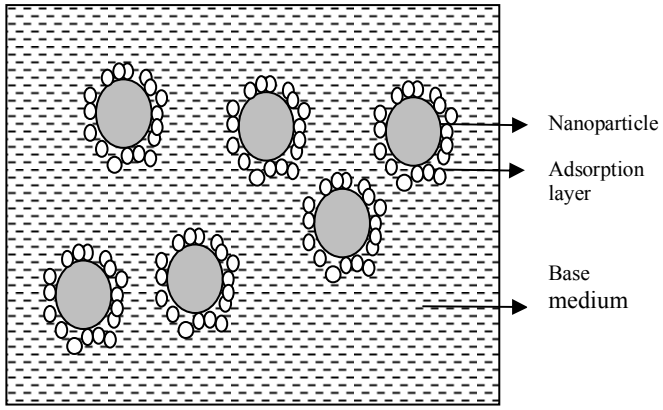

Figure 3.1 Schematic illustration of the formation Polymeric nanolayer around a spherical nanoparticle.

For a polymeric fluid, the apparent thickness (t_{ad}) of the adsorption layer formed around the nanoparticle is obtained by subtracting the radius of the bare nanoparticle r from the hydrodynamic radius (R_h) of the layered nanoparticle. The hydrodynamic radius of the layered nanoparticle can be estimated from the Stokes- Einstein equation as,

$$R_h = \frac{kT}{6\pi\mu D} \tag{3. 13}$$

where μ the viscosity of the base fluid and D is the diffusion coefficient of the layered nanoparticle. Studies on the adsorption of PVA like liquid polymers around solid particles (Becker *et al.*, 1989) have shown that the effective adsorption layer thickness t, varies with nanoparticle radius r as

$$t = \frac{\left[(r + t_{ad})^3 - r^3 \right]}{3r^2} \tag{3.14}$$

Upon performing this calculation we obtain an apparent adsorption layer thickness in the range 1-5 nm for a typical polymeric nanofluid.

We try to explain the observed effective thermal conduction in a polymeric nanofluid in terms of the formation of adsorption layer and the associated nanoparticle clustering. Though different authors have modified the effective medium theory including the formation of liquid adsorption layer around particles, most of these modifications have been done for nanofluids made of low molecular weight base fluids. We adopt similar formalism to the two systems studied in this work. For polymeric nanofluids, we have tried to establish the thermal conduction properties analytically following the theoretical models given by Yu and Choi (2003), and Liang and Tsai (2011) which consider the particle clustering in the nanofluid. Detailed descriptions of the theoretical models that we have adopted in our theoretical analysis and their comparison are given in the following sections.

3.3.2 Renovated Maxwell–Garnett model including adsorption layers

Yu and Choi (2003) modified the Maxwell –Garnett model to derive the effective thermal conductivity of nanofluids composing of nanoparticles with adsorption layer as follows.

In order to include the effect of the liquid adsorption layer, Yu and Choi (2003) considered that nanoparticles of radius r and volume fraction ϕ_v are suspended in a base fluid. Assume that the solid-like adsorption layer of thickness t around the particles is more ordered than the bulk liquid and that the thermal conductivity k_{layer} of the ordered liquid layer is higher than the base liquid. In high molecular weight based fluid, t is estimated as a difference between the hydrodynamic radius and the radius of the suspended nanoparticles in the medium (Becker *et al*., 1989). One can find theoretical as well as experimental findings on this subject in literature (Becker *et al*., 1989, Schwartz *et al*., 1995).

In order to simplify the analysis, assume that the nanolayer around each particle could be combined with the particle to form an equivalent particle and that the particle volume fraction is so low that there is no overlap of these equivalent particles. The above assumptions result in an equivalent particle radius $r+t$ and an increased volume fraction ϕ_v' , which can be expressed as

$$\phi_v' = \frac{4}{3}\pi(r+t)^3 n = \frac{4}{3}\pi r^3 n(1+ t/r)^3 = \phi_v(1+\beta)^3 \qquad (3.15)$$

where n is the particle number per unit volume and $\beta = t/r$ is the ratio of the nanolayer thickness to the original particle radius.

Based on the effective medium theory, Schwartz *et al*. (1995) investigated the electrical conductivity of mortars including the enhanced electrical conduction in the matrix-sand grain inter-facial region. They evaluated the electrical conductivity by a combination of finite element, finite difference, and random walk methods for periodic and disordered models for the mortar. Since the effective conductivity within the inter-facial zone is often much higher than the bulk matrix conductivity, the qualitative features of

transport in these systems is often controlled by the connectivity of the interfacial zone. A family of effective medium approximations has given a good qualitative description of the effective electrical properties of this physical system in terms of the properties of its components, interfacial layer and that of the base matrix. The detailed mathematical steps followed by Schwartz et al. are available in literature (Schwartz *et al*., 1995). Adapting an analogous mathematical formalism to the case of nanofluids having layered nanoparticles, Yu and Choi (2003) have expressed the effective thermal conductivity of layered nanoparticle in terms of the nanoparticle thermal conductivity (k_p), thickness of the adsorption layer and thermal conductivity of the base medium (k_m).

Following the above approach, equivalent thermal conductivity k_{pe} of the equivalent particles can be obtained as (Schwartz *et al*., 1995)

$$k_{pe} = \left(\frac{[2(1-\gamma)+(1+\beta)^3(1+2\gamma)]\gamma}{-(1-\gamma)+(1+\beta)^3(1+2\gamma)} \right) k_p \qquad (3.16)$$

where $\gamma = k_{layer}/k_p$ is the ratio of nanolayer thermal conductivity to particle thermal conductivity. For the extreme case of $k_{layer} = k_p$ (i. e. $\gamma = 1$), Equation (3. 16) reduces to $k_{pe} = k_p$. This model assumes that the value of k_{layer} lies in between k_m and k_p.

Replacing k_p by k_{pe} and ϕ_v by ϕ_v' , the Equation (3. 11) can be modified into ,

$$k_{eff} = \frac{k_{pe}+2k_m+2(k_{pe}-k_m)(1+\beta)^3\phi_v'}{k_{pe}+2k_m-(k_{pe}-k_m)(1+\beta)^3\phi_v'} k_m \qquad (3.17)$$

This Equation (3. 17) represents the effective thermal conductivity of a nanofluid having nanoparticles with adsorption layers around them.

In addition to the formation of adsorption layer around the nanoparticle, another mechanism simultaneously at work in a nanofluid system is the formation of nanoparticle clusters in the liquid medium at comparatively high particle concentrations (Liang and Tsai, 2011). In order to include the effect of clustering along with interfacial layering we have followed the modified form of effective medium theory introduced by Liang and Tsai (2011).

3.3.3 Effective medium theory including clustering of nanoparticles with interfacial adsorption layers

Liang and Tsai (2011) developed a modified form of a three-level particle clustering model originally developed by Prasher (Prasher *et al*., 2006) assuming the formation of nanoparticle clusters along with formation of interfacial layers. They have used the nonequilibrium Molecular Dynamics (MD) simulation for a nanofluid assuming it as an inhomogeneous system in which the solid-liquid interactions are assumed to be much stronger than liquid-liquid interactions. They have incorporated the simulation results in to a three-level clustering model to evaluate the effective thermal conductivity of nanofluids. They have assumed that the nanoparticle clusters are embedded in a sphere of radius R_a and the cluster spheres are uniformly distributed in the liquid medium. Each cluster consists of linear chains of nanoparticles, termed back-bone of the cluster, and side chains called dead-end particles. These clustered nanoparticles are assumed to have a significant influence on the thermal conductivity of the interfacial layers. By combining the idea of nanoparticle clustering with liquid layering, Liang and Tsai have introduced a new model to evaluate the thermal conductivity of nanofluids. As mentioned above, Liang and Tsai (2011) assumed that particle clusters are embedded within a sphere of radius R_a and these cluster spheres are uniformly distributed

in the liquid. Clustering of nanoparticles including the back-bone of the cluster and dead-end particles are pictorially demonstrated in Figure 3. 2.

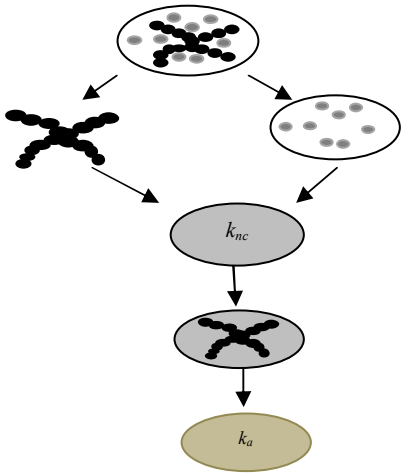

Figure 3. 2 Schematic of a single nanoparticle cluster consisting of the backbone (black circles) and dead ends (gray circles). The nanoparticle cluster is decomposed into dead ends with the fluid and the backbone. Thermal conductivity of the aggregate only with particles belonging to the dead ends k_{nc}. Linear chains are embedded inside a medium with effective conductivity of k_{nc}. Here k_a *i*s the overall thermal conductivity of a single cluster consisting of back-bone particles and dead end particles.

The volume fractions of the nanoparticles (ϕ_{int}), the backbone particles (ϕ_c), and the dead-end particles (ϕ_{nc}) in the cluster spheres are, obtained from fractal theory (Hui and Stroud, 1990; Hui and Stroud, 1994) as

$$\left.\begin{aligned} \phi_{\text{int}} &= \left(R_a / a\right)^{d_f - 3} \\ \phi_c &= \left(R_a / a\right)^{d_l - 3} \\ \phi_{nc} &= \phi_{\text{int}} - \phi_c \end{aligned}\right\} \qquad (3.\ 18)$$

where d_f and d_l are, respectively, the fractal dimensions and chemical dimensions of clustered spheres. In this calculation, we assume $R_a = 5a$ and set $d_f = 1.8$ and $d_l = 1.4$, following Prasher *et al*. (2006). Due to number conservation of the particles, we can write

$$\phi_v = \phi_{\text{int}}\phi_a \tag{3.19}$$

where ϕ_v and ϕ_a are the volume fractions of nanoparticles and cluster spheres in the liquid respectively. After defining the above parameters, Prasher's model (Prasher *et al.,* 2006) starts with the first level of homogenization, which is performed with only particles belonging to the dead ends. The effective thermal conductivity of the cluster sphere in the presence of the dead-end particles only, k_{nc}, can be determined based on the Bruggeman model, which has adopted a mean field approach (Bruggeman, 1935). The Bruggeman equation to determine k_{nc} can be easily derived from the Maxwell-Garnett equation, given by Equation (3.11), by applying an integration scheme to take into account of the concentration of dispersed particles in the immediate neighborhood of a certain particle. For this, assume that the large sphere of radius R_0 is embedded in the matrix of thermal conductivity k_{eff} rather than k_m; then rearrange and differentiate equation (3.11) to obtain

$$\frac{dk_{eff}}{d\phi_v} = \frac{1}{1-\phi_v}\frac{3k_{eff}(k_p - k_{eff})}{2k_{eff} + k_p} \tag{3.20}$$

which upon integration from $\phi_v = 0$ (k_{eff}=k_m) to $\phi_v = \phi_{nc}$ (k_{eff}= k_{nc}) leads to

$$1 - \phi_v = \frac{k_p - k_{nc}}{k_p - k_m}\left(\frac{k_m}{k_{nc}}\right)^{1/3} \tag{3.21}$$

Rearrangement of terms in equation (3. 21) leads to a model which is particularly suitable for composites with high-concentration of additives and is given by,

$$\phi_{nc}\left(\frac{k_p - k_{nc}}{k_p + 2k_{nc}}\right) + (1-\phi_{nc})\left(\frac{k_f - k_{nc}}{k_f + 2k_{nc}}\right) = 0 \qquad (3.\ 22)$$

Solution of this equation yields the value of k_{nc} as,

$$k_{nc} = (3\phi_v - 1)k_p + [3(1-\phi_v) - 1]k_f + \sqrt{\Delta} \qquad (3.\ 23)$$

where

$$\Delta = (3\phi_v - 1)^2 k_p^2 + [3(1-\phi_v) - 1]^2 k_m^2 + 2[2 + 9\phi_v(1-\phi_v)]k_p k_m \qquad (3.\ 24)$$

where k_p is the thermal conductivity of the nanoparticle. Equation (3. 22) does not consider the effect of interfacial layers. In order to include the influence of the interfacial layers, consider each nanoparticle with radius of r to be covered with an interfacial layer of thickness t. The volume fraction of a nanoparticle in this structure, therefore, is

$$\phi_e = r^3 / (r+t)^3 \qquad (3.\ 25)$$

The effective thermal conductivity of the particle-interfacial layer structure for dead-end particles, k_{ed}, can be obtained by solving Equation. (3. 22) after necessary substitutions.

Then we get

$$\frac{k_{ed}}{k_{layer}} = \frac{k_p + 2k_{layer} + 2\phi_e(k_p - k_{layer})}{k_p + 2k_{layer} - \phi_e(k_p - k_{layer})} \qquad (3.\ 26)$$

The numerical steps for solving this equation are available in literature (Xue and Xu 2005). The results of the MD simulation performed by Liang and Tsai (2011) have shown that $k_{layer}=2k_m$ and $k_p=200k_m$. While incorporating the effect of interfacial layers we have to replace k_p and ϕ_{nc} in equation (3. 22) by k_{ed} and ϕ_{nc}/ϕ_e, respectively.

In the second level of homogenization in Prasher's model k_a, the effective thermal conductivity of the cluster sphere, including the particles belonging to the back-bone, is calculated assuming that the backbone is embedded in a medium with an effective thermal conductivity k_{nc} obtained from Equation (3. 21). A methodology to predict the effective thermal conductivity of particulate composites with interfacial thermal resistance following the effective medium approach, combined with interfacial thermal resistance, or Kapitza resistance, was developed by Nan *et al.* (1997). The details of Nan *et al.* 's model for effective thermal conductivity of nanosolids will be discussed in the next section. This approach has been able to predict the thermal conductivity of a composite medium with particle inclusions. When this model is adapted to a nanofluid system, the value of k_a, the effective thermal conductivity of the cluster sphere, can be obtained as

$$\frac{k_a}{k_{nc}}=\frac{3+\phi_c[2\beta_{11}(1-L_{11})+\beta_{33}(1-L_{33})}{3-\phi_c(2\beta_{11}L_{11}+\beta_{33}L_{33})} \tag{3. 27}$$

where, $L_{11}=0.5p^2/(p^2-1)-0.5p/(p^2-1)^{1.5}.\cosh^{-1}p$

$$p=R_a/r\ ;\ L_{33}=1-2L_{11}$$

$$\beta_{11}=(k_e-k_{dc})\Big/(k_{dc}+L_{11}(k_e-k_{dc}))$$

$$\beta_{33}=(k_e-k_{dc})\Big/(k_{dc}+L_{33}(k_e-k_{dc}))$$

However in back-bone structure of clustered sphere, the nanoparticles belonging to the backbone are so close to each other that the interfacial layers are connected to one another and they form a percolating network. Thus by assuming the nanoparticles in the backbone are embedded in the interfacial layer medium, we can also calculate the effective thermal conductivity of the backbone-interfacial layer structure k_e using the Bruggeman model (1935) as has been performed above. So we have

$$\phi_e\left(\frac{k_p-k_e}{k_p+2k_e}\right)+(1-\phi_e)\left(\frac{k_{layer}-k_e}{k_{layer}+2k_e}\right)=0 \qquad (3.\ 28)$$

While incorporating the effect of interfacial layers, the k_p and ϕ_c in Equation (3. 27) have to be replaced by k_e and ϕ_c / ϕ_e. By including the effects of particle clustering and interfacial adsorption layering, the expression for effective thermal conductivity based on EMT can be obtained as

$$\frac{k_{eff}}{k_m}=\frac{k_a+2k_m+2\phi_a(k_a-k_m)}{k_a+2k_m-\phi_a(k_a-k_m)} \qquad (3.\ 29)$$

This expression gives the effective thermal conductivity of nanofluids consisting of clustered nanoparticles with interfacial layers. Equations (3. 11), (3. 17) and (3. 29) have been used to evaluate the effective thermal conductivity of polymeric nanofluids in this work.

In this work we have presented the thermal conduction mechanisms in nanofluids by measuring the variations of effective thermal diffusivity with particle volume fraction using a thermal wave interference technique. Since the parameter measured is thermal diffusivity (α_{eff}), it is required to express thermal conductivity in terms of thermal diffusivity. These two are related through the following expression (Zhang *et al.,* 2006b),

$$\alpha_{eff} = {k_{eff}}/{\rho_{eff} c_{eff}} \quad (3.30)$$

where ρ_{eff} and c_{eff} defines the effective mass density and effective specific heat capacity of nanofluids. In an effective medium approach, these are given by

$$\text{where } \rho_{eff} = \phi_v \rho_p + (1-\phi_v)\rho_m \quad (3.31)$$

$$c_{eff} = \phi_w c_p + \left(1-\phi_w\right) c_m \quad (3.32)$$

Here ρ_p, ρ_m are the densities of the nanoparticle and base fluid respectively, and c_p and c_f are the specific heat capacities of the nanoparticle and the base fluid respectively. These expressions also follow from the respective effective medium approximations.

By analyzing the experimental results obtained with polymeric nanofluids, we have tried to describe the effective thermal conductivity of a polymeric nanofluid by comparing the experimental results with the corresponding ones calculated using the above mentioned theoretical models (Equations (3. 11), (3. 17) (3. 29) and (3. 30)). Our experimental results agree best with the conventional mean field theory with an essential concept of interfacial layering. The detailed descriptions of the experimental results on thermal conduction properties of polymeric nanofluids obtained as a function of nanoparticle volume fraction and nanoparticle sizes are presented in the following chapters.

3.4 Thermal conduction in polymeric nanosolids

While comparing thermal conduction properties of polymeric nanofluids with values derived from the above described theoretical models, it can be

clearly seen that the mechanisms which mainly control the effective thermal properties of liquid composites is the diffusion of thermal waves through the solid inclusions. But in the case of a solid composite mixture the situation is rather different especially in the case of a polymeric nanosolid material obtained by condensing the respective polymeric nanofluid. In a nanosolid material another mechanism which works dominantly in transporting thermal energy is the scattering of thermal waves at matrix-particle interfaces. This is due to the smaller dimensions of the solid particle inclusions compared to the mean free path of phonons in the solid matrix. The interfacial thermal wave scattering, demonstrated pictorially in Figure 3.3, causes an interfacial thermal resistance, known as Kapitza resistance R_k, which constitutes a barrier to heat flow at the nanoparticle-matrix boundaries. The magnitude of the Kapitza resistance at an interface can be estimated following an acoustic mismatch model (AMM) or a diffusion mismatch model (DMM). Even while phonons are backscattered from the interfaces, normal thermal diffusions through the nanoparticles do occur as demonstrated in Figure 3. 3. This can be accounted for in terms of the transmission probability of the propagating thermal waves through the dispersed nanoparticles in the host matrix. The strength of diffusion would be greater at an interface of a nanoparticle with higher mass density and thermal conductivity (higher transmission probability), compared to the host matrix, while back scattering would be predominant when the nanoparticles have a lower mass density and thermal conductivity (lower transmission probability). While dealing with a nanosolid consisting of nanoparticles embedded in a base material like a polymer, a combination of above two mechanisms (diffusion and scattering) will control the overall thermal conduction in the material.

In the present work on thermal conductivity of nanosolid materials obtained by condensing nanofluids we have tried to establish the validity of our experimental results by combining relevant theoretical models which include the modified form of the Maxwell-Garnett effective medium model for this special material. We have employed a modified EMT which takes into account

(i) Thermal diffusion through the constituent phases of the composite medium, and

(ii) Interfacial scattering of thermal waves at matrix-particle interfaces.

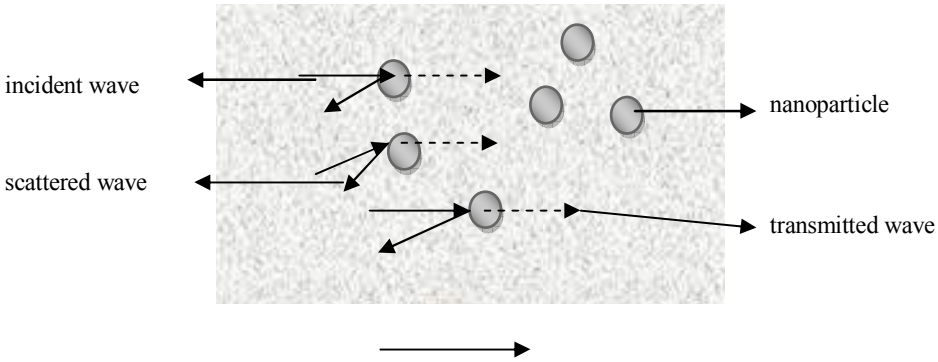

Figure 3.3: Demonstration of heat flow in a nanosolid, controlled by interfacial scattering at matrix-particle interfaces and diffusion through particles

We have followed the modified model based on EMT, including the above two mechanisms. These mechanisms have been considered earlier for other systems by previous workers; interfacial scattering by Nan *et al.* (1997) for composites in which the phonon mean free path are greater than the size of constituent phases and diffusion by Cheng and Vachon (Cheng and Vachon, 1969) for general solid composite mixtures. We have employed Nan's model (Nan *et al.,*1997) for describing the scattering part of thermal conduction mechanisms through polymeric nanosolids. The role of thermal diffusion mechanisms has been included in the Cheng-Vachon model (Cheng and Vachon, 1969; Shabde *et al.,* 2006). An expression for the overall thermal

conductivity of polymeric nanosolids has been derived combining these two mechanisms and adopting these to polymeric nanosolids.

3. 4. 1 EMT in the limit of diffusion

As mentioned earlier, thermal diffusion through the particles play a significant role in determining the thermal conduction in a nanosolid sample. Conventionally, for a two component mixture, earlier researchers have generally tried models such as the series and parallel resistance models to describe effective thermal conductivity of composites. Cheng and Vachon (1969) proposed a modified form of effective medium theory following an analogy between heat flow and electric current flow to express the effective thermal conductivity of a composite as determined by thermal diffusion. Cheng and Vachon started their theoretical formalism by modifying Tsao's model (Tsao, 1961) for predicting the thermal conductivity of a two phase material. This model assumes a discontinuous material phase (one component) dispersed in a continuous material phase. They have assumed a parabolic distribution of the discontinuous phase in the background matrix. The constants of the parabolic distribution are determined by a numerical analysis and are presented as a function of the volume fraction of the discontinuous phase. The equivalent thermal conductivity of a unit cube of the mixture is derived in terms of a distribution function, and the thermal conductivity of the constituents. In order to derive the expression for effective thermal conductivity of a two component heterogeneous mixture, Cheng and Vachon model makes the following assumptions.

For a unit cube of the mixture in an x-y-z co-ordinate system

(i) the heat flux is unidirectional in the x-direction,

(ii) thermal convection and radiation are negligible,

(iii) contact resistance between the continuous and discontinuous phases is negligible,

(iv) no porosity exists in the mixture,

(v) the discontinuous phase is uniformly dispersed in the continuous phase,

(vi) thermally, the mixture is isotropic,

(vii) in a mechanical mixing process, no chemical reaction occurs.

Assume that the unit cube cell of the nanosolid is sliced into differential elements of width *dx* which are perpendicular to the direction of the heat flow. Here it is assumed that *dx* is parallel to the *y-z* plane. A two dimensional picture of this assumption is shown in Figure 3. 4.

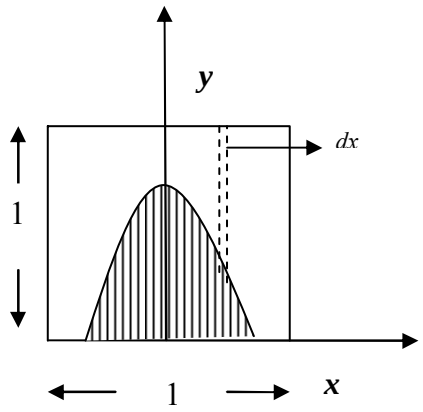

Figure 3.4 Model used for the study of the thermal conductivity of a two-phase mixture.

Here the thermal conductivity of the composite medium is evaluated in terms of *y(x)* in the configuration given in Figure 3.4. It can be shown the equivalent resistance of the solid composite as per the configuration given in Figure 3.4 is;

$$R_e = \int_0^x \frac{dx}{k_m + (k_p - k_m)y} + \frac{1-2x}{k_m} \tag{3.33}$$

and thermal conductivity k_{eff1} is given by,

$$k_{eff1} = \frac{1}{R_e} \tag{3.34}$$

Here $y(x)$ represents the volume fraction of dispersed discontinuous phase. It is a normal distribution curve due to the assumed randomness of the discontinuous phase embedded in the continuous phase. Thus,

$$y = C\exp(-C_2 x^2) \tag{3.35}$$

$$y = C_1\left(1 - C_2 x^2 + \frac{C_2^2 x^4}{2!} - \ldots\ldots\right) \quad \text{for } -1/2 \le x \le +1/2 \tag{3.36}$$

$$\text{or } y = B + Cx^2 \tag{3.37}$$

Thus the normal distribution can be reduced into a parabolic distribution. So it is possible to express the constants B and C as a function of the given volume fraction of ϕ_v of the discontinuous phase. Since the discontinuous volume fraction would be a known volume for a given two phase mixture, we can write

$$\phi_v = 2\int_0^{1/2} y.dx \tag{3.38}$$

In order to evaluate B and C one can apply the following boundary conditions,

$$y = 1 \quad \text{at} \quad x = 0$$

and

$$y = 0 \quad \text{at} \quad x = 1/2$$

This represents the maximum volume fraction for the discontinuous phase.

Equation (3. 37) is an even function of x, hence only the positive value of x need to be considered. i. e $0 \le x \le 1/2$. Applying this boundary conditions, one obtain B=1 and C= - 4.

Now, the maximum volume fraction ϕ_v of the discontinuous phase is calculated to be 0. 669 which is the maximum volume fraction for discontinuous phase which equation (3. 37) can accommodate. The boundary conditions will change as ϕ_v deviates from the maximum value.

When $\phi_v < 0.669$, the general conditions are,

$$y = B + Cx^2 \text{ at } |x| \le a \le 1/2 \ ,$$

$$y = 0 \text{ at } a \le |x| \le 1/2 \ , \text{ and}$$

$$y < 1 \text{ at } x = 0$$

It is easy to show that, $B = -4/C$

Thus it is possible to calculate B and C in terms of ϕ_v as follows;

$$\phi_v = 2 \int_0^{B/2} y.dx$$

$$= 2 \int_0^{B/2} (B + Cx^2) dx$$

$$= \frac{2B^2}{3} + C'$$

$$\text{Or } B = \sqrt{\left(3\phi_v / 2\right)} \qquad \text{and} \quad C = -4\sqrt{2/3}\,\phi_v$$

This is the situation when a two-phase mixture is reduced to the limiting case of single phase when $y = 0$ at $x = 0$ and $\phi_v = 0$. Substituting Equation (3. 37) in (3. 33) and letting $C=C'$ since C<0 yield

$$\mathrm{R_e} = 2\int_0^{B/2} \frac{dx}{[k_m + B(k_p - k_m)] - C(k_p - k_m)] - C(k_p - k_m)x^2} + \frac{1-B}{k_m} \qquad (3.\ 39)$$

Rearranging the first term in the denominator of Equation (3. 39), one gets

$$k_m + B(k_p - k_m) = Bk_p + k_m(1-B),$$

which is always greater than zero since B varies from 0 to 1. Integration of Equation (3. 39) resulting in the effective thermal conductivity (k_{eff1}) due to diffusion of thermal waves through nanoparticles having volume fraction ϕ_v.

Consider the following two cases.

(i) $k_m > k_p$

In this case Equation (3. 39) reduces to

$$k_{eff\,1} = R_e^{-1} = \frac{2}{\sqrt{C(k_m - k_p)}} \times \arctan\left(\frac{B}{2}\sqrt{\frac{C(k_m - k_p)}{k_p + B(k_m - k_p)}} + \frac{1-B}{k_m}\right) \qquad (3.\ 40)$$

(ii) $k_m < k_p$

In this case Equation (3. 39) reduces to

$$\frac{1}{k_{eff1}} = \frac{1}{\sqrt{C(k_m - k_f)(k_m + B(k_f - k_m))}} \ln \frac{\sqrt{k_m + B(k_f - k_m)} + 0.5B\sqrt{(C(k_m - k_f))}}{\sqrt{k_m + B(k_f - k_m)} - 0.5B\sqrt{(C(k_m - k_f))}} + \frac{1-B}{k_m} \quad (3.41)$$

Equations (3. 40) and (3. 41) express the effective thermal conductivities of medium embedded with particles. This model describes the effective thermal conductivity of composites as an overall effect of thermal diffusion among spherical nanoparticles distributed parabolically in a continuous base matrix.

3. 4. 2 EMT in the limit of interfacial scattering

As has been outlined earlier, while dealing with nanoparticle inclusions in a continuous base matrix, thermal wave scattering plays a significant role in determining the effective thermal conductivity of nanosolids. So we have employed a modified effective medium theory (EMT) including the contributions from interfacial thermal wave scattering, proposed earlier by Nan *et al.* (1997), to describe the role of thermal wave scattering at matrix-particle interfaces on the effective thermal conductivity of these nanosolids. Nan *et al.* modified Maxwell's model including the concept of interfacial thermal resistance to describe the thermal conductivity of a two-component composite (Nan *et al.,* 1997), under the following basic assumptions.

(i) A composite material consists of different constituent phases; the different mechanical or chemical adherences at the interfaces, as well as thermal expansion mismatch result in the scattering of thermal waves at the interfaces.

(ii) Scattering rates at the interfaces vary with the aspect ratio (ratio of the longitudinal to transverse dimensions) of the dispersed particles.

(iii) The interfacial thermal resistance influences the total thermal conductivity of the composite significantly.

In order to obtain an expression for thermal conductivity, this model considers a composite medium with multiple scatterers in the medium. In such a situation the thermal conductivity inside the composite varies from point to point. The variations in thermal conductivity can be written as,

$$k\ (r) = k^0 + k'(r) \tag{3. 42}$$

where k^0 is the constant part of the thermal conductivity for the homogeneous medium and $k'(r)$ is the arbitrary fluctuating part. Using Green's function G for a homogeneous medium defined by k^0 and the transition matrix T for the entire composite medium, a rigorous solution for the distribution of the temperature gradient can be obtained. The resulting effective thermal conductivity k^* is given by

$$k^* = k^0 + \langle T \rangle (I + \langle GT \rangle)^{-1} \tag{3. 43}$$

where I is the unit tensor and, symbol $\langle\ \rangle$ denotes spatial averaging. The matrix T is

$$T = \sum_n T_n + \sum_{n,m \neq n} T_n G T_m + ..., \tag{3. 44}$$

Here the first term is the sum of the T matrices of n particles and the succeeding term represents the interaction between particles. An accurate calculation of T is a formidable problem. For simplicity of calculation we approximate T as,

$$T \cong \sum_n T_n = \sum_n K_n' (I - GK_n')^{-1} \tag{3. 45}$$

there by neglecting inter-particle multiple scattering. Obviously, this approximation is valid only when the inclusion particles are dispersed uniformly in the base matrix.

Now, let us consider an ellipsoidal particle in the matrix, which is surrounded by a semisolid interface layer of thickness δ and thermal conductivity k_s, as a composite unit cell. Substituting $k^0 = k_s$ we directly obtain the equivalent thermal conductivities k_{ii}^C ($i=1, 2, 3$) along the X_i' symmetric axis of this ellipsoidal composite unit cell as

$$k_{ii}^{\,c} = k_s \frac{k_s + L_{ii}(k_p - k_s)(1-u) + u(k_p - k_s)}{k_s + L_{ii}(k_p - k_s)(1-u)} \qquad (3.46),$$

with

$$u = a_1^2 a_3 / (a_1 + \delta)^2 (a_3 + \delta) ,$$

Here k_p is the thermal conductivity of the ellipsoidal particle; a_1 and a_3 are respectively, the radii of the ellipsoid along the X_1' and X_3' axes; and L_{ii} are the well known geometrical factors dependent on the particle shape, and are given by (Nan et al. 1997)

$$L_{11}=L_{22} = \frac{p^2}{2(p^2-1)} - \frac{p^2}{2(p^2-1)^{3/2}} \cosh^{-1} p \quad \text{for } p > 1, \qquad (3.47)$$

and

$$= \frac{p^2}{2(p^2-1)} + \frac{p^2}{2(p^2-1)^{3/2}} \cosh^{-1} p \quad \text{for } p < 1 \qquad (3.48)$$

Also, $L_{33} = 1 - 2L_{11}$.

In the above expressions, $p = a_3/a_1$ is the aspect ratio of the ellipsoid, and $p > 1$ and $p < 1$ are for a prolate ($a_1 = a_2 < a_3$) and an oblate ($a_1 = a_2 > a_3$) ellipsoidal inclusion, respectively.

By ultimately passing to the limit that $\delta \to 0$ at $k_s \to 0$, the interfacial thermal resistance is thought of as the limiting case of heat transport across bulk phase by a thin, poorly conducting interface region, we rewrite Equation. (3. 46) as

$$k_{ii}^{C} = k_p / (1 + \gamma L_{ii} k_p / k_m) \tag{3. 49}$$

with

$$\left.\begin{aligned} &\gamma = (2 + 1/p)\alpha \ , \text{ for } p \geq 1 \\ &\text{and, } \gamma = (1 + 2p)\alpha \ , \text{ for } p \leq 1 \end{aligned}\right\} \tag{3. 50}$$

Here a dimensionless parameter, α, is introduced, which is defined by

$$\left.\begin{aligned} &\alpha = a_k / a_1 \text{ for } p \geq 1 \\ &\alpha = a_k / a_3 \text{ for } p \leq 1 \end{aligned}\right\} \tag{3. 51}$$

where a_k is the Kapitza radius defined by $a_k = R_{bd} k_m$, where R_{bd} is the interfacial Kapitza resistance, and k_m is the thermal conductivity of the host matrix phase.

When the inclusions become spheres, $p=1$, so that

$L_{11}=L_{33}=1/3$, and $\langle \cos^2 \theta \rangle = 1/3$;

then Equation (3. 49) reduces to

$$K_{11}^{C} = K_{22}^{C} = K_{33}^{C} = k_p / (1 + \alpha k_p / k_m)$$

and thermal conductivity limited by interfacial scattering is then given by,

$$k_{eff\,2} = k_m \frac{k_p(1 + 2\alpha) + 2k_m + 2\phi_v[k_p(1 - \alpha) - k_m]}{k_p(1 + 2\alpha) + 2k_m - \phi_v[k_p(1 - \alpha) - k_m]} \tag{3. 52}$$

This expression represents the thermal conductivity under the effective medium approximation including interfacial thermal resistance. It is evident that a large enough value for α can give rise to a de-enhancement in the effective thermal conductivity for a nanosolid of this type. Here also assuming an analogy between thermal conductivity and electrical conductivity we can also express k_{eff2} in terms of corresponding resistance value as expressed in the diffusion limited case.

3. 4. 3 Overall effective thermal conductivity of a nanosolid

From the foregoing discussions we can see that it is possible to combine the resistance due to diffusion and scattering of thermal waves at the interfaces. We define the overall conductivity of a polymeric nanosolid as a combined effect of the mechanisms described by Equations (3. 41) and (3. 52). Assuming that the two mechanisms work in parallel we can write the effective thermal conductivity of a nanosolid as

$$k_{ns} = \frac{k_{eff1} * k_{eff2}}{k_{eff1} + k_{eff2}} \tag{3. 53}$$

In this work we have employed Equation (3. 53) to compute and discuss the variations in effective thermal properties of polymeric nanosolids. Experimental and theoretical variations of the thermal conduction properties of polymeric nanosolids are presented and discussed in chapter 6.

Chapter 4

Thermal conduction in Polymeric and water based nanofluids

4.1 Introduction

As discussed in previous chapters, great deal of studies has been carried out by earlier researchers to determine the thermal conductivity of nanofluids for the past two decades. Most of the experimental studies and theoretical analysis in this field have been focused to determine the thermal conductivity of nanofluids consisting of metallic or metallic oxide nanoparticle suspensions in low molecular weight base fluids such as water, Ethylene Glycol etc. In order to measure thermal conductivity of nanofluids, previous workers have used different experimental techniques such as transient hot wire technique, steady state technique, optical beam deflection technique etc. Researchers have prepared nanoparticles of different materials like metals, metallic oxides, alloys etc. which are the prime components that determine the effective thermal conductivity of nanofluids. As mentioned in chapter 1, the preparation of nanofluids for experimental analysis has been done either by single step or two step method. Most of the metallic nano suspensions such as Cu/water, Cu/Ethylene Glycol etc. have been prepared following the single step method (Zhu *et al.,* 2004). The metallic oxides suspensions like TiO_2/water, Al_2O_3/water and CuO/water etc. have been prepared following the two step method (Kwak and Kim, 2005).

In this chapter we present and discuss the variations of thermal conductivity of polymeric nanofluids with particle loading that have been measured by a Thermal Wave Interferometer. Experimentally our approach is different from that of previous authors (Murshed *et al.,* 2005; Wang *et al.*, 1999; Xie *et al.*, 2002a). Here we determine the thermal diffusivity rather than thermal conductivity to define the thermal conduction properties of nanofluid samples. This is because of the fact that thermal diffusivity measures the speed with which thermal waves propagate through a sample. Thermal diffusivity measurements are more accurate than thermal conductivity measurements as the former one is independent of the heat losses from the sample. In the present work we have investigated thermal conduction properties of polymer based nanofluids as well as water based nanofluids. The details of the thermal wave interference method to measure thermal diffusivity of nanofluids have already been described in chapter 2.

In a polymeric nanofluid, the base fluid is a polymer liquid with very high molecular weight (> 100,000 g/mol) so that the interaction between nanoparticles and the base fluid molecules are entirely different from their low molecular weight counterparts. The adsorption of base fluid molecules around nanoparticles is a strong function of the molecular weight of the base fluid. In this chapter we present the results of the investigation on the effect adsorption of polymer molecules around nanoparticles on the thermal conductivity of these nanofluids. The details of preparation of nanofluid systems that we have selected for experimental studies are described in the following sections.

4.2 Systems selected and preparation of nanofluids

Two sets of polymer based nanofluid samples, each with different nanoparticle concentrations, were prepared for the measurements reported in this

chapter. These were, TiO_2/PVA nanofluids prepared by uniformly dispersing TiO_2 nanoparticles in Poly vinyl alcohol (PVA) acting as base fluid and Cu/PVA nanofluids with copper nanoparticles dispersed uniformly in Poly vinyl alcohol. TiO_2 and copper nanoparticles were selected because they have wide difference in thermal conductivity in their respective bulk forms, and we wanted to bring out the effect of particle thermal conductivity on the interfacial thermal resistance and its effect on overall thermal conductivity. The preparation of these nanofluids has been done following a two step method. In a two step method, the first step involves the preparation of nanoparticles and the second step is the dispersion of desired concentration of nanoparticles in the base fluid.

4.2.1 Preparation of TiO_2 nanoparticles

Various synthesis methods such as hydrolysis (Chhabra *et al.*, 1995), sol-gel (Lal *et al.*, 1988; Campbell *et al.*, 1992; Selvaraj *et al.,* 1992), micro emulsion or reverse micelles (Sugimoto *et al.*, 1997; Kumazava *et al.*, 1993; Basca and Gratzel, 1996), and hydrothermal synthesis (Kutty *et al.,* 1988; Qian *et al.,* 1993) have been used to prepare nanoparticles of titanium dioxide. Compared to other methods, hydrolysis could be carried out at conditions close to ambient to produce nanoparticles of TiO_2. The nanocrystalline anatase titanium dioxide powder reported in this study was prepared by the hydrolysis of $TiCl_4$ at room temperature (Reddy *et al.*, 2001). Titanium tetrachloride (98% Sigma Aldrich) was used as the starting material without any further purification. When $TiCl_4$ was dissolved in water, the heat of exothermic reaction effects the formation of orthotitanic acid [Ti (OH) $_4$]. Since the formation of the species disturbed homogeneous precipitation, appreciable amount of $TiCl_4$ was initially digested in hydrochloric acid and then diluted in distilled water; all these while keeping the reaction vessel in ice-water bath. The

concentration of titanium tetrachloride was adjusted to 3M in water. The initial p^H was found to be about 1.8. A solution of hydrazine hydrate H_6N_2O in water (5M) was added drop wise to the solution until the final p^H was about 8.0. The hydrolysis and condensation reaction started immediately upon mixing, as indicated by the rapid increase in turbidity and the formation of large flocs, which precipitated to the bottom of the reaction vessel. The mixture was kept under high-speed constant stirring on a magnetic stirrer for 1 hour at room temperature. Subsequently, the precipitated titanium dioxide ($TiO_2.nH_2O$) was filtered and repeatedly washed with hot distilled water to make $TiO_2.nH_2O$ free of chloride ions. The hydrous oxide was dried at 90-100^{0}C over night and then grounded to a fine powder. Then polycrystalline titanium dioxide powders were then calcined at 100, 200, 300, 400, 500, or 600^{0}C for 2 hours to observe the phase changes accompanying heat treatments. Here we preferred nanofluids with different concentrations of nanoparticles having same particle size. To fulfill our requirement we have calcined the titanium dioxide powders at 200^{0}C to get the crystalline size as minimum as possible. After calcination, X-ray Powder diffraction (XRD) technique was used for crystal phase identification and estimation of particle size. The X-ray diffraction measurements were performed with a Bruker Model AXS D8 Advance X-ray Powder diffractometer. The X-ray diffraction pattern obtained for TiO_2 nanopowders calcined at 200^{0}C is shown in Figure 4.1. The structural analysis performed using this XRD pattern helped the phase identification of nanocrystals of this anatase TiO_2. From the line broadening of corresponding X-ray diffraction peaks and using Scherrer formula (Equation 2.3), nanoparticle size *d* has been estimated (Cullity, 1978)

$$d = \frac{0.9\lambda}{B\cos\theta_B} \qquad (2.3)$$

where λ=0.154 nm is the wavelength of the X-ray radiation, B is the line width at half maximum height and θ_B is the diffracting angle. The estimated average size of the titanium dioxide powders calcined at 200^0C is ~ 15 nm.

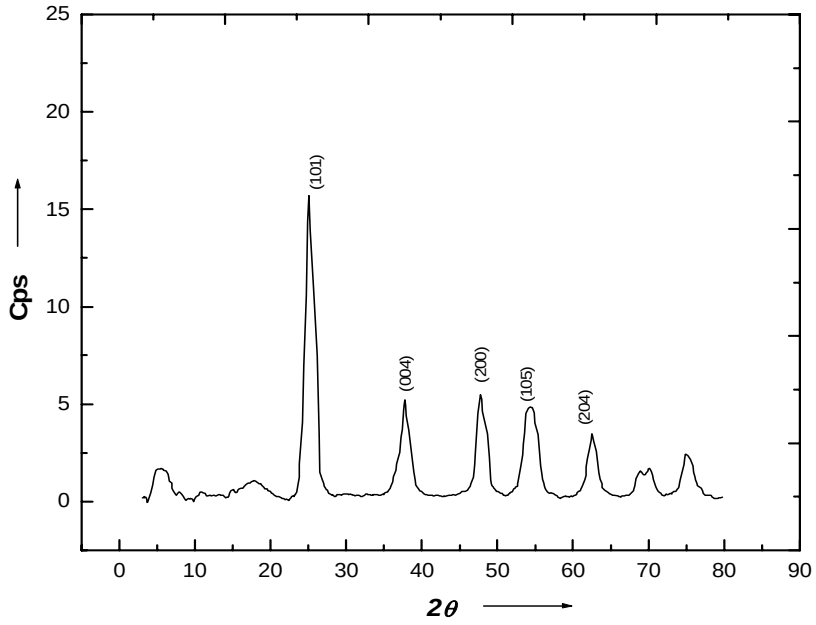

Figure 4.1 XRD pattern of TiO_2 calcined at 200^0C

4.2.2 Preparation of copper nanoparticles

We have prepared copper nanoparticles following a chemical reduction method. The main steps in the synthesis of copper nanoparticles following the chemical reduction method are described below. Considerable attention has been paid to metallic copper nanoparticles in the past two decades due to their unusual properties and potential applications in many fields (Lu *et al.,* 2000; Tatasov *et al.,* 2002). A number of methods such as micro emulsion (Qi *et al.,* 1997), reverse micelles (Lisiecki *et al.,* 1995), reduction of aqueous copper salts (Zheng *et al.,* 1998), UV light irradiation (Kapoor *et al.,* 2002), γ- irradiation (Joshi *et al.,* 1998) etc. have been developed for the preparation of metallic

copper nanoparticles. Among the various methods, chemical reduction of copper salts with hydrazine or hydrogen in aqueous systems has been known for nearly a hundred years. In the present work, we have prepared copper nanoparticles by a chemical reduction of Ethylene glycol in the presence of hydrazine (Zhu *et al.*, 2005). In a typical procedure, 20 ml Ethylene glycol (EG) solution (0.1M) of $CuSO_4.5H_2O$ was mixed with 20 ml Ethylene Glycol mixed

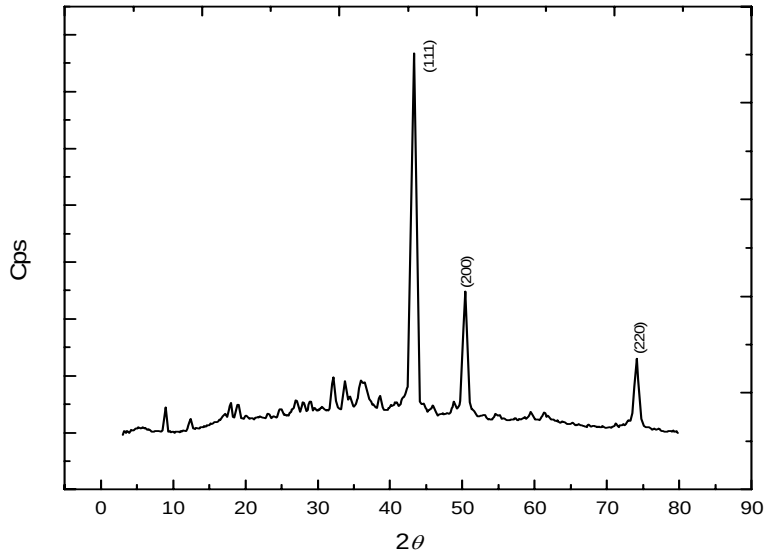

Figure 4.2 XRD pattern of copper nanoparticles obtained by the chemical reduction method

solution of NaOH and $N_2H_4.H_2O$ under magnetic stirring. The molar ratio of $N_2H_4.H_2O$/ $CuSO_4$ was 1.5 and molar ratio of NaOH/$CuSO_4$ was 0.05. The solution mixture was placed in a microwave oven (2.45GHz, Galanz WP750) and reacted under a medium power of 750W. After cooling to room temperature the mixture was filtered, washed in ethanol and dried to obtain copper nanopowders. The structure analysis performed using X-ray Powder diffractometer helped phase identification and particle size determination of these metallic nanoparticles. The XRD pattern obtained for copper

nanoparticles is shown in Figure 4.2. The line broadenings in the XRD pattern give the average nanoparticle size as ~ 16 nm. The phase analysis by XRD revealed that FCC metal Copper was the only phase in the prepared nanopowder. No oxides or hydroxides were found.

The second step in the two step method included the dispersion of TiO_2 or copper nanoparticles in Poly Vinyl alcohol. The details of the dispersing nanoparticles in Poly Vinyl alcohol can be found in the following sections.

4.2.3 Dispersion of nanoparticles in Poly Vinyl Alcohol

In order to obtain the TiO_2/PVA and copper/PVA (or Cu/PVA) nanofluids for experimentation, we dispersed desired mass fractions of TiO_2 and copper nanoparticles in PVA. Here the base fluid selected is Poly Vinyl alcohol (PVA) having high molecular weight of the order of 1, 25,000 g/mol. The PVA base fluid was prepared by mixing PVA granules in water under constant stirring for several hours. The degree of hydrolysis of PVA used was about 90%. Nanoparticles of desired mass fraction were added to the base fluid, thoroughly mixed and sonicated for several hours to obtain highly uniform nanofluid samples for experimentation. The thermal conduction properties such as thermal conductivity and thermal diffusivity of these nanofluids samples were measured using the thermal wave interferometer described in chapter 2. In the following sections we discuss the details of the experimental methods and the results obtained in these polymeric nanofluids prepared by two step method.

4.3 Experimental details

A thermal wave resonant cavity (TWRC) cell has been set up to measure the thermal diffusivity of the prepared nanofluids by forming thermal wave interference peaks in the cavity (Shen *et al.*, 1996; Shen and Mandelis, 1995). Detailed descriptions of the Thermal Wave Interferometer and the experimental

procedure to measure the thermal diffusivity of nanofluids are given in chapter 2. The determination of thermal diffusivity of nanofluids has been done by performing the cavity length scan experiment. To determine the thermal diffusivity of a nanofluid, a desired volume (< 1ml) of the nanofluid was filled inside the Thermal Wave Resonant Cavity. Cavity length scan was performed with the help of a stepper motor controller and a computer, and the thermal wave interference peaks were detected. The cavity lengths corresponding to successive thermal wave interference maxima or minima have been used to determine the thermal diffusivity of nanofluid samples (Equation (2.15)).

The thermal wave interference patterns that have been used to determine the thermal diffusivity of two typical concentrations of TiO_2/PVA and Cu/PVA nanofluids are shown in Figures 4.3(a) and 4.3(b) respectively. Positions of thermal wave interference peaks are different for metallic and nonmetallic nanofluids as these are determined by the magnitude of the thermal diffusivity of the fluid. This also varies with volume fraction of dispersed nanoparticles. The detection of thermal wave interference peaks for thermal diffusivity measurements have carried out in a vibration free environment because an external vibration can change the positions of consecutive maxima and minima in a thermal wave interference pattern. So we have taken all precautions to obtain a well sustained thermal wave interference pattern. For this we have designed our whole experimental set up (as shown in Figure 2.6) in a vibration free table for thermal diffusivity measurement of nanofluids. The vibration free table protects the resonant cavity from the disturbances produced due to external physical movements, vibration produced due to the working of any other equipment such as air conditioner, exhaust fan, ceiling fan etc. In order to nullify the effect of other external noises we switched off all noisy devices to produce a vibration free environment for the measurement.

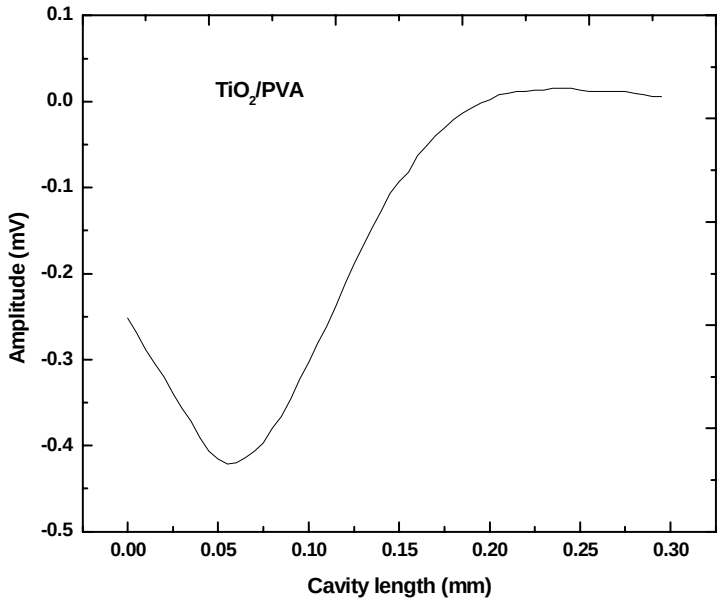

Figure 4.3 (a) A typical thermal wave interference pattern obtained for volume concentration 0.1% of TiO_2 nanoparticles dispersed in PVA (TiO_2/PVA nanofluid).

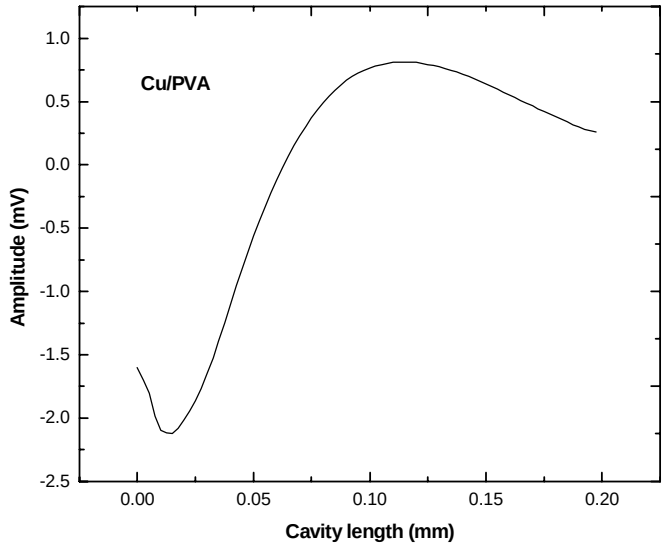

Figure 4.3 (b) A typical thermal wave interference pattern obtained for volume concentration 0.1% of Cu nanoparticles dispersed in PVA (Cu/PVA nanofluid).

From the experimental values of thermal diffusivity, the thermal conductivity of these nanofluids have also been determined by multiplying the diffusivity values with the effective mass density and specific heat capacity of the respective nanofluids.

If α_{eff} represents the experimental value of effective thermal diffusivity, then the value of effective thermal conductivity k_{eff} is given by Equation (3.30),

$$k_{eff} = \alpha_{eff} \rho_{eff} c_{eff}$$

Here ρ_{eff} and c_{eff} respectively represent the values of effective mass density and specific heat capacity of nanofluids. ρ_{eff} and c_{eff} can be evaluated from the density and specific heat values of the nanoparticles and base fluid using the following relations.

$$\rho_{eff} = \phi_v \rho_p + (1 - \phi_v) \rho_m \tag{3.31}$$

$$c_{eff} = \phi_w c_p + (1 - \phi_w) c_m \tag{3.32}$$

Parameter ϕ_v stands for the particle volume fraction and ϕ_w for the particle mass fraction, and the subscripts p and m stand for the particle and the base fluid (or the base matrix) respectively. Then the normalized values of thermal diffusivity/conductivity have been determined as the ratio of the effective thermal diffusivity of nanofluid to the corresponding base fluid thermal diffusivity/conductivity.

The uncertainty in the measurement of thermal diffusivity (or thermal conductivity) of a particular concentration of nanofluid has been obtained by performing the repeat measurements. Here the uncertainty of the measurement is obtained as the standard deviation of set of thermal diffusivity values obtained as a result of repetition of the cavity length scan experiment for a

particular concentration of nanofluid. Then we have assumed a rectangular distribution to estimate the mean value of the thermal diffusivity/thermal conductivity of the nanofluid measured following thermal wave interference technique. Rectangular distribution indicates the possibility for the diffusivity value to occur between an upper and lower value which is decided by the measurement uncertainty. For example, in the case of TiO_2/PVA nanofluid system the estimated uncertainty in thermal diffusivity value is ±0.9%.

4.4 Results

The results of measurement of thermal diffusivity/conductivity of TiO_2/PVA and Cu/PVA nanofluids are presented in the following sections. While discussing the results on the thermal conduction properties of polymeric nanofluids, we have compared the experimental values of thermal diffusivity and thermal conductivity with theoretical values obtained from various theoretical models published earlier, which consider the effects of interfacial layers and nanoparticle clustering (Maxwell, 1873; Yu and Choi, 2004; Liang and Tsai, 2011).

4.4.1 Thermal conduction in TiO_2/PVA nanofluid

TiO_2/PVA nanofluids are obtained by dispersing a desired concentration of TiO_2 nanoparticles of average size ~ 15 nm in Poly Vinyl alcohol (PVA). We have prepared TiO_2/PVA nanofluids having different concentrations of TiO_2 nanoparticles to study the variations of their effective thermal conductivity and thermal diffusivity with particle volume fraction. The experimental and theoretical variations of effective thermal conductivity and effective thermal diffusivity as a function of nanoparticle volume fraction are as shown in Figure 4.4(a) and 4.4(b). The theoretical variations of thermal properties shown in Figures 4.4(a) and 4.4(b) have been plotted following three models described in

chapter 3, viz. modified form of Maxwell model (1873), model proposed by Yu and Choi (2003) and the model proposed by Liang and Tsai (2011).

While Maxwell's model assumes effective thermal transport in mixtures as essentially diffusive, modifications to this model considers effects like formation of adsorption layer around the nanoparticles, and the consequent interfacial effects at fluid-particle boundaries, and nanoparticle clustering in the fluid medium to describe the effective thermal conductivity of these nanofluids. The model developed by Yu and Choi (2003) considers the effect of adsorption layer around the nanoparticles in modifying the effective thermal conductivity of nanofluids, while the model based on molecular dynamics, recently developed by Liang and Tsai (2011) considers the formation of adsorption layers around particles and the particles forming clusters embedded in interfacial fluid shells. In a two component mixture consisting of particles dispersed in a high molecular weight polymeric fluid such as PVA the adsorption of liquid molecules around solid medium is a pre-defined phenomenon (Becker *et al.*, 1989), which cannot be neglected. So we have compared our experimental results with these models to arrive at conclusions on the effective thermal conductivity of polymeric nanofluids. The theoretical values of thermal diffusivities have been determined from the corresponding thermal conductivities calculated following these models. Evaluations of thermal conductivity/diffusivity based on the above three models, described by Equations. (3.11), (3.17) and (3.29), have been carried out for three values of adsorption layer thickness, viz. 1, 3 and 5 nm. This limit of layer thicknesses has been set based on the hydrodynamic model described in chapter 3. It is found that the best agreement with experimental values are obtained with $t = 3$ nm for TiO_2/PVA nanofluid system.

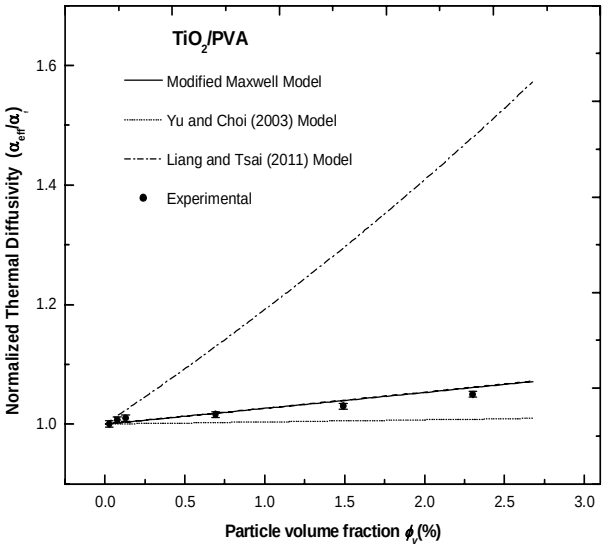

Figure 4.4(a): The variations of normalized thermal diffusivity of TiO_2/PVA nanofluids with volume fraction of nanoparticle. Experimental points as well as comparison with different theoretical models are shown.

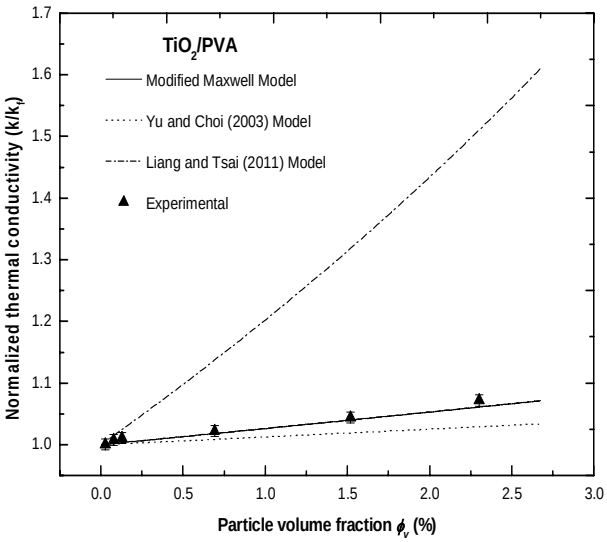

Figure 4.4(b) The variations of normalized thermal conductivity of TiO_2/PVA nanofluids with the volume fraction of nanoparticle. Experimental points as well as comparison with different theoretical models are shown.

For TiO_2/PVA nanofluids the experimental points agree best with the modified model based on the Maxwell's theory, which considers the nanofluid system as a uniform mixture of the base fluid, solid nanoparticles and interfacial adsorption layers formed at the boundary between the nanoparticles and base fluid. The interfacial adsorption layer around the particles acts as a thermal bridge between the nanoparticle and base fluid. The percolation network created by these interfacial thermal layers enhances the overall thermal conductivity of the nanofluid. The enhancement in effective thermal diffusivity obtained in this case is about 5 % at a particle volume fraction of 2.4%, while the corresponding enhancement in thermal conductivity is about 7%. This enhancement in thermal conductivity, as per the original Maxwell's theory (without considering adsorption layers), is only about 2%. This extra enhancement can be considered as due to enhanced thermal conduction through the interfacial adsorption layers.

4.4.2 Thermal conduction in Cu/PVA nanofluid

We have also prepared Cu/PVA nanofluids by dispersing desired volume fractions of copper nanoparticles of average size ~ 16 nm in PVA. We have varied the concentration of copper nanoparticles in PVA to get the respective variations of normalized thermal diffusivity and thermal conductivity of these nanofluids with particle volume fraction. The variations of normalized thermal diffusivity and thermal conductivity of these nanofluids are shown in Figure 4.5(a) and 4.5(b) along with the corresponding theoretical variations obtained using the theoretical models discussed earlier.

In the case of Cu/PVA nanofluid system, the maximum enhancement in effective thermal diffusivity obtained is about 30% at a particle volume fraction of

1.3%, while the corresponding enhancement in thermal conductivity is about 33%. These enhancements as per the original Maxwell's model are only about 4% and 5% respectively. The experimental variations of thermal diffusivity and conductivity agree best with the theoretical values obtained based on the model of Liang and Tsai (2011). According to this model also the main cause of thermal

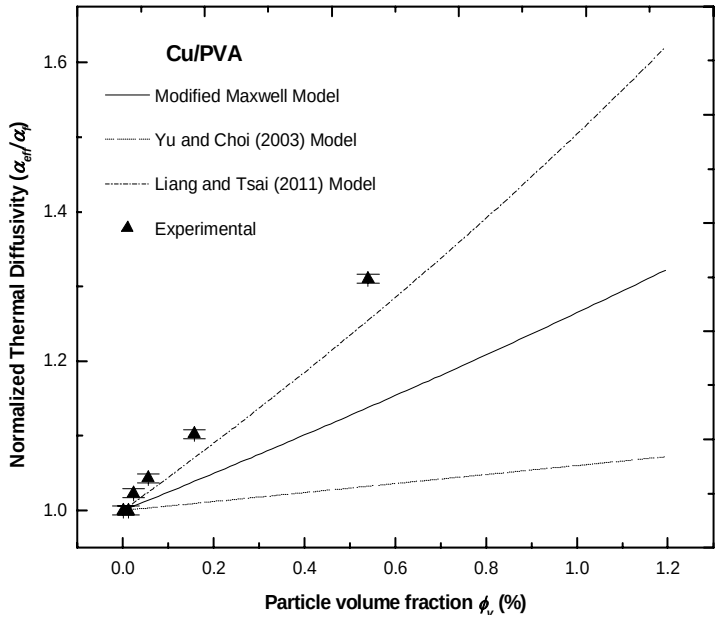

Figure 4.5(a): The variations of normalized thermal diffusivity of Cu/PVA nanofluids with volume fraction of nanoparticles. Experimental and theoretical values based on different models are also shown.

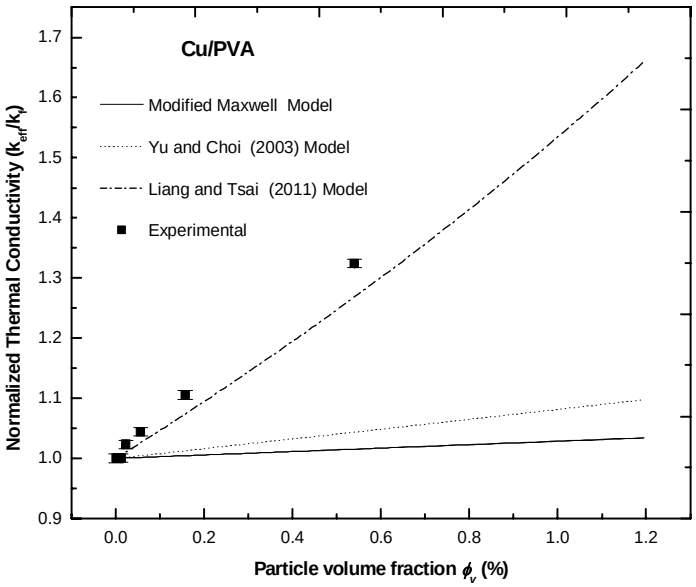

Figure 4.5(b): The variations of normalized thermal conductivity of Cu/PVA nanofluids with volume fraction of nanoparticles. Experimental and theoretical values based on different models are also shown.

conductivity enhancement beyond the predictions of Maxwell's model is the formation of adsorption layers around nanoparticles. What makes this model different from the modified Maxwell model or the Yu and Choi model is the inclusion of particle clustering. Here the formation of adsorption layers together with particle clustering is responsible for the effective thermal conduction in these nanofluids. The chances for particle clustering are greater in metallic nanofluids than in nanofluids dispersed with nonmetallic nanoparticles. The physical phenomenon behind the thermal diffusivity/conductivity enhancement is the diffusion of thermal waves through clustered nanoparticles embedded in adsorption layers.

In order to distinguish between the effect of interfacial layer in high as well as low molecular weight based nanofluids, we have measured thermal diffusivity and thermal conductivity of a water based nanofluid system

consisting of different concentrations of TiO_2 nanoparticles dispersed in deionised water. We prepared different concentrations of water based nanofluids and their thermal diffusivity has been measured by the Thermal Wave Resonant Cavity technique as described earlier. The results for TiO_2/water nanofluids are shown in figures 4.6(a) and 4.6(b).

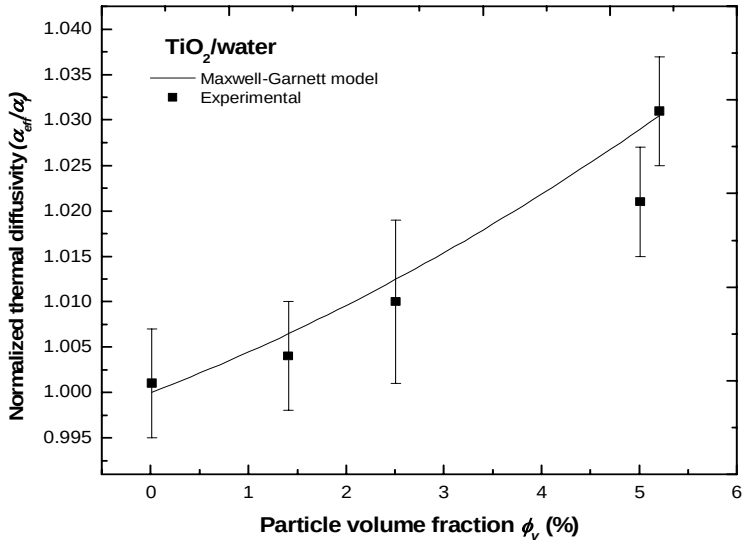

Figure 4.6(a): The experimental as well as theoretical (Maxwell-Garnett model without considering adsorption layer) variation of normalized thermal diffusivity of TiO_2/water nanofluid system.

The estimation of experimental uncertainty has been carried out as outlined earlier for PVA based nanofluids. We have then compared the theoretical values of thermal conductivity computed using Maxwell- Garnett model with and without considering the effect of adsorption layer. It can be seen that our experimental results on water based system agrees better with the effective medium theory without considering the effect of adsorption layer. Thus we see that the adsorption layers do not have much influence on the effective thermal conductivity of a low molecular weight based nanofluid.

The experimental results of the INPBE studies performed by Buongiorno et al. (2009) also support the above argument. The theoretical variations of the normalized thermal diffusivity and thermal conductivity of TiO_2/water nanofluids are also shown in Figures 4.6(a) and 4.6(b) respectively for comparison.

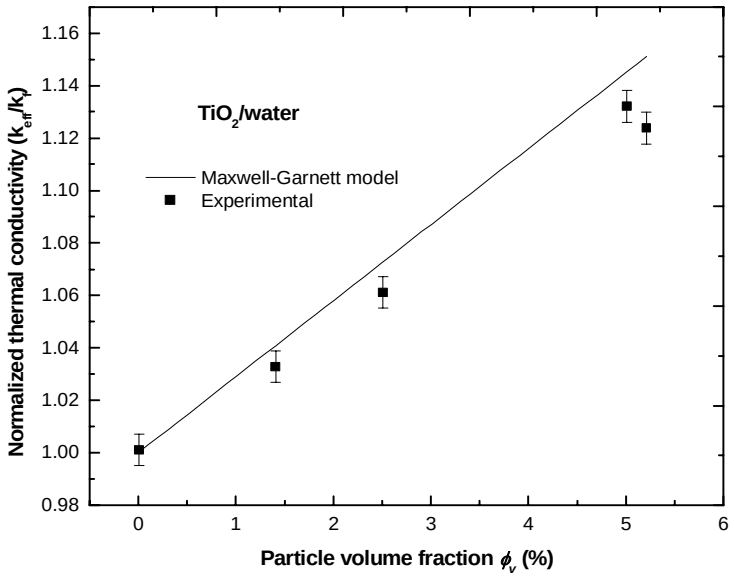

Figure 4.6(b): The experimental as well as theoretical (Maxwell-Garnett model without considering adsorption layer) variation of normalized thermal conductivity of TiO_2/water nanofluid system.

We could not perform measurements on Cu/water nanofluid system as it was found difficult to form stable nanofluids without sedimentation even after sonication for long periods of time.

4.5 Conclusions

We have measured the thermal diffusivity of high molecular weight as well as low molecular weight based nanofluid systems following the thermal wave interference technique. We have plotted the experimental variations of thermal conductivity from the measured thermal diffusivities of nanofluids.

From the observed variations it can be seen that in high molecular weight nanofluid systems such as TiO_2/PVA and Cu/PVA effective thermal diffusivity/conductivity increases with concentration of nanoparticles. The percentage of enhancements of the effective values of thermal diffusivity and thermal conductivity are higher than the values predicted by the effective medium theory. This has been explained in terms of the formation interfacial nanolayers around the nanoparticles and nanoparticle clustering. The interfacial layer formed around the nanoparticle act as a thermal bridge between the nanoparticle and the base fluid. The percolating network created by this nanolayer enhances the effective thermal conduction in nanofluids. At the high particle concentration regime, the percentage of enhancement is decided by clustering of nanoparticles. While the mechanism which controls the thermal conduction in a normal low molecular weight nanofluid is the diffusion of thermal waves through a nanoparticle-fluid mixture, the same is not true for a high molecular weight nanofluid.

From the analyses presented in this chapter, we can conclude that formation of interfacial adsorption layers around nanoparticles and nanoparticle clustering play significant roles in determining the effective thermal conduction in a polymeric nanofluid. A comparison of the results for metallic and nonmetallic nanoparticles indicate that metallic nanofluids show much higher effective thermal conductivity than the corresponding nonmetallic ones, and this is due to the higher thermal conductivity of the metallic nanoparticles and greater clustering of particles in the fluid. Measurements on the variation in thermal conduction properties with particle sizes will throw more light on the mechanisms involved. The detailed description on this aspect is discussed in chapter 5.

Chapter 5

Influence of particle size on the effective thermal conductivity of nanofluids

5.1 Introduction

Chapter 4 essentially describes the variation in effective thermal conductivity and thermal diffusivity of polymeric as well as water based nanofluids recorded as a function of the volume fraction of nanoparticles. It could be found that the mechanisms which control the thermal conduction in a high molecular weight nanofluid are the formation of adsorption layers around nanoparticles and nanoparticle clusters in the base medium. But in a low molecular weight nanofluid like a water based nanofluid system, the mechanism of thermal conduction is the enhanced diffusion of thermal waves through nanoparticles in a nanofluid. For a strong confirmation on this aspect we extended the thermal conduction studies in these two types of nanofluids by varying the size of the dispersed nanoparticles, keeping the volume fraction a constant. As mentioned in chapter 4 here also we measured the thermal diffusivity and thermal conductivity following thermal wave interference technique using a Thermal wave resonant cavity described earlier. The theoretical predications of our experimental findings have been done following the Maxwell-Garnett effective medium model (1873) and its modified forms which considers the effects like the adsorption of liquid molecules around the surface of nanoparticles (Yu and Choi, 2003) and the clustering of nanoparticles (Liang and Tsai, 2011). This chapter describes the experimental as well as

theoretical findings on the influence of nano particle size on the effective thermal conductivity of nanofluids formed by dispersing nanoparticles in high as well as low molecular weight base fluids. The following section briefly describes the materials and methods used in our experimental analysis.

5.2 Sample preparation and characterization

Two sets of nanofluids, each with different nanoparticle sizes and concentrations, were prepared for the measurements reported in this work. These were nanofluids prepared by dispersing TiO_2 nanoparticles in PVA as well as in water. The preparation involves synthesis of the nanoparticles, preparation of PVA and dispersing nanoparticles uniformly in PVA or water.

TiO_2 nanoparticles of average sizes approximately 5nm, 20nm, 50nm and 100nm were prepared following a chemical route (Reddy *et al.*, 2006). The technique basically involved hydrolysis of Titanium tetrachloride ($TiCl_4$) to form TiO_2. The titanium dioxide powder so obtained as a product of the hydrolysis of $TiCl_4$ was then calcined at 100, 200, 400, or 600^0 C for 2 hours each to obtain nanoparticles with different average sizes. The particle sizes were estimated following powder XRD technique. Powder XRD spectra were recorded with a Bruker D8 Advanced X-ray diffractometer. The estimated particle size is ~5 nm, ~20 nm, ~50 nm and ~100 nm etc. The XRD pattern obtained for the phase identification and particle size determination are shown in figures 5.1(a), 5.1(b), 5.1(c) and 5.1(d). In order to prepare a set of TiO_2/PVA nanofluids with different nanoparticle size, fixed mass fractions of the nanoparticles with different average sizes were uniformly dispersed in PVA. The mixture was sonicated for several hours to ensure uniformity of the nanofluid. By changing the base fluid to water, the same procedure was followed to prepare TiO_2/water nanofluid samples.

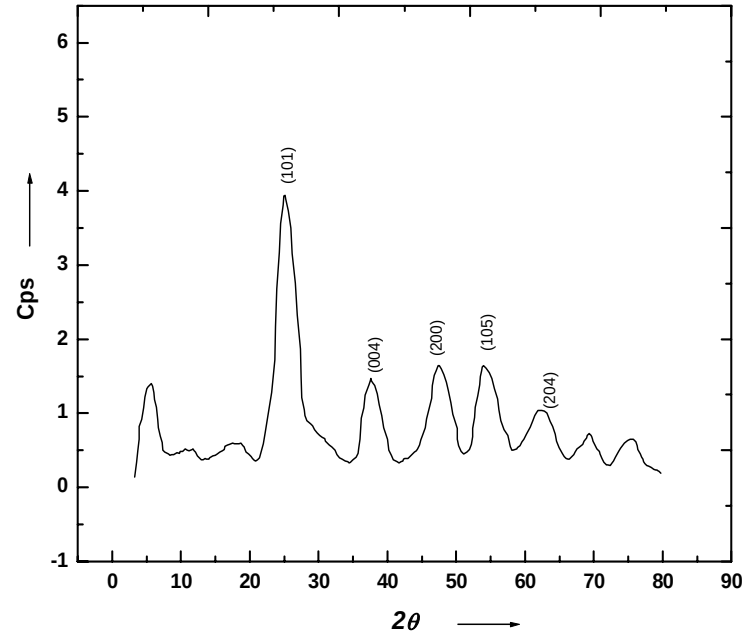

Figure 5.1(a). The XRD pattern TiO_2 nanopowder calcined at 100^0C.

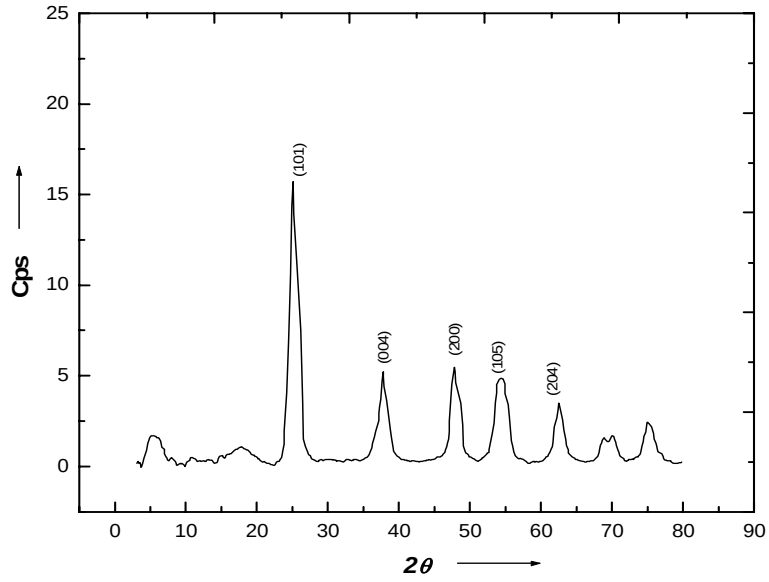

Figure 5.1(b). The XRD pattern TiO_2 nanopowder calcined at 200^0C.

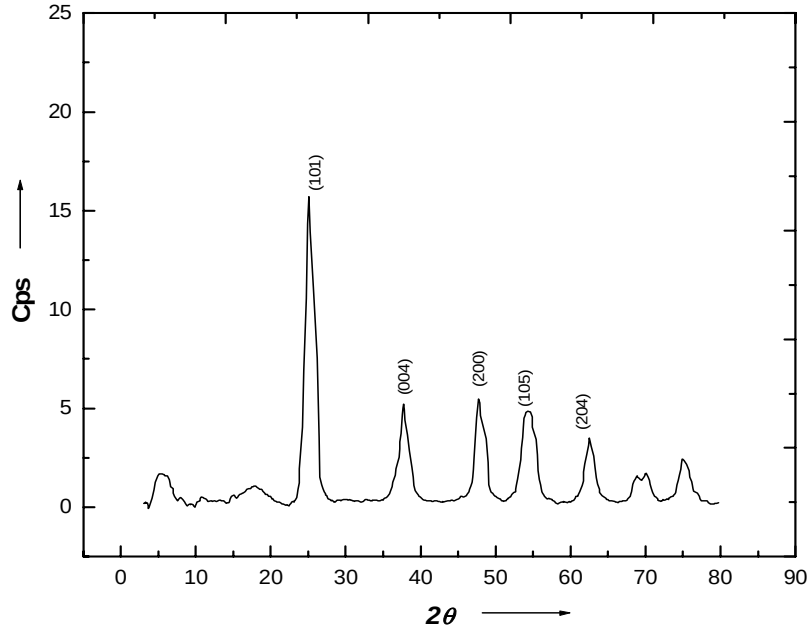

Figure 5.1(c). The XRD pattern TiO_2 nanopowder calcined at 400^0C.

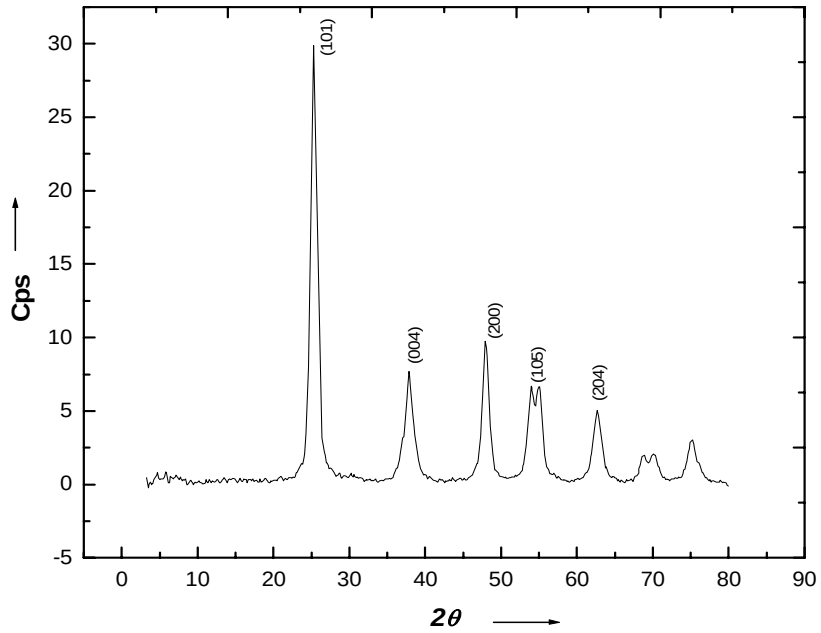

Figure 5.1(d). The XRD pattern TiO_2 nanopowder calcined at 600^0C.

In order to measure the thermal diffusivity of nanofluids accurately, the thermal wave resonant cavity (TWRC) cell was used (Shen and Mandelis, 1996) which works based on thermal wave interference occurring in a resonant cavity. The principle and method of the measurement of thermal diffusivity and thermal conductivity of nanofluids following thermal wave intereference in a TWRC cell described in detail in chapter 2.

5.3 Experimental methods

We have prepared TiO_2/PVA and TiO_2/water nanofluids by varying the dispersed nanoparticle size and kept the volume fraction of nanoparticle a constant for each sample. Then a desired volume of the prepared nanofluid is filled in the resonant cavity of the TWRC cell. By performing a cavity length scan experiment, thermal diffusivity of this nanofluid has been determined from thermal wave interference maxima and minima. The same procedure has been adopted for the prepared PVA as well as water based nanofluids. Thus we evaluated the experimental variations of the normalized thermal diffusivity and thermal conductivity for polymeric as well as water based nanofluids.

If $L_1^{(IP)}$ and $L_2^{(IP)}$ are the cavity lengths corresponding to consecutive interference maxima and minima, then the thermal diffusivity of the medium in the cavity is given by the expression (Shen *et al.,* 1996)

$$\alpha = \frac{f}{\pi}\left(L_2^{(IP)} - L_1^{(IP)}\right)^2 \qquad (2.15)$$

The technique provides accuracy better than ±1% in the measurement of thermal diffusivity.

5.4 Results and Discussion

In order to bring to light the dependence of nanoparticle size on the effective thermal diffusivity/conductivity of polymeric as well as water based nanofluids, we have compared the obtained experimental variation of effective thermal diffusivity and thermal conductivity of PVA and water based systems with selected theoretical models which consider the effect of interfacial layering and clustering of nanoparticles (Maxwell, 1873; Yu and Choi, 2004; Liang and Tsai, 2011). The detailed descriptions of these theoretical models and comparison procedure have already been described in chapter 3 and chapter 4. In chapter 4 we discussed the experimental variations of thermal diffusivity/conductivity of these nanofluids as a function of volume concentration. For polymeric nanofluids, we have obtained an experimental variation in thermal properties which agrees best with Maxwell model, which considers a change only in the volume concentration of nanoparticles due to the adsorption of liquid molecules around nanoparticles. However, in the renovated Maxwell model proposed by Yu and Choi (2003), both the volume fraction modifies the thermal conductivity of nanoparticles. But in water based systems, thickness and stability of the adsorption layer around the nanoparticle is much less due to the low viscosity and low molecular weight of the base fluid. Moreover, results from previous experimental findings (Buongiorno *et al.,* 2009) and simple calculation of adsorption layer thickness using Langmuir formula (less than 1 nm) support the idea to neglect the effect of adsorption layer on effective thermal conductivity or thermal diffusivity for water based nanofluids. In such systems, the dominant mechanism which causes enhancement in thermal conductivity is the clustering of nanoparticles in the fluid medium. So a comparison of the theoretical results obtained for these systems has been done following the nanoparticle clustering models based on effective medium theory

proposed by previous workers (Maxwell, 1873; Prasher *et al.,* 2006, Wang *et al.*, 2003).

5.4.1 Thermal conduction in TiO_2/PVA nanofluid

Figures 5.2(a) and 5.2(b) respectively depict the measured variations of effective thermal diffusivity and thermal conductivity of TiO_2/PVA nanofluid with particle size, along with the corresponding theoretical variations.

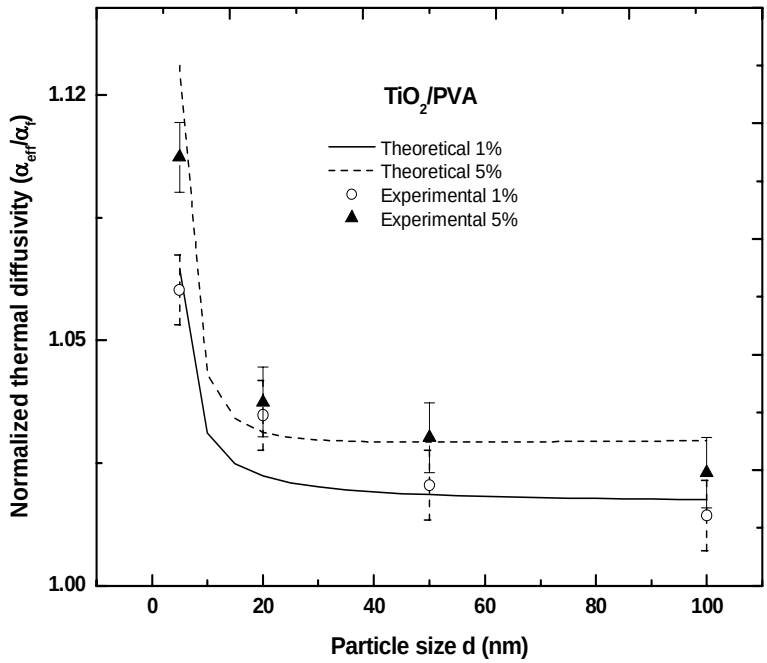

Figure 5.2(a) Variations of the effective thermal diffusivity of TiO_2/PVA nanofluids recorded as a function of particles size. Corresponding theoretical curves following modified Maxwell-Garnett model are also shown. Curves drawn are for two different particle volume fractions.

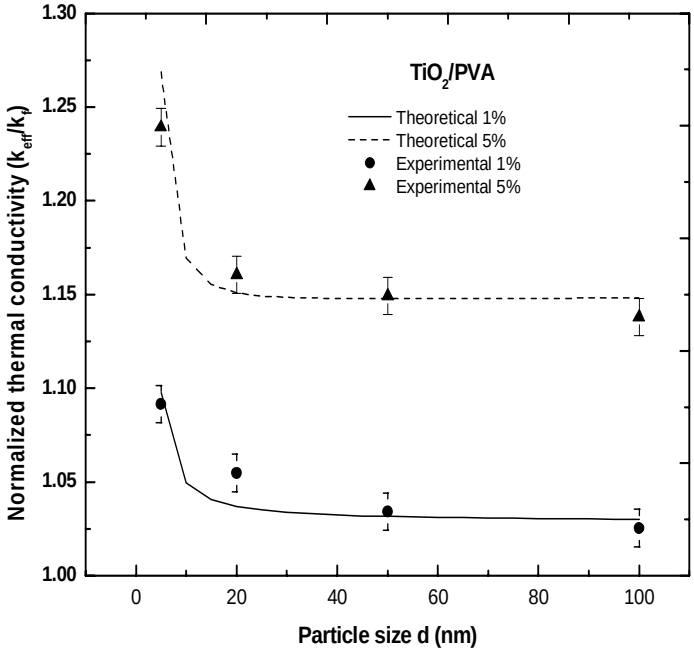

Figure 5.2(b) Variations of the effective thermal conductivity of TiO_2/PVA nanofluids recorded as a function of particles size. Corresponding theoretical curves following modified Maxwell-Garnett model are also shown. Curves drawn are for two different particle volume fractions.

It may be noted that there is good agreement between experimental and theoretical variations. The variation of effective thermal diffusivity with average particle size for TiO_2/PVA nanofluids is such that it tends to decrease with increase in nanoparticle size. We have obtained maximum enhancement in the thermal diffusivity/conductivity for the nanofluid with low average particle size such as ~5 nm. The maximum enhancements in thermal diffusivity obtained are 6% and 10% respectively for 1% and 5% volume fractions of the dispersed nanoparticles and the corresponding enhancements in thermal conductivity are about 9% and 23 % respectively. But for the nanofluid dispersed with particles of average size ~100 nm, the corresponding variations in thermal diffusivity are about 1% and 2%, while those for thermal

conductivity are about 2% and 13 % respectively. These variations in thermal diffusivity or thermal conductivity can be explained by considering the effect of liquid adsorption layers formed around nanoparticles. For low size of the nanoparticles, say ~ 5 nm, due to the high surface area to volume ratio of nanoparticles and high viscosity of the base fluid, the percolating network formed by the adsorbed nanolayer enhances the overall thermal conductivity of TiO_2/PVA nanofluid system. These adsorption layers act as continuous percolation paths for easy transport of thermal energy through the medium. As the nanoparticle size increases the effect of adsorption layer becomes less due to its smaller thickness (following Equation (3.14)). In addition to this, the scattering of thermal waves at fluid-particle boundaries causes a decrease in thermal conductivity at higher particle sizes as well as particle concentrations (Kapitza resistance).

As is evident from Equation (3.14), the theoretical formalism based on adsorption does not work for particle sizes less than the apparent adsorption layer thickness. Such a situation is not physically realistic and the minimum particle size for which a realistic adsorption layer formation is possible is ~ 3 nm for a nanofluid made from a polymeric base fluid such as PVA.

5.4.2 Thermal conduction in TiO_2/water nanofluid

In the case of TiO_2/water nanofluid, the effective thermal diffusivity and thermal conductivity of nanofluids increase as the particle concentration increases. The experimental as well as theoretical variations of effective thermal diffusivity and thermal conductivity of these nanofluids with average particle size are shown in Figures 5.3(a) and 5.3(b) respectively. Here the observed experimental variation is in such a way that as the average nanoparticle size increases the effective thermal diffusivity as well as thermal conductivity increases.

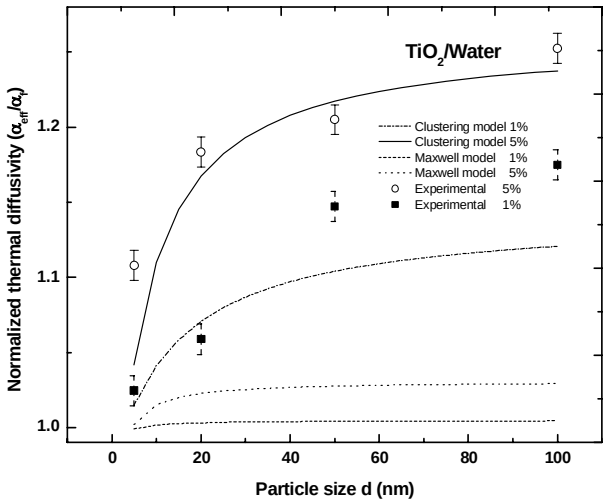

Figure 5.3(a) Variations of the effective thermal diffusivity of TiO_2/water nanofluids recorded as a function of particles size. Corresponding theoretical curves (using Maxwell model and clustering model) are also shown. Curves drawn are for two different particle volume fractions (1% and 5 %).

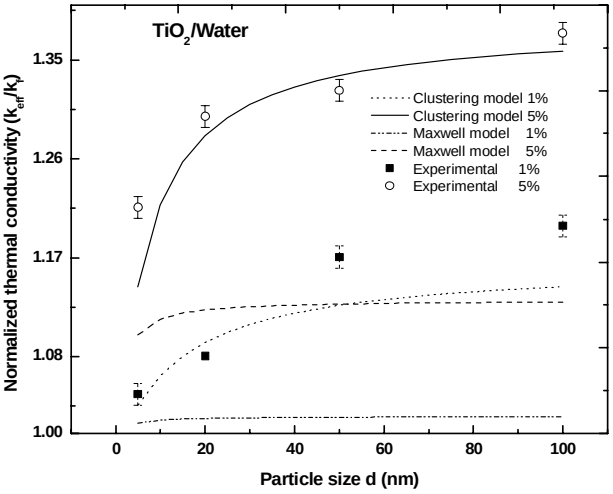

Figure 5.3(b) Variations of the effective thermal conductivity of TiO_2/water nanofluids recorded as a function of particles size. Corresponding theoretical curves (using Maxwell model and clustering model) are also shown. Curves drawn are for two different particle volume fractions (1% and 5 %).

The maximum enhancement in thermal diffusivity for 100 nm sized particles is about 17% and 25% for particle volume fractions 1% and 5% respectively, while the corresponding enhancements in thermal conductivity are about 19% and 37% respectively. The nature of variations of thermal diffusivity and thermal conductivity with particle size is in tune with the effective medium theory, but the experimental values of the thermal conductivity and thermal diffusivity at high particle concentrations for these fluids are beyond the values predicted by this theory. So we tried to interpret the experimental findings including the clustering of nanoparticles, which increases as particle concentration increases, in the nanofluid. Equation (1.19), which includes the effect of particle clustering, has been used to compute the thermal conductivity and diffusivity values. These results, along with the corresponding values computed following the Maxwell model (given by Equation (3.11)) are plotted in Figures 5.3(a) and 5.3(b) for comparison. It can be noted that experimental and theoretical plots agree very well when the effect of clustering is included in the theory. We think that particle clustering results in the formation of interconnecting channels between nanoparticle clusters, which grow as fractal structure as particle concentration increases (Wang *et al.,* 2003). Such interconnected particle clusters form easy channels for thermal energy to propagate resulting in an overall enhancement in thermal conductivity and thermal diffusivity beyond values predicted by effective medium theory. Figures 5.3(a) and 5.3(b) shows the variations in effective thermal conduction properties of nanofluids. The first one is that as the particle concentration increases, thermal diffusivity/conductivity increases. This can be accounted for in terms of particle clustering at higher concentrations. The second result is that thermal diffusivity/conductivity increases exponentially as the particle size increases and saturates at high particle sizes. These results indicate that particle

clustering and increase in particle size have comparable roles in determining the thermal diffusivity/conductivity of nanofluids. The INPBE results published do not favor particle clustering and are silent about the role of particle size on thermal conductivity, but those results pertain mostly to nanofluids at low concentrations (volume fractions less than 1 %) of nanoparticles and low particle sizes (~ 10 nm). At such low particle concentrations and sizes our experimental results are more or less in agreement with the effective medium theory.

5.5 Conclusions

From the experimental and theoretical analysis presented for the variations of effective thermal conductivity and thermal diffusivity with nanoparticle size for PVA as well as water based nanofluids reveal the role of adsorption layers in enhancing the effective thermal conductivity of nanofluids. The results based on effective medium theory, including the role of adsorption layers has been developed and compared with available experimental results. In a water based nanofluid system, it is shown that the effective thermal conductivity or thermal diffusivity at high particle concentrations are controlled by the formation of nanoparticle clusters.

It is evident from the presented results that for a nanofluid made from a high molecular weight base fluid, such as a polymeric nanofluid, the effective thermal diffusivity/conductivity decreases exponentially with increase in particle size whereas for a nanofluid made from a low molecular weight base fluid, such as TiO_2/water, the effective thermal diffusivity/conductivity increases exponentially with increase in particle size. This difference is accounted for in terms of the formation of adsorption layers in polymeric

nanofluids, and in terms of nanoparticle clustering at high particle concentrations in water based nanofluids.

For a high molecular weight nanofluid system, for larger particle sizes at higher concentrations (> 10%), one cannot neglect chances for condensation of the nanofluids, in which case the variation of effective thermal conductivity could not possibly be predicted by the present effective medium model. Through latest experiments, inter-laboratory comparisons and theoretical models, scientists working on nanofluids have arrived at the conclusion that semi-solid layer formation and particle clustering do not possibly have any significant influence in taking the thermal conductivity of nanofluids beyond the values predicted by effective medium theories. The results presented in this chapter show that this conclusion is applicable only to nanofluids made from low molecular weight base fluids and at low particle concentrations and particle sizes. For high molecular weight nanofluids, like polymeric nanofluids, formation of adsorption layer, controlled by hydrodynamic radius of the particle and viscosity of the fluid, does occur, which influences the values of thermal conductivity at low particle sizes and concentrations. The adsorption layer thickness varies with particle size, which influences the thermal conductivity of nanofluids as described earlier. We show that the adsorption layer largely influences the thermal conductivity at low particle concentrations and sizes. Moreover, the results in this chapter bring out the role of base fluid molecular weight on the nature of thermal conductivity enhancements in nanofluids.

Chapter 6

Thermal conduction in Polymeric nanosolids

6.1 Introduction

The previous chapters describe the effective thermal conduction in polymeric nanofluids in the light of effective medium theories which consider effect of adsorption layer, effect of nanoparticle clustering etc. After having evaluated the thermal conduction properties of polymeric nanofluids, we thought it would be interesting to extend these investigations to their solid counterparts. So as an extension of our experimental analysis, we have carried out an investigation of the effective thermal conduction in the condensed form of polymeric nanofluids termed as polymeric nanosolids. For this we have prepared uniform suspensions of single phase nanomaterials dispersed uniformly in a liquid and condensed them to form solid counterparts of the corresponding polymeric nanofluids. A polymeric nanofluid is obtained by uniformly dispersing a known concentration (or volume fraction) of nanoparticles (typically < 1% volume fraction) in a polymeric fluid and directly condensing it at room temperature, which results in the formation of the respective solid nanosolid. The volume fraction of nanoparticles in such a nanosolid is higher compared to the corresponding nanofluid due to the net decrease in the volume of the base fluid upon condensation. Moreover, such solid nanosolids, whose thermal properties could possibly be tuned, may lead to the design of special heat transfer systems and accessories. As has been demonstrated by earlier workers, composites have the distinct advantage of

possessing tunability of their properties, which is of great advantage in the design of heat transfer systems. Thermal properties of heat transfer materials are relevant to applications in fields such as thermoelectric and thermal management systems (Prasher, 2006a; Prasher, 2006b).

In the work presented in this thesis we have tried to extend investigations on thermal properties of Polymeric nanosolids, the condensed form of polymeric nanofluids, composing of metallic or nonmetallic nanoparticles embedded in a polymer matrix. In our studies the preparation of uniform nanosolids have been done by the direct condensation of the corresponding nanofluids which are easier than the preparation of the same by mixing the components uniformly in the solid state under controlled temperatures. Two sets of polymer based nanosolids consisting of TiO_2 or copper nanoparticles dispersed uniformly in PVA have been prepared and their thermal conductivities measured as a function of particle volume fraction following the Photopyroelectric (PPE) technique. Their thermal diffusivities have also been measured separately employing the Photoacoustic (PA) technique for confirmation. We have then described the effective thermal conductivity of this two phase solid composite under the combined effects of thermal boundary resistance arising due to the scattering of thermal waves at the interfaces of the two phases, and thermal diffusion across the interfaces of this two phase material (Chen and Vachon, 1969). For this we have employed two forms of modified effective medium approximation (EMA) which describes the mechanism of thermal conduction in Polymeric nanosolids in terms of increased interfacial scattering (Nan *et al.*, 1997) and thermal wave diffusion through a two phase composite (Cheng and Vachon, 1969). Detailed descriptions of sample preparation methods and experimental methods employed for measurements on these materials are given in the following sections.

6.2 Sample Preparation

We prepared the Polymeric nanosolid samples by the direct condensation of PVA based nanofluids, dispersed uniformly with copper (or Cu) or TiO_2 nanoparticles at room temperature. Two sets of nanofluid samples, each with different nanoparticle concentrations have been prepared following the two step method (Kwak *et al.*, 2005). These were TiO_2/PVA nanofluids prepared by uniformly dispersing TiO_2 nanoparticles in PVA and Cu/PVA nanofluids with copper nanoparticles dispersed in PVA. TiO_2 and copper nanoparticles were selected because we wanted to bring out the effect of particle thermal conductivity on the interfacial thermal resistance and the consequent thermal conductivity.

In order to prepare TiO_2/PVA nanofluids, first TiO_2 nanoparticles of average size ~15 nm were prepared by the hydrolysis of $TiCl_4$ (Reddy *et al.* 2001). For this 99% $TiCl_4$ was initially digested in concentrated hydrochloric acid and then mixed with water. The p^H of the solution was about 1.8. In order to precipitate TiO_2, 5 M Hydrazine hydrate was added drop by drop so as to raise the p^H to ~ 8. The precipitate was then stirred, filtered, washed and dried. The powder was calcined at 200^{o}C for a few hours to obtain TiO_2 nano powder. The average particle size was estimated using powder XRD technique. Copper nanoparticles of average size ~ 16 nm were prepared by chemical reduction of $CuSO_4$ with hydrazine in ethylene glycol under microwave irradiation in a medium power of 750 W for a few minutes (Zhu *et al.*, 2005). After cooling to room temperature the mixture was filtered, washed in ethanol and dried to obtain the Cu nano powder. More detailed descriptions of the synthesis of TiO_2 and copper nanoparticles have already been discussed in chapter 4.

In order to get uniform dispersions of nanoparticles in PVA initially we have prepared PVA base fluid by mixing PVA granules in water under constant

stirring for several hours. The degree of hydrolysis of PVA used was about 90%. Nanoparticles of desired mass fractions were added to the base fluid, thoroughly mixed and sonicated for several hours to obtain highly uniform nanofluid samples. In order to condense the nanofluid, we kept 5ml of nanofluid in a petridish and allowed it to condense slowly at room temperature. After 2 - 3 days, condensed forms of nanofluids, or polymeric nanosolids, were formed. The volume of the fluid was so chosen that the thickness of the sample after solidification was about 0.5 mm, which was suitable for direct measurements following any of the two photo thermal methods mentioned above. The change in mass fraction as the fluid that got condensed to solid was determined by measuring the loss of weight of pure PVA after it got condensed. The nanosolids prepared by this method were found to be highly uniform. We have tried to investigate the thermal properties of these polymeric nanosolids by following the well established Photoacoustic (PA) and Photopyroelectric (PPE) techniques. A brief description of the experimental procedures that we have followed is given in the following sections.

6.3 Measurement of Thermal Properties

6.3.1 Measurement of thermal diffusivity by Photoacoustic (PA) technique

Photoacoustic (PA) measurement of the thermal diffusivity of a solid is based on the sensitive detection of acoustic waves generated by the absorption of modulated electromagnetic radiation, the most popular radiation source nowadays being lasers. It is now well established that the PA effect (Rosenswaig, 1980) involves the production of acoustic waves as a consequence of the generation of thermal waves in the medium due to non-radiative de-excitation processes in the sample as a result of periodic heating by the absorption of modulated light. The PA technique constitutes a

comparatively simple and reliable experimental tool (Adams and Kirkbright, 1977), which has been extensively used for the measurement of thermal properties such as thermal diffusivity and conductivity of solid samples (Charpentier *et al.,* 1982; Madhusoodanan *et al.,* 1987). The method is based on the analysis of the variations in the amplitude and phase of the PA signal with light modulation frequency, which is also the frequency of the generated acoustic waves. The sample is kept in an enclosed volume provided with a window to irradiate the sample and a sensitive microphone (electrets microphone in our measurements) to pick up the PA signals, which are amplified and processed with a Lock-in amplifier. The experiment needs to be carried out in a vibration free environment so that a sufficiently high signal to noise ratio can be achieved. In the present work we have measured the variations of the PA amplitude with modulation frequency to arrive at the thermal diffusivity values of the samples. More details of experimental techniques are described in chapter 2 of the thesis.

The sample thicknesses chosen are such that at low modulation frequencies (say < 50 Hz) the thermal diffusion length of the sample is more than the physical thickness of the sample, in which case the sample is said to be thermally thin. By increasing the modulation frequency to higher values (say > 100 Hz) the thermal diffusion length decreases, and at a high enough modulation frequency, it becomes less than the physical thickness of the sample, which takes the sample to a thermally thick regime. The modulation frequency at which the sample changes over from thermally thin to thermally thick regime is called the critical frequency. Critical frequency can be determined by measuring the variation of PA amplitude or phase with modulation frequency, which appears as a distinct slope change in the PA amplitude plot or as a maximum in the phase plot. The amplitude plots that have been used to determine the thermal diffusivity for a typical concentration 0.1 % of TiO_2/PVA nanosolid and the copper/PVA

nanosolid are shown in Figures 6.1 (a) and 6.1(b) respectively. In each case change of slope in amplitude versus frequency plot gives the critical frequency f_c. Once the critical frequency f_c is determined, thermal diffusivity α can be determined from the relation

$$\alpha = \pi f_c l_s^2 \tag{2.21}$$

where l_s is the sample thickness. Here the thickness of the condensed nanofluid samples were measured at a large number of points with an accurate micrometer of least count 0.01mm, and the mean values of thickness l_s were recorded. Similar plots have been obtained for other samples with different concentrations of nanoparticles in the PVA polymer matrix.

6.3.2 Measurement of thermal properties by Photopyroelectric (PPE) technique

The thermal properties of the nanosolid samples were also measured by the photo pyroelectric (PPE) technique (Mandelis and Zver, 1985; Menon and Philip, 2000). In this technique, an intensity modulated beam of light (from a laser) incident on the sample generated a thermal wave, which propagated through the sample generating a corresponding temperature rise on the opposite side of the sample. This temperature rise was picked up with a pyroelectric detector (metal coated PVDF film) thermally attached to the sample. The sample thicknesses used in the present measurements were of the order of 0.5 mm. The amplitude and phase of the pyroelectric signal were recorded as a function of modulation frequency with a dual phase Lock-in amplifier. From the frequency dependence of the amplitude and phase of the thermal wave, thermal properties such as thermal conductivity, thermal diffusivity and specific heat capacity of the samples could be evaluated. The amplitude and phase plots that have been used to determine thermal properties of the two sets of polymeric

nanosolids, TiO_2/PVA and copper/ PVA, are shown in Figures 6.2(a), 6.2(b), 6.2(c) and 6.2(d).

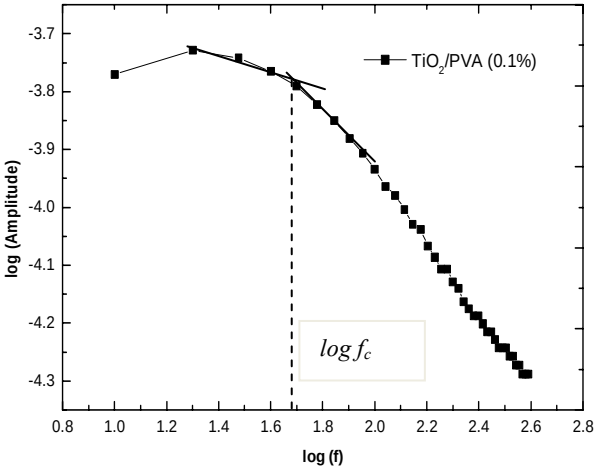

Figure 6.1(a) The variation of the amplitude as a function of the modulation frequency of the photoacoustic signal obtained to measure the thermal diffusivity of 0.1% TiO_2/PVA polymeric nanosolid.

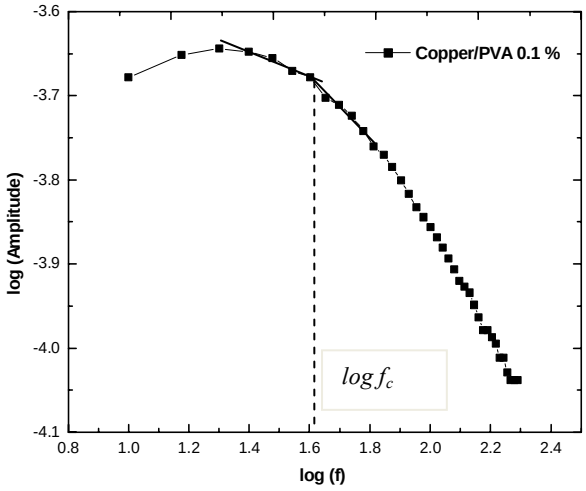

Figure 6.1(b) The variation of the amplitude as a function of the modulation frequency of the photoacoustic signal obtained to measure the thermal diffusivity of 0.1% copper/PVA polymeric nanosolid.

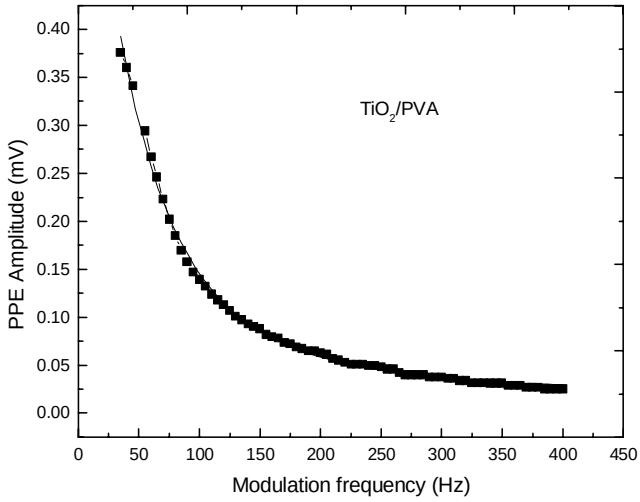

Figure 6.2(a) The variation of the amplitude of the photopyroelectric signal recorded as a function of modulation frequency for TiO_2/PVA nanosolid having a volume fraction 0.1%.

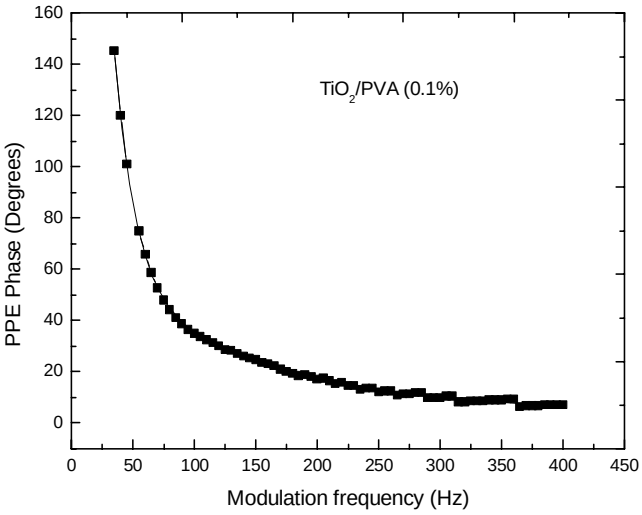

Figure 6.2(b) The variation of the phase of the photopyroelectric signal recorded as a function of modulation frequency for TiO_2/PVA nanosolid having a volume fraction 0.1%.

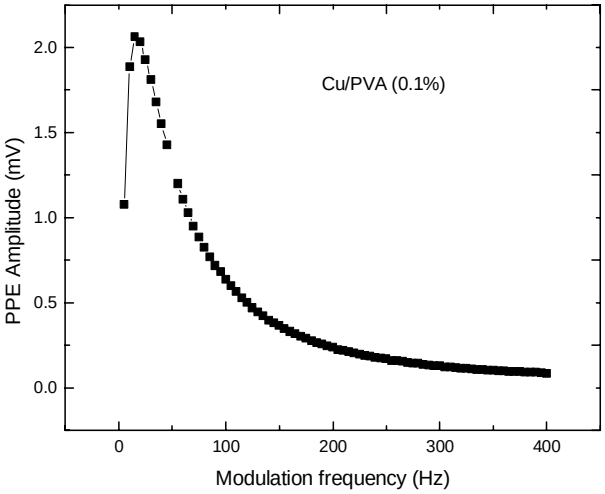

Figure 6.2(c) The variation of the amplitude of the photopyroelectric signal recorded as a function of modulation frequency for copper/PVA nanosolid having a volume fraction 0.1%.

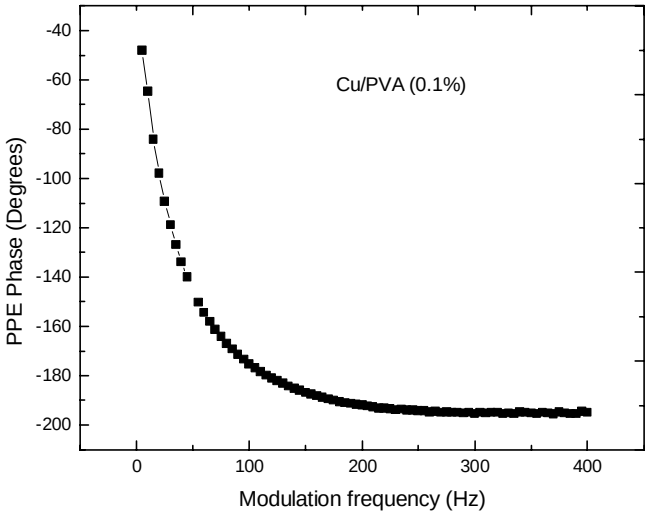

Figure 6.2(d) The variation of the phase of the photopyroelectric signal recorded as a function of modulation frequency for copper/PVA nanosolid having a volume fraction 0.1%.

More details of the experimental techniques adopted in these measurements can be found in chapter 2. The PA as well as PPE measurements

were carried out on samples prepared with different volume fractions of nanoparticles. The thermal properties of pure PVA, condensed following the same procedure, were also measured for comparison. From these the thermal properties of each sample, normalized by the corresponding properties for pure condensed PVA, have been plotted against the volume fractions of the nanoparticles.

6.4 Results and Discussion

The experimental and theoretical variations of the normalized thermal conductivity and normalized thermal diffusivity of TiO_2/PVA and Cu/PVA nanosolids with volume fractions of nanoparticles are shown in Figures 6.3(a), 6.3(b), 6.4(a) and 6.4(b) respectively. The experimental plots of thermal conductivity shown in these figures are from PPE measurements. Thermal diffusivity values of the two sets of polymeric nanosolids have been obtained from the PA measurements. It can be seen that the variations of normalized thermal conductivity as a function of particle volume fraction are different for the two sets of samples. Since in this case the properties of materials at particle-matrix interfaces are nearly the same, effects like thermal wave scattering at the particle-matrix boundaries cannot be accounted for within the framework of these conventional models, which are essentially diffusion based. These models consider only the mechanism of diffusion as responsible for the effective thermal conduction in a solid composite. However, while dealing with nanoparticle inclusions in a host matrix one has to consider effects like interfacial scattering that arises due to thermal impedance mismatch at particle-matrix boundaries.

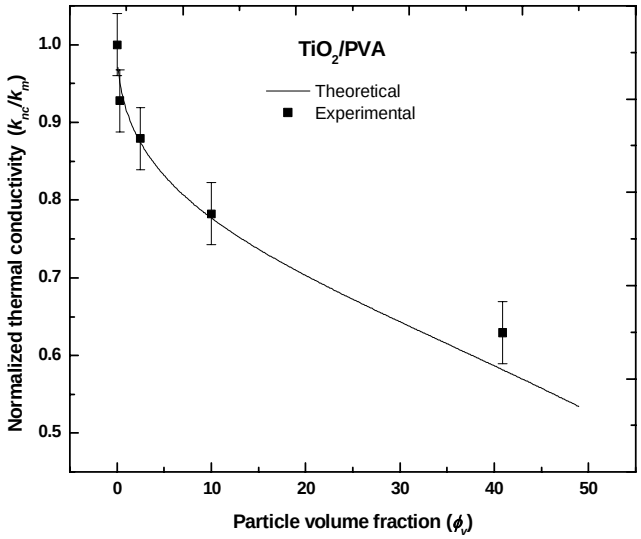

Figure 6.3 (a) Theoretical and experimental variations of effective thermal conductivity of TiO_2/PVA nanosolids as a function of volume fraction of TiO_2 nanoparticles. Experimental values are from PPE measurements.

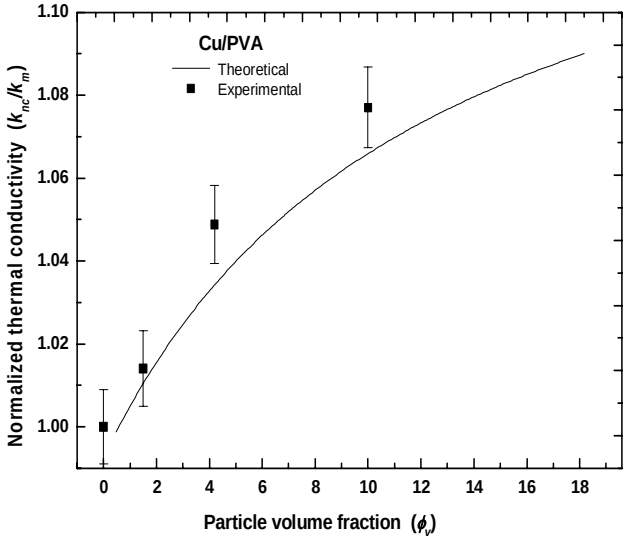

Figure 6.3 (b) Theoretical and experimental variations of effective thermal conductivity of Cu/PVA nanosolids as function of volume fraction of copper nanoparticles. Experimental values are from PPE measurements

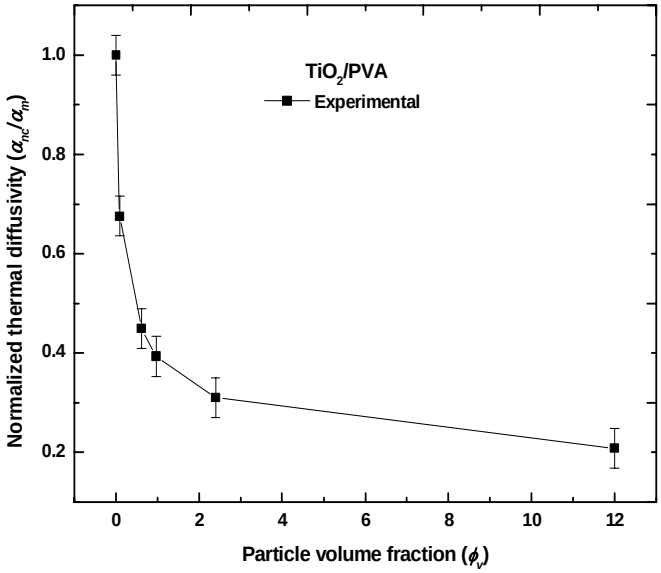

Figure 6.4(a) Experimental variation of effective thermal diffusivity of TiO_2 /PVA nanosolids with nanoparticle volume fraction. Values are from PA measurements.

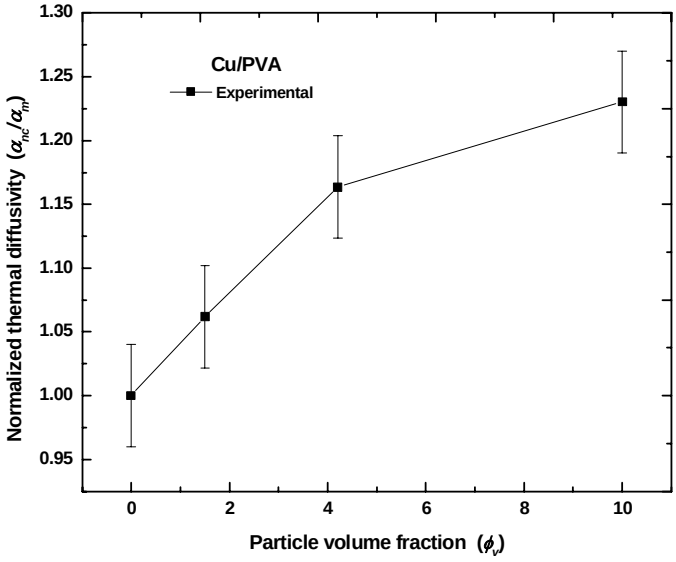

Figure 6.4(b) Experimental variation of effective thermal diffusivity of Cu/PVA nanosolids with nanoparticle volume fraction. Values are from PA measurements

The uncertainties in the measured values of thermal diffusivity or thermal conductivity have been estimated as standard deviations of set of experimental values of thermal diffusivity or thermal conductivity obtained by repeating the measurements a fixed number of times.

The essential mechanisms that mainly work out in polymeric nanocompistes are (i) diffusion through the constituents of the medium, which forms the basis of effective medium approximation, and (ii) interfacial scattering of thermal waves at matrix-particle interfaces. In the present work we have tried to explain the observed variations in effective thermal conductivity of the polymeric nanosolids under investigation as a combined effect of relevant mechanisms proposed by previous authors (Nan *et al.*, 1997; Cheng and Vachon, 1969). We have employed the effective medium model proposed by Nan *et al.* (1997), which describes the effective thermal conductivity of a two phase composite, which includes thermal boundary resistance arising due to the scattering of thermal waves at the interfaces of two phases and the effective medium model proposed by Cheng and Vachon (1969), which describes an effective thermal diffusion in composite solids. Cheng and Vachon model (1969) considered an analogy between heat flow and electric current flow to derive the effective thermal conductivity of composite materials. This model assumes a parabolic distribution for the discontinuous phase (nanoparticle inclusions) with the constants of the distribution determined by the analysis and presented as a function of the volume fraction of the discontinuous phase. The equivalent thermal conductivity of a unit cube of the mixture is derived in terms of the distribution function, and the thermal conductivity of the constituents. Detailed theoretical descriptions of these models have already been outlined in chapter 3.

In order to explain our experimental results on the thermal properties of polymeric nanosolids we assumed that the effective thermal conductivity of nanosolid, including diffusion and scattering effects, can be obtained by adopting a series resistance model for conduction at the nanoparticle - matrix interface. The model proposed by Nan *et al.* (1997) describes the effective thermal conductivity of a nanosolid as controlled by interfacial effects (k_{sct}), while the Cheng -Vachon model (1969) discusses the heat transport mechanism in a solid composite in terms of diffusion of thermal waves (k_{dif}). In our theoretical formalism we have described the overall conductivity of the nanosolid under consideration as a combination of these two mechanisms, defined by Equations (3.41) and (3.52), so that we can write the effective thermal conductivity of a nanosolid k_{nc} as

$$k_{nc} = \frac{k_{sct} \times k_{dif}}{k_{sct} + k_{dif}} \tag{3.53}$$

This expression has been used to calculate the thermal conductivity of nanosolids presented in this work and compare with experimental results.

6.4.1 Variations of thermal conductivity

The experimental and theoretical variations of the normalized thermal conductivity of TiO_2/PVA and Cu/PVA nanosolids with volume fractions of nanoparticles are shown in Figures 6.3(a) and 6.3(b) respectively. The experimental plots shown in these Figures are from PPE measurements. It can be seen that the variations of normalized thermal conductivity as a function of particle volume fraction are different for the two sets of samples. From these curves it is clear that the interfacial thermal resistance and thermal conductivity of nanoparticles have strong influence on the effective thermal conductivity of nanosolids. For TiO_2/PVA nanosolid, the calculated effective thermal resistance

is of the order of 10^{-7}, and the low thermal conductivity of bare TiO_2 nanoparticles results in a decrease in effective thermal conductivity with the increase in nanoparticle volume fraction. Thus, we see that the scattering mechanism is dominant over thermal wave diffusion for TiO_2/PVA samples because of the low transmission probability for thermal waves through TiO_2 nanoparticles. From the theoretical and experimental variations it can be seen that a decrease of about 40% in effective thermal conductivity occurs as the particle volume fraction increases to about 45%. This decrease in thermal conductivity can be interpreted as due to Kapitza scattering of short wavelength phonons from the polymer matrix-nanoparticle interfaces, with the nanoparticles acting as impurities. The limited diffusion due to low transmission probability as a consequence of low thermal conductivity of bare TiO_2 nanoparticles cannot compensate for the strong decrease due to scattering in the system.

In the case of Cu/PVA samples the normalized value of effective thermal conductivity increases as the nanoparticle volume fraction increases. The reason for this is the higher thermal conductivity of the included copper nanoparticles. It is found that for about 5% copper nanoparticle concentration, the effective thermal conductivity increases by about 7%. Though phonon scattering from the particles acting as impurities is present in this regime also, strong diffusion of thermal waves takes place in to the particles, resulting in an effective enhancement. At higher volume fractions the competing effects of scattering and diffusion tend to make the thermal conductivity saturate.

6.4.2 Variations of thermal diffusivity

Normalized thermal diffusivity of the Polymeric nanosolids TiO_2/PVA and copper/PVA are shown in Figures 6.4(a) and 6.4(b) respectively. The

thermal diffusivity values obtained from PA measurements agree well with the corresponding values obtained and calculated from PPE measurements, using the relation between thermal conductivity and thermal diffusivity.

From these figures it is clear that the effective thermal diffusion in these nanosolids is also determined by scattering as well as diffusion mechanisms. As expected, variations of thermal diffusivity follow the corresponding variations of thermal conductivity.

Using the PPE technique, we have also measured the variation in the specific heat capacity of the TiO_2/PVA nanosolids with the concentration of TiO_2 nanoparticles. The variation is as shown in Figure 6.5

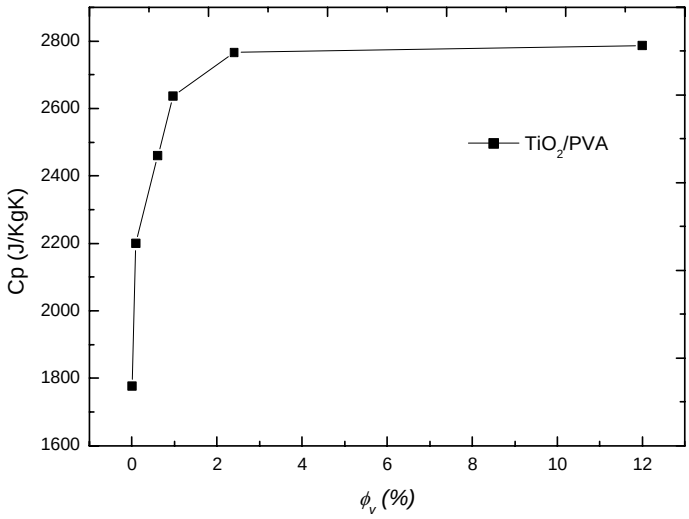

Figure 6.5 The variation in the specific heat capacity of TiO_2/PVA nanosolids with concentration of TiO_2 nanoparticles.

6.5 Conclusions

From the thermal conductivity analysis presented in this work, it is clear that polymeric nanosolids with metallic inclusions exhibit a total reversal in thermal conduction compared to the corresponding materials with nonmetallic inclusions. We see that the effective thermal conductivity of these polymeric nanosolids is essentially determined by particle volume fraction and particle thermal conductivity, and are controlled by the competing mechanisms of scattering and diffusion. Our experimental results as well as theoretical predictions for polymeric nanosolids open up the possibility to tune the normalized thermal conductivity of nanosolids from a low negative to high positive values compared to the thermal conductivity of the base solid.

Chapter 7

Summary and Conclusions

For the past two decades, nanofluids prepared by uniformly dispersing nanoparticles in a conventional fluid have attracted the attention of the scientific community due to their enhanced thermal conduction properties and their possible use as efficient heat transfer fluids. Nanoparticle-fluid suspensions (nanofluids) have been reported to possess enhanced thermal conductivity and convective heat transfer performance due to the higher thermal conductivity of dispersed nanoparticles compared to the base fluid. A great deal of theoretical modeling has also appeared in literature on this subject to account for the observed experimental findings. Most of the successful theoretical models published in literature on this subject have their base in the effective medium theory put forward by Maxwell in the nineteenth century to evaluate the effective properties of mixtures. According to the effective medium theory, the addition of solid particles in to a liquid matrix improves its thermal conductivity by convective heat transfer across the matrix-particle interfaces. As a matter of fact many authors reported enhancements in thermal conductivity far more than those predicted by the well established effective medium theories. This fact and the inconsistencies in the values of thermal conductivity of nanofluids reported by different researchers forced scientists to develop theoretical models including various other mechanisms such as the formation of a semisolid layer around nanoparticle surface, formation of fractal like nanoparticle clusters, Brownian motion of nanoparticles at finite temperatures and interfacial

scattering of thermal waves at fluid-particle boundaries. Experimentalists have not been able to confirm the above mechanisms unambiguously, perhaps due to the differences in the experimental techniques and conditions, differences in sample preparation methods, differences in particle sizes etc. The elaborate inter-laboratory comparison initiated by International Nanofluids Property Benchmark Exercise (INPBE) involving over 30 laboratories across the world, arrived at a general consensus that effects such as liquid layering around nanoparticles and formation of fractal like nanoparticle clusters do not lead to anomalous enhancements in thermal conductivity of nanofluids and that the observed enhancements are well within the framework of effective medium theories. However, this comparison work has been limited to nanofluids prepared by dispersing nanoparticles in low molecular weight base fluids, such as water, ethylene glycol, oil etc. An important issue that still remains unresolved is the influence of particle sizes on the enhancement in thermal conductivity of nanofluids. Conflicting experimental reports have appeared in literature on this subject matter, while theoretical models based on effective medium approach and results published based on the INPBE experiments are silent about this and many other issues.

In this thesis we have reported the thermal conduction in nanofluids prepared by dispersing nanoparticles in a high molecular weight base fluid such as a polymeric fluid. We have then tried to investigate the effect of mechanisms like adsorption of liquid molecules around nanoparticles and clustering of nanoparticles on the effective thermal conductivity of nanofluids. For this we have studied the variation in effective thermal diffusivity and thermal conductivity with volume fraction of nanoparticles as well as size of the dispersed nanoparticles. In polymer based nanofluids the adsorption layer

formed around the nanoparticle are stable due to the high viscosity of the polymeric base fluid compared to that in a low molecular weight base fluid such as water. We have presented a theoretical model specific to a polymeric nanofluid which has its roots in the basic Maxwell-Garnett effective medium theory, but including the effect of adsorption layer around the nanoparticles. Then we have tried to describe the effective thermal conductivity of the polymeric nanofluid by comparing the experimental data with conventional effective medium theory, originally proposed by Maxwell to predict the effective thermal conductivity of homogeneous solid mixtures. Maxwell's model assumes that the effective thermal transports in mixtures are essentially diffusive. While dealing with polymeric nanofluids we consider one additional modification to this model including the effect of formation of adsorption layer around nanoparticles and the consequent interfacial effects at fluid-particle boundaries. In a two component mixture consisting of particles dispersed in a high molecular weight polymeric fluid, viz. Poly Vinyl alcohol (PVA), the adsorption of liquid molecules around a solid medium is a pre-defined phenomenon, which cannot be neglected. So we have tried to determine the variations of the effective thermal diffusivity and thermal conductivity of nanofluids with the volume fraction of nanoparticles. The theoretical predictions have been verified experimentally by performing accurate measurement of thermal diffusivity of two representative polymeric nanofluids; TiO_2/PVA nanofluid, prepared by dispersing TiO_2 nanoparticles in polyvinyl alcohol (PVA), and Cu/PVA nanofluid obtained by dispersing Copper nanoparticles in PVA and estimating thermal conductivity from it.

In order to measure the thermal diffusivity of nanofluids accurately, a thermal wave resonant cavity (TWRC) cell has been designed and fabricated,

which works on the principle of thermal wave interference in a defined volume of the fluid. Measurement uncertainties have been estimated following standard techniques, and it is found that the uncertainty of measurement is within ± 1%. We think that this technique is more convenient and accurate than other techniques such as transient hot wire or parallel hot plate methods generally used to measure thermal conductivity of nanofluids. The measurements have been extended to the corresponding nanofluids with water as the base fluid for comparison and verification with reported results.

For the confirmation of the validity of the mechanisms proposed for describing the effective thermal conductivity of polymeric nanofluids we have performed measurements of effective thermal diffusivity and thermal conductivity in a low molecular weight based nanofluid system such as TiO_2/water nanofluid. In this case the experimental variations obtained are well in tune with well established Maxwell-Garnett model, and are in agreement with the INPBE results.

The experimental variations of the effective thermal conductivity and diffusivity obtained as a function of volume fraction of nanoparticles reveal that the adsorption layer formed around nanoparticles and nanoparticle clustering play decisive roles in deciding the effective thermal conductivity of polymeric nanofluids. The experimental results obtained are in good agreement with the Maxwell-Garnett model including the effect of adsorption layer around nanoparticles. These adsorption layers act as continuous percolation paths for easy transport of thermal energy through the medium. The experimental studies on the dependence of particle size on effective thermal conductivity of the polymeric as well as water based nanofluid systems strongly reveal the validity of these mechanisms in high molecular weight nanofluid systems. The

difference in experimental results observed with polymeric nanofluids having metallic and nonmetallic suspensions of nanoparticles opens up the possibility for the design of high efficiency heat transfer systems for heat conduction application.

As the second part of the research work we have extended the study of thermal conduction properties of the condensed PVA based nanofluids with the concentration nanoparticles. For this, first we prepared two sets of PVA based nanofluids with different concentrations of TiO_2 and copper nanoparticles and dried them at room temperature to obtain nanosolids. The thermal characterization of the nanosolid samples is done by the photopyroelectric (PPE) and photoacoustic (PA) techniques. In the PPE technique, an intensity modulated beam of light (from a laser) incident on the sample generates a thermal wave, which propagates through the sample generating a corresponding temperature rise on the opposite side of the sample. This temperature rise is picked up with a pyroelectric detector (such as metal coated PVDF film) thermally attached to the sample. From the frequency dependence of the amplitude and phase of the PPE signal, thermal properties such as thermal conductivity and thermal diffusivity could be evaluated. The photoacoustic technique is based on the PA effect which involves the production of acoustic waves as a consequence of the generation of thermal waves in the medium due to non-radiative de-excitation processes in the sample as a result of periodic heating by the absorption of modulated light. The PA technique constitutes a comparatively simple and reliable experimental tool, which has been extensively used for the measurement of thermal properties such as thermal diffusivity and conductivity of solid samples. The method is based on the analysis of the variations in the amplitude and phase of the PA signal with the

light modulation frequency, which is also the frequency of the generated acoustic waves. Here we have evaluated the variation in thermal diffusivity of the nanosolids by performing a frequency scan experiment in a photoacoustic cell.

We have tried to explain the observed variations in effective thermal conductivity of the nanosolids under investigation as a combined effect of relevant mechanisms proposed by previous authors; such as diffusion through the constituents of the medium, which forms the basis of effective medium approximation, and interfacial scattering of thermal waves at matrix-particle interfaces. In order to interpret the experimental results we have employed modified forms of theoretical models such as Nan *et al.*'s model and Cheng-Vachon model. Nan *et al.*'s model is a modified form of Maxwell's model including the concept of interfacial thermal resistance in the composite and describes the role of thermal wave scattering at matrix-particle interfaces on the effective thermal conductivity of these nanosolids . The Cheng–Vachon model essentially describes and discusses the mechanism of heat transport in a solid composite in terms of diffusion of thermal waves. Cheng and Vachon proposed this model for effective thermal conductivity following the analogy between heat flow and electric current flow and considered a parabolic distribution for the discontinuous phase (nanoparticle inclusions) with the constants of the distribution determined by the analysis and presented as a function of the volume fraction of the discontinuous phase. We have combined these two mechanisms to obtain an expression for the overall thermal conductivity for polymeric nanosolids. Based on our theoretical analysis we have concluded that nanosolids with metallic inclusions exhibit a total reversal in thermal conduction compared to the corresponding materials with nonmetallic

inclusions. We see that the effective thermal conductivity of these polymeric nanosolids is essentially determined by particle volume fraction and particle thermal conductivity, and are controlled by the competing mechanisms of scattering and diffusion.

Most work reported on nanofluids is on nanofluids made from low molecular weight nanofluids. Perhaps ours is the first systematic measurement of the thermal diffusivity and associated properties of nanofluids made from high molecular weight base fluid such as polymeric nanofluids. We have invoked several mechanisms to explain our experimental findings. We do not claim that we have been able to identify and solve all the issues related to thermal properties of polymeric nanofluids. More work is required to be done on other polymeric nanofluids with different types of nanoparticles dispersed in the base fluid. It would also be interesting to disperse highly anisotropic nanoparticles such as carbon nanotubes in polymeric fluids and measure their thermal properties. More experimentation and results may lead to further modeling and better understanding of their properties, and hence may lead to new applications.

In the case of condensed form of polymeric nanofluids known as polymeric nanosolids it can be seen that nanosolids with metallic inclusions exhibit a total reversal in thermal conduction compared to the corresponding materials with nonmetallic inclusions. In the case of experimental results as well as theoretical predictions done with polymeric nanosolids open up a possibility to tune the normalized thermal conductivity of nanosolids from a low negative to high positive values compared to the thermal conductivity of the base solid. Thermal conductivity of the polymeric nanofluids generally depends on the values of constituent particle thermal conductivity, volume

fraction, size and shape of the constituent phases. Future research on this subject is based on the possibility for designing polymeric nanosolids with positive or negative thermal conductivity which can be achieved by trying polymeric nanosolids with variable nanoparticle size and shape. This may lead to the fabrication of advanced cooling and heat transfer systems. More systematic measurements and analysis of the thermo-physical properties are needed for testing and establishing the applications of these materials.

- Adams M. J. and Kirkbright G. F. (1977). Analytical optoacoustic spectrometry. Part III. The optoacoustic effect and thermal diffusivity, *Analyst*. **102:** 281.
- Amrollahi A., Hamidi A. A. and Rashidi A. M. (2008). *Nanotechnology*. **19:** 315701.
- Artus R. G. C. (1996). Measurement of novel thermal conduction of a porphoritic heat sink paste, *IEEE Transactions on Components Packaging and Manufacturing-Part B*. **19:** 601.
- Azmi B. Z., Sing L. T., Saison E. B. and Wahab Z. A. (2006). Thermal wave resonant cavity technique in measuring thermal diffusivity of sucrose solution, *Pertanika: J. Sci. & Technol*. **14:** 33.
- Bang I. C. and Chang S. H. (2005). Boiling heat transfer performance and phenomena of Al_2O_3-water nanofluid from a plain surface in a pool, *Int. J. Heat Mass Transfer*. **48:** 2407.
- Basca R. R. and Gratzel. M. (1996). *J. Am. Ceram. Soc*. **79:** 2185.
- Beck M. P., Yuan Y., Warrier P. and Teja A. S. (2008). The effect of particle size on the thermal conductivity of alumina nanofluids, *J. Nanoparticle. Res*. **11:** 1129.
- Becker J. A., Pearson R. A. and Berg J. C. **(**1989). Influence of particle curvature on polymer adsorption layer thickness, *Langmuir*. **5:** 339.
- Belleet M. and Sengelin S. (1975). Determination des proprietes thermophysiques de liquides non-Newtoniens a l'aide d'une cellule a cylindres coaxiaux, *Int. J. Heat Mass Transfer*. **18:** 1177.

- Bentely J. P. (1984). Temperature sensor characteristics and measurement system design, *J. Phys. E. Sci. Instrum.* **17:** 430.
- Bruggeman D. A. G. (1935). The calculation of various physical constants of heterogeneous substances, 1. The dielectric constants and conductivities of mixtures composed of isotropic substances, *Ann. Phys. (Leipzig)*. **24:** 636.
- Buongiorno J. *et al*. (2009). A benchmark study on the thermal conductivity of nanofluids, *J. Appl. Phys.* **106:** 094312-1.
- Campbell L. K., Na B. K. and Ko E. I. (1992). Synthesis and characterization of titania aerogels, *Chem. Mate*. **4:** 1329.
- Chandrasekhar M. and Suresh S. (2009). A review on the mechanisms of heat transport in nanofluids, *Heat Transf. Eng*. **30:** 1136.
- Charpentier P., Lepoutre F. and Bertrand L. (1982). Photoacoustic measurements of thermal diffusivity description of the ''drum effect'', *J. Appl. Phys*. **53:** 608.
- Chen G. (1996). Nonlocal and nonequilibrium heat conduction in the vicinity of nanoparticles, *ASME J Heat Transf*. **118:** 539.
- Chen G. (2000). Particularities of heat conduction in nanostructures, *J. Nanoparticle. Res.* **2:** 199.
- Chen G., Yu W. H., Singh D., Cookson D., and Routbort J. (2008). *J. Nanopart. Res*. **10:** 1109.
- Cheng H., Ma J., Zhao Z. and Qi L. (1995). Hydrothermal Preparation of Uniform Nanosize Rutile and Anatase Particles**,** *Chem. Mater*. **7:** 663.

- Cheng S. C. and Vachon R. I. (1969). The prediction of thermal conductivity of two and three phase heterogeneous mixtures, *Int. J. of Heat Mass Transfer*. **12:** 249.
- Chhabra V., Pillai V., Mishra B. K., Morrone A. and Shah D. O. (1995). Synthesis, Characterization, and Properties of Microemulsion-Mediated Nanophase TiO_2 Particles, *Langmuir*. **11:** 3307.
- Chhabra V., Pillai V., Mishra B. K., Morrone A. and Shah. D. O. (1995). Synthesis, Characterization, and Properties of Microemulsion-Mediated Nanophase TiO_2 Particles, *Langmuir*. **11:** 3307.
- Choi S. U. S (2009). Nanofluids**:** from vision to reality through research, *J. Heat Transf* . **131:** 033106.
- Choi S. U. S. (1995). Enhancing thermal conductivity of fluids with nanoparticles; Development and applications of non-Newtonian flows, *ASME. New York FED*. Vol. **231**/MD **66:** 99.
- Choi S. U. S., Zhang Z. G., Yu W., Lockwood F. E. and Grulke E. A. (2001). Anomalous thermal conductivity enhancement in nanotube suspensions, *Appl. Phys. Lett.* **79:** 2252.
- Chon C. H. and Kihm K. D. (2005). Thermal conductivity enhancement of nanofluids by Brownian motion, *J. Heat. Transfer*. **127:** 810.
- Chon C. H., Kihm K. D., Lee S. P., and Choi S. U. S. (2005). *Appl. Phys. Lett*. **87:** 153107.
- Chopkar M., Das P. K. and Manna I. (2006). Synthesis and characterization of nanofluid for advanced heat transfer applications, *Scripta Materialia*. **55:** 549.

- Chopkar M., Sudarshan S., Das P. K. and Manna I. (2008). Effect of particle size on thermal conductivity of nanofluid, *Metallurgical and Materials Transactions*. **39A:** 1535.
- Cullity B. D. (1978). *Elements of X-ray Diffraction*. (Addison-Wesley: Philippines).
- Das S. K., Choi S. U. S., Yu W., Pradeep T. (2007). *Nanofluids Science and Technology* (Wiley**:** New Jersey).
- Das S. K., Putra N., Theisen P. and Roetzel W. (2003). Temperature dependence of thermal conductivity enhancement for nanofluids, *Journal of Heat Transfer*. **125:** 567.
- De Witt J. A. and M van de Ven' T. *G*. (1992). Kinetics and Reversibility of the Adsorption of Poly (viny1 alcohol) onto Polystyrene Latex Particles, *Langmuir*. **8:** 788.
- Eapen J., Williams W. C., Buongiorno J., Hu L. W., Yip S., Rusconi R. and Piazza R. (2007). Mean-field versus micro-convection effects in nanofluid thermal conduction, *Phys. Rev. Lett*. **99:** 095901-1.
- Eastman J. A., Choi S. U. S., Li S., Yu W. and Thomson L. J. (2001). Anomalously increased effective thermal conductivities of ethylene glycol based nanofluids containing copper nanoparticles, *Appl. Phys. Lett*. **78:** 718.
- Eastman J. A., Phillipot S. R., Choi S. U. S. and Keblinsky P. (2004). Thermal transport in nanofluids, *Annual Review of material Research*. **34:** 219.
- Evans W., Prasher R., Fish J., Meakin P., Phelan P. and Keblinski P. (2008). Effect of aggregation and interfacial thermal resistance on

thermal conductivity of nanocomposites and colloidal nanofluids. *Int. J. Heat Mass Transf* . **51:** 1431.

- Faulkner D. J., Rector D. R,Davidson J. J. and Shekkariz R. (2004). Enhanced Heat Transfer Through the use of nanofluids in Forced Convection, *ASME paper No. IMECE*. **3:** 219.
- Glass J. E. (1968). The Adsorption Characteristics of Water-Soluble Polymers. I. Poly (viny1 alcohol) and Poly (vinylpyrro1idone) at the Aqueous-Air Interface, *Journal of Physical Chemistry*. **72:** 4450.
- Griffith D. J. (1999). *Introduction to Electrodynamics.* (Prentice Hall**:** U. S. A).
- Hamilton R. L., Crosser O. K. (1962). Thermal conductivity of heterogeneous two-component systems, *Ind. Eng. Chem. Fundam* **1:** 187.
- Hasselman D. P. H. and Johnson L. F. (1987). Effective thermal conductivity of composites with interfacial thermal barrier resistance, *J. Compos. Mater*. **21:** 508.
- Hasselman D. P. H. and Johnson L. F. (1987). *J. Compos. Mater*. **21:** 508.
- Holman J. P. (1990). *Heat Transfer* (McGraw-Hill**:** New York,).
- Hong K. S., Hong T. K. and Yang H. S. (2006). Thermal conductivity of Fe nanofluids depending on the cluster size of nanoparticles, *Appl. Phys. Lett* . **88:** 1.
- Hong T. K., Yang H. S. and Choi C. J. (2005). Study of the enhanced thermal conductivity of Fe nanofluids, *J. Appl. Phys*. **97:** 1.

- Hua L. Y., Wei Q. and Cho F. J. (2008). Temperature Dependence of Thermal Conductivity of Nanofluids, *Chin. Phys. Lett.* **25:** 3319.
- Hui P. M. and Stroud D. (1990). Complex dielectric response of metal-particle clusters, *Phys. Rev. B.* **33:** 2163.
- Hui P. M. and Stroud D. (1994). Effective linear and nonlinear response of fractal clusters, *Phys. Rev. B.* **49:** 2163.
- Izadi M., Hossainpour S., Jalali V. D. (2009). Effects of nanolayer structure and Brownian motion of particles in thermal conductivity enhancement of nanofluids, *Int. J. Mechanical Industrial and Aerospace Eng.* **3:** 4201.
- Jacob Klein and Paul F. Luckham (1986). Variation of Effective Adsorbed Polymer Layer Thickness with Molecular Weight in Good and Poor Solvents, *Macromolecules.* **19*:*** 2007.
- Jana S., Salehi-Khojin A. and. Zhong W. H. (2007). *Thermochem. Acta.* **462:** 45.
- Jang S. P. and Choi S. U. S. (2004). Role of Brownian motion in the enhanced thermal conductivity of nanofluids, *Appl. Phys. Lett.* **84:** 4316.
- Jang S. P. and Choi S. U. S. (2006). Cooling performance of a microchannel heat sink with nanofluids, *Appl. Thermal. Engg.* **26:** 2457.
- Jeffrey D. J. (1973). Conduction through a random suspension of spheres, *Proc. R. Soc. London, Ser. **A*** **335:** 355.
- John P. K., Miranda L. C. M., and Rastogi A. C. (1986). Thermal diffusivity measurement using the photopyroelectric effect, *Phys. Rev. B.* **34:** 4342.

- Joshi S. S., Patil S. F., Iyer V. and Mahumuni S. (1998). *Nanostruct. Mater*. **10:** 1135.
- Kang H. U., Kim S. H. and Oh J. M. (2006). *Exp. Heat. Transfer*. **19:** 181.
- Kapoor S., Palit D. K. and Mukherjee T. (2002). *Chem. Phys. Lett*. **355:** 383
- Keblinski P., Eastman J. A. and Cahill D. A. (2005). Nanofluids for thermal transport, *Materials. Today*. **8:** 36.
- Keblinski P., Phillpot S. R., Choi S. U. S. and Eastman J. A. (2002). Mechanisms of heat flow in suspensions of nano-sized particles (nanofluids), *Int. J. Heat. Mass. Transf*. **45:** 855.
- Kim H., Kim J. and Kim M. (2005). Experimental study on CHF characteristics of water-TiO_2 nanofluids, *Nuclear Engg, and Technol*. **38:** 61.
- Kim S. H., Choi S. R., and Kim D. (2007). *ASME J. Heat Transfer*. **129:** 298.
- Kim S. J., McKrell T., Buongiorno J. and Hu L. W. (2008). "Alumina Nanofluids Enhance The critical Heat Flux of water at a Low Pressure, *ASME J. Heat Transfer*. **130:** 044501.
- Kinsler L. E. and Fray A. R. (1962). *Fundamentals of Acoustics*. (Wiley**:** New York).
- Koo J. and Kleinstreuer C. (2004). A new thermal conductivity model fornanofluids, *J. Nanopart. Res*. **6:** 577.
- Kumazava H., Otuski H. and Sada. E. (1993). *J. Mater. Sci. Lett*. **12:** 839.

- Kutty T. R. N., Vivekanandan R. and Murugaraj P. (1988). Precipitation of rutile and anatase (TiO_2) fine powders and their conversion to $MTiO_3$ (M = Ba, Sr, Ca) by the hydrothermal method, *Mater. Chem. Phys.*, **19:** 533.
- Kwak K. and Kim C. (2005). Viscosity and Thermal Conductivity of copper oxide Nanofluid dispersed in ethylene glycol, *Korea-AUST rheol. J.* **17:** 35.
- Lal M., Chhabra V., Ayyub P. and Maitra A. (1988). *J. Mater. Res.* **13:** 1249.
- Lee S., Choi S. U. S., Li S. and Eastman J. A. (1999). Measuring thermal conductivity of fluids containing oxide nanoparticles, *ASME J. Heat Transf*. **121:** 280.
- Li C. H. and Peterson G. P. (2006). Experimental investigation of temperatureand volume fraction variations on the effective thermal conductivity of nanoparticle suspensions (nanofluids). *J. Appl. Phys.* **99:** 1.
- Li C. H. and Peterson G. P. (2007). *J. Appl. Phys.* **101:** 044312.
- Li C. H., Williams W., Buongiorno J., Hu L. W. and Peterson G. P. (2008a). Transient and steady-state experimental comparison study ofeffective thermal conductivity of Al_2O_3/water nanofluids, *J. Heat. Transf*. **130:** 042407.
- Li Q., Xuan Y. (2000). *Experimental investigation on transport properties of nanofluids*. (Heat transfer science and technology Higher Education Press**:** Beijing).
- Li Yu-Hua, Qu W., Feng J. C. (2008). Temperature Dependence of Thermal Conductivity of Nanofluids, *CHIN. PHYS. LETT.* **25:** 3319.

- Liang Z. and Tsai H-L (2011). Thermal conductivity of interfacial layers in nanofluids, *Physical Review. E* **83:** 041602.
- Lisiecki I., Biorling M., Motte L., Ninham B. and Pileni M. P. (1995). *Langmuir*. **11:** 2385.
- Lu L., Sui M. L. and Lu K. (2000). *Science*. **287:** 1463.
- Madhusoodanan K. N., Thomas M. R. and Philip J. (1987). Photoacoustic measurements of the thermal conductivity of some bulk polymer samples, *J. Appl. Phys*. **62:** 1162.
- Mandelis (1993a). *Progress in Photothermal and Photoacoustic Science and Technology*. (Prentice-Hall, Englewood Cliffs**:** N. J).
- Mandelis A. and Zver M. M. (1985). *Theory of photopyroelectric spectroscopy of solids, J. Appl. Phys*. **57:** 4421.
- Mandelis A., Vanniasinkam J., Budhuddu S., Othonos A., and Kokta M. (1993b). Absolute nonradiative energy-conversion-efficiency spectra in Ti^{3+}**:** Al_2O_3 crystals measured by noncontact quadrature photopyroelectric spectroscopy, *Phys. Rev. B1*. **48:** 6808.
- Masuda H., Ebata A., Teramae K., Hishinuma N. (1993). Alteration of thermal conductivity and viscosity of liquid by dispersing ultrafine particles (dispersion of c-Al_2O_3, SiO_2, and TiO_2 ultra-fine particles), *Netsu Bussei*. **4:** 227.
- Masui T., Fujiwara K., Machida K. and Adachi G. (1997). *Chem. Mater*. **9:** 2197.
- Maxwell J. C (1873). *A Treatise on Electricity and Magnetism*. (Oxford**:** Clarendon)

- Menon C. P. and Philip J. (2000). Simultaneous determination of thermal conductivity and heat capacity near solid state phase transitions by a photopyroelectric technique, *Meas. Sci. and Tech*. **11:** 1744.
- Moghadassi A. R., Hosseini S. M. and Henneke D. E. (2010). Effect of CuO nanoparticles in enhancing the thermal conductivities of monoethylene glycol and paraffin fluids, *Ind, Engg, Chem ,Res*. **49:** 1900.
- Munidasa M. and Mandelis A. (1994). A comparison between conventional photothermal frequency scan and the lock-in rate window method in measuring thermal diffusivity of solids, *Rev. Sci. Instrum*. **65:** 2344.
- Muralidharan V. S. and Subrahmanya A. (2009). *Nanoscience and Technology*. (Anne Books: New Delhi).
- Murshed S. M. S., Leong K. C. and Yang C. (2005). Enhanced thermalconductivity of TiO_2-water based nanofluids, *Int. J. Therm. Sci*. **44:** 367.
- Murshed S. M. S., Leong K. C. and Yang C. (2008a). Thermophysical and electrokinetic properties of nanofluids—a critical review, *Appl. Therm. Eng.*, **28:** 2109.
- Murshed S. M. S., Leong K. C., Yang C. (2008b). Investigations of thermal conductivity and viscosity of nanofluids, *Int. J. Therm. Sci*. **47:** 560.
- Nan C. W and Birringer R. (1997). Effective thermal conductivity of particulate composites with interfacial thermal resistance, *J. Appl. Phys*. **81:** 6692.

- Nash D. C., McCreath G. E. and Chase H. A. (1997). Modification of polystyrenic matrices for the purification of proteins: Effect of the adsorption of poly(vinyl alcohol) on the characteristics of poly(styrene-divinylbenzene) beads for use in affinity chromatography, *Journal of Chromatography A.* **758:** 53.
- O'Neill M. J. (1964). The analysis of a temperature-controlled scanning calorimeter, *Anal. Chem.* **36:** 1238.
- Parthasarathy G. and Asokan S. (1987). Effect of high-pressure on the optical-absorption and thermal- diffusivity in gexte100-x glasses by the photoacoustic technique, *Physical Rev. B.* **35:** 8269.
- Patel H. E., Das S. K., Sundararajan T., Nair A. S., George B. and Pradeep T. (2003). Thermal conductivities of naked and monolayer protected metal nanoparticle based nanofluids**:** Manifestation of anomalous enhancement and chemical effects, *Appl. Phys. Lett.* **83:** 2931.
- Petra N., Roetzel W., Das S. K. (2003). Natural convection of nano-fluids, *Heat and Mass Transfer*. **39:** 775.
- Philip J. and Nisha M. R. (2009). Thermal diffusion in dilute nanofluids investigated by photothermal interferometry, *J. Phy. Conference Series.* **214:** 012035.
- Prakash M. and Giannelis E. P. (2007). Mechanism of heat transport in nanofluids, *J. Computer-Aided Mater Design*, **14:** 109.
- Prasher R. (2006a). Thermal conductivity of composites of aligned nanoscale and microscale wires and pores, *J. Appl. Phys.* **100:** 034307.

- Prasher R. (2006b). Transverse thermal conductivity of porous materials made from aligned nano- and microcylindrical pores, *J. Appl. Phys.* **100:** 064302.
- Prasher R., Phelan P. E. and Bhattacharya P. (2006). Effect of aggregation kinetics on the thermal conductivity of nanoscale colloidal solutions (nanofluid), *Nano Lett.* **6:** 1529.
- Preethy C. Menon (2001). *Photopyroelectric study of thermalproperties and phase transitions in selected solids*, (Thesis submitted to Cochin University of Science and Technology).
- Putnam S. A., Cahill D. A., Ash B. J. and Schadler L. S. (2003). High-precision thermal conductivity measurements as a probe of Polymer/nanoparticle interfaces, *J. Appl. Phys.* **94:** 6785.
- Qi L. M., Ma J. M. and Shen J. L. (1997). *J. Colloid Interface Sci.* **186:** 498.
- Qian Y., Chen Q., Chen Z., Fan C. and Zhou G. (1993). *J. Mater. Chem.,* **3:** 203.
- Rayleigh L. (1892). *Philos. Mag.* **34:** 481.
- Reddy K. M., Reddy C. V. G. and Manorama S. V. (2001). Preparation, Characterization, and Spectral Studies on Nanocrystalline Anatase TiO_2, *J. Solid State Chem.* **158:** 180.
- Rosencwaig A. (1980). *Photoacoustics and Photoacoustic Spectroscopy*. (Wiley**:** New York).
- Roy G., Nguyen C. T., Doucet D., Suiro S. and Mare T. (2006). Temperature dependent thermal conductivity of alumina based nanofluids, *In: Davis GV, Leonardi E (eds) Proceedings of 13th*

International Heat Transfer Conference. (*Begell House Inc, Redding: CT)*.

- Schrock V. and Starkman S. (1958). Spherical Apparatus for Measuring the Thermal Conductivity of Liquids, *Rev. Sci. Instrum*. **29:** 625.
- Schwartz L. M., Garboczi E. J. and Bentz D. P. (1995). Interfacial transport in porous media**:** Application to DC electrical conductivity of mortars, *J. Appl. Phys*. **78:** 5898.
- Selvaraj U., Prasadrao A. V., Komerneni S. and Roy R. (1992). *J. Am. Ceram. Soc*. **75:** 1167.
- Shabde V. S., Hoo K. A. and Gladysz G. M. (2006). Experimental determination of the thermal conductivity of three-phase syntactic foams, *J. Mater. Sci.* **41:** 4061.
- Shaikh S., Lafdi K., and Ponnappan R. (2007). *J. Appl. Phys.* **101:** 064302.
- Shen J. and Mandelis A. (1995). Thermal Wave Resonant Cavity *Rev. Sci. Instrum*. **66:** 4999.
- Shen J., Mandelis A. and Aloysius B. D. (1996). Thermal Wave Resonant Cavity Measurements of the Thermal Diffusivity of Air: A Comparison between Cavity length scan and Modulation frequency scan, *International Journal of Thermophysics*. **17:** 1241.
- Shima P. D., Philip J., and Raj B. (2009). *Appl. Phys. Lett*. **94:** 223101.
- Stathatos E., Lianos P., Del Monte F., Levy D. and Tsiourvas D. (1997). *Langmuir*. **13:** 4295.
- Stratton J. A. (1941). *Electromagnetic Theory*. (McGraw-Hill**:** New York).

- Sugimoto T., Okada K. and Itoh H. (1997). Synthetic of Uniform Spindle-Type Titania Particles by the Gel–Sol Method, *J. Colloid. Interface Sci*. **193:** 140.
- Syam Sundar L. and Sharma K. V. (2008). Thermal conductivity enhancement of nanoparticles in distilled water, *Int. J. Nanoparticle*. **1:** 66.
- Tatasov S., Kolubaev A., Belyaev S., Lerner M. and Tepper F. (2002). *Wear*, **252:** 63.
- Timofeeva E. V., Routbort J. L. and Singh D. (2009). Particle shape effects on thermophysical properties of alumina nanofluids, *J. Appl. Phys*. **106:** 014304.
- Tsao G. T-N (1961). Thermal conductivity of two-phase materials, *Ind. Engng Chem*. **53:** 395.
- Vadasz J., Govender S. and Vadasz P. (1987). *Int. J. Heat Mass Transfer*. **1:** 343.
- Van Beek L. K. H. (1967). Dielectric behavior of heterogeneous system,Progr. Dielectr, **7:** 69.
- Vanniasinkam J., Mandelis A., Budhuddu S., and Kokta M. (1994). Photopyroelectric deconvolution of bulk and surface optical-absorption and nonradiative energy conversion efficiency spectra in Ti**:** Al_2O_3 crystals, *J. Appl. Phys*. **75:** 8090.
- Vassallo P., Kumar R., and D'Amico S. (2004). Pool Boiling Heat Transfer Experiments in Silica Water Nanofluids, *Int. J. Heat Mass Transfer*. **47:** 407-411.
- Vladkov M., Barrat J – L. (2006). Modeling transient absorption and thermal conductivity in simple nanofluids, *Nano Lett*. **6:** 1224.

- Wang B. X., Sheng W. Y. and Peng X. F. (2009). A novel statistical clustering model for predicting thermal conductivity of nanofluid, *Int. J. Thermophys.* **30:** 1992.
- Wang B-X., Zhou L-P. and Peng X-F. (2003). A fractal model for predicting the effective thermal conductivity of liquid with suspension of nanoparticles, *Int. J. Heat Mass Transfer*. **46:** 2665.
- Wang X. Q. and Majumdar A. S. (2007). Heat transfer characteristics of nanofluids**:** a review, *Int. J. Thermal Sci.* **46:** 1.
- Wang X., Xu X. and Choi S. U. S. (1999). Thermal conductivity of nanoparticle- fluid mixture, *J. Thermal Physics Heat Transfer*. **13:** 474.
- Watson E. S., O'Neill M. J., Justin J. and Berrnerr N. A. (1964). Differential scanning calorimeter for quantitative differential thermal analysis, *Anal. Chem.* **36:** 1233.
- Wen D. and Ding Y. (2004). *J. Thermophys. Heat Transfer*. **18:** 481.
- Wen D. and Ding Y. (2005). Experimental investigation into the pool boiling heat transfer of aqueous based alumina nanofluids, *J. of Nanoparticle Res.* **7:** 265.
- Wen D., Lin G., Vafaei S., Zhang K. (2009). Review of nanofluids for heat transfer application, *Particuology*. **7:** 141.
- Wilson O. M., Hu X., Cahill D. G., Braun P. V. (2002). Colloidal metal particles as probes of nanoscale thermal transport in fluids, *Phys. Rev. B*. **66:** 224301-1.
- Xie H., Fujii M., Zhang X. (2005). Effect of interfacial nanolayer on the effective thermal conductivity of nanoparticle–fluid mixture, *Int. J. Heat Mass. Transf.* **48**: 2926.

- Xie H., Wang J., Xi T., and Ai F. (2002). *J. Appl. Phys.* **91:** 4568.
- Xie H., Wang J., Xi T., Liu Y. (2002a). Thermal conductivity of suspensions containing nanosized SiC particles, *Int J Thermophys*. **23:** 571.
- Xie H., Wang J., Xi T., Liu Y. and Ai F. (2002b). Dependence of the thermal conductivity of nanoparticle–fluid mixture on the base fluid, *J. Mater. Sci. Lett*. **21:** 1469.
- Xuan Y. and Li Q. (2000). Heat transfer enhancement of nanofluids, *Int. Journal Heat Fluid Flow.* **21:** 58.
- Xuan Y. and Li Q. (2003). Investigation on convective heat transfer and pressure loss of alumina/ Water and Flow features of nanofluids, *ASME J. Heat Transfer*.**125**: 151.
- Xuan Y., Li Q. and Hu W. (2003). Aggregation structure and thermal conductivity of nanofluids, *AIChE. J.* **49:** 1038.
- Xue Q. and Xu W. (2005). *Mater. Chem. Phys.*, **90:** 298.
- Yan J. M., Zhang Q. Y. and Gao J. Q. (1986). *Adsorption and Agglomeration Surface and Porosity of Solid*. (Science Press**:** Beijing).
- You S. M., Kim J. H., Kim K. M. (2003). Effect of nanoparticle on critical heat flux of water in pool boiling of heat transfer, *Appl. Phys. Lett*. **87:** 233107.
- Yu W. and Choi S. U. S. (2003). The role of interfacial layers in the enhanced thermal conductivity of nanofluids**:** A renovated Maxwell model, *J. Nanopart. Res.* **5:** 167.

- Yu W., France D. M., Routbort J. L. and Choi S. U. S. (2008). Review and comparison of nanofluid thermal conductivity and heat transfer enhancements, *Heat Transfer Eng.* **29:** 432.
- Yu W. and Choi S. U. S. (2004). *J. Nanoparticle Research*. **6:** 355
- Zhang X., Gu H. and Fujii M. (2006a). Effective thermal conductivity and thermal diffusivity of nanofluids containing spherical and cylindrical nanoparticles, *J. Appl. Phys* **100:** 1.
- Zhang X., Gu H. and Fuji M. (2006b). Experimental study on the effective thermal conductivity and thermal diffusivity of nanofluids, *Int. J. Thermophysics*. **27:** 569.
- Zheng H., Li C., Liu Y., Zeng J. and Li Y. (1998). *J. Univ. Sci. Technol. China*. **28:** 722.
- Zhu H., Lin Y. and Yin Y. (2004). A novel one-step chemical method for preparation of copper nanofluids, *J. Colloid Interface Sci.* **277:** 100.
- Zhu H., Zhang C., Yin Y. (2005). *Nanotechnology*. **16:** 3079.